

Impact Assessment for a High Penetration of Distributed Generators in Medium and Low Voltage Grids

Master Thesis



Institute of Electrical Power Systems
TU Graz

Author

Florian Otto BSc

Supervisor

Univ.-Prof. DI Dr.techn. Lothar Fickert

Mentor

DI Thomas Wieland

Head of the Institute: Univ.-Prof. DI Dr.techn. Lothar Fickert

A - 8010 Graz, Inffeldgasse 18-I
Telephon: (+43 316) 873 - 7551
Telefax: (+43 316) 873 - 7553
<http://www.ifea.tugraz.at>
<http://www.tugraz.at>

Graz / July - 2012



Statutory Declaration

I declare that I have authored this thesis independently, that I have not used other than the declared sources / resources, and that I have explicitly marked all material which has been quoted either literally or by content from the used sources.

Graz, 25.07.2012

Florian Otto

Acknowledgemend

This thesis would not have been possible without the guidance and support of several people who helped me during my work. First of all I want to thank my supervisor Univ.-Prof. DI Dr.techn. Lothar Fickert and my mentor DI Thomas Wieland as well as the Institute of Electrical Power Systems at Graz University of Technology with all its employees for their excellent support and professional advises.

Furthermore I want to show my deepest gratitude to the employees of the company Wien Energie Stromnetz GmbH. My special thanks go to DI Dr.techn. Gerhard Lavicka, DI Dr.techn. Thomas Schuster and DDI. Andreas Bolzer who supported my thesis and made it possible.

Last but not least I also want to thank all my friends and fellow students for their abundance of patience during the time I spent for this work and for their continuous assistance.

Abstract

This thesis assesses the effects of a large-scale implementation of distributed micro-generators in medium and low voltage grids. In a first step three generally applicable generic model grids for network areas with urban, suburban and rural characteristics are developed from real distribution network structures. Power flow simulations are performed with these model grids, in order to examine their feed-in capacity, regarding distributed generation. The distributed generators are therefore represented by evenly distributed photovoltaic rooftop systems. Extended simulations with different measures (grid reinforcement, decentralized and centralized reactive power management, regulating distribution transformers) determine the possibilities to increase the achievable feed-in capacities of the particular grids. The assessment criteria for the evaluations are defined by the appropriate national and international standards and grid codes. To analyze the behavior of the developed model grids, parameter and equipment variations including a sensitivity analysis are carried out, altering their specific network parameters (line length, distribution transformer parameters and consumer loads).

Keywords: distributed micro-generation, generic model grids, photovoltaic (PV), increased feed-in capacity, power flow calculation

Kurzfassung

Diese Arbeit beschäftigt sich mit den Auswirkungen einer großflächigen Implementierung von dezentralen Micro-Erzeugungsanlagen am Mittel- und Niederspannungsnetz. In einem ersten Schritt werden aus realen Netzgebieten mit städtischem, vorstädtischem und ländlichem Charakter, drei allgemein gültige generische Musternetze entwickelt. Um die Aufnahmefähigkeit dieser Netze, bezüglich dezentraler Einspeisung, zu ermitteln werden Lastflussberechnungen durchgeführt. Die dezentralen Erzeugungsanlagen werden dabei durch gleichmäßig verteilte Photovoltaik Aufdachanlagen dargestellt. Erweiterte Simulationen mit verschiedenen Maßnahmen (Netzverstärkung, dezentrales und zentrales Blindleistungsmanagement, regelbare Verteiltransformatoren) dienen dazu, den Effekt dieser Maßnahmen bezüglich der Erhöhung der Einspeisekapazität der jeweiligen Netze zu untersuchen. Nationale und internationale Normen sowie Anschlussbedingungen stellen die dafür benötigten Bewertungskriterien dar. Eine Parameter und Betriebsmittel Variation, inklusive einer Sensitivitätsanalyse soll das Verhalten der entwickelten Musternetze bei der Veränderung typischer Netzparameter (Leitungslänge, Parameter der Verteiltransformatoren, Verbraucherlast) veranschaulichen.

Schlüsselwörter: Dezentrale Micro-Erzeugung, generische Musternetze, Photovoltaik (PV), Erhöhung der Einspeisekapazität, Lastfluss Berechnung

Table of Contents

1. Introduction	7
2. Fundamentals	8
2.1. Photovoltaic Basics	8
2.2. Photovoltaic Modules	11
2.3. Photovoltaic Inverters	12
2.4. Photovoltaic Systems	15
2.4.1. Islanded Systems	15
2.4.2. Grid-Connected Systems	16
2.5. Grid Structures	16
2.5.1. Distribution Grid Structures - Medium Voltage Level	17
2.5.2. Distribution Grid Structures - Low Voltage Level	17
2.6. Influence of Distributed Generator Infeeds on Distribution Systems	20
2.6.1. Voltage Rises due to Distributed Generation	22
2.6.2. Approximation of the Voltage Rise	25
2.7. Applied Grid Codes and Standards	27
2.7.1. Power Frequency	27
2.7.2. Voltage Magnitude Variations	28
2.7.3. Rapid Voltage Changes	28
2.7.4. Supply Voltage Unbalance	28
2.7.5. Voltage Rise Constraints for Distributed Generators	28
2.7.6. Reactive Power Management	28
2.8. Measures to Decrease the Voltage Rise	29
2.8.1. Line Impedance	29
2.8.2. Decentralized Reactive Power Management	30
2.8.3. Centralized Reactive Power Management	33
2.8.4. Regulating Distribution Transformers	34
3. Model Grid Development	36
3.1. General Model Grid Parameters	38
3.1.1. Transformers	38
3.1.2. Cable Lines	39
3.1.3. Overhead Lines	39
3.1.4. Consumer Loads	40
3.1.5. Residential Photovoltaic System Configuration - Distributed Generator	41
3.2. Representative Real Grids	42
3.2.1. Urban Model Grid	42
3.2.2. Suburban Model Grid	44

3.2.3. Rural Model Grid	46
4. Simulations	48
4.1. Urban Model Grid	49
4.1.1. Simulation Parameters	51
4.1.2. Simulation Sequence	52
4.1.3. Simulation Results	55
4.1.4. Achievable Feed-In Capacity	57
4.1.5. Parameter Variation - Sensitivity Analysis	58
4.1.6. Equipment Variation	60
4.2. Suburban Model Grid	65
4.2.1. Simulation Parameters	67
4.2.2. Simulation Sequence	68
4.2.3. Simulation Results	71
4.2.4. Achievable Feed-In Capacity	73
4.2.5. Parameter Variation - Sensitivity Analysis	74
4.2.6. Equipment Variation	75
4.3. Rural Model Grid	77
4.3.1. Simulation Parameters	79
4.3.2. Simulation Sequence	80
4.3.3. Simulation Results	84
4.3.4. Achievable Feed-In Capacity	86
4.3.5. Parameter Variation - Sensitivity Analysis	87
5. Conclusion	90
Bibliography	92
Appendix	93
A. Voltage Profiles - Urban Model Grid	93
A.1. 630 kVA Distribution Transformers	93
A.2. 800 kVA Distribution Transformers	94
A.3. 1000 kVA Distribution Transformers	95
B. Voltage Profiles - Suburban Model Grid	96
B.1. Reactive Power Provision through PV-Systems	96
B.2. Overhead Line / Cable Comparison	97
B.3. Regulating Distribution Transformer	98
B.4. Central Reactive Power Management at 0,4 kV Busbar	99
C. Voltage Profiles - Rural Model Grid	100
C.1. Reactive Power Provision through PV-Systems	100
C.2. Overhead Line / Cable Comparison	103
C.3. Regulating Distribution Transformer	106
C.4. Central Reactive Power Management at 0,4 kV Busbar	109

1. Introduction

Decentralized energy production gained extensive importance during the past years. Especially the number of distributed generators with small output powers in the kVA range, connected to the low and medium voltage grid, increased steadily. The traditional public power supply network, with its hierarchic energy production, transmission and distribution structure, experiences a transition into a distributed system with an increasing number of detached micro-generation facilities.

The purpose of this thesis is the evaluation of different effects onto the networks system voltages and equipment loadings, caused by a high penetration of distributed generators operated at the medium and low voltage level. From special interest are small-scale micro-generators, which are for example: photovoltaic (PV) systems, wind turbines, hydro energy, micro gas turbines or micro combined-heat and power plants (micro-CHP). The distributed generators in this document are represented by domestic photovoltaic systems, due to their growing popularity, mainly caused by sinking prices of photovoltaic panels and grid connected inverters, as well as interesting government fundings.

The thesis is divided into three main chapters, starting with a fundamental part, which explains the basic functions of photovoltaic generators and their system integration, as well as principle distribution system structures and the effects of distributed generation onto the grid. Different constraints, stated in the relevant grid codes and standards, define thresholds, which must not be violated by the increased occurrence of distributed generation. Therefore this document also lists the appropriate guidelines and thresholds forming the assessment base for the evaluation.

In the second part, three characteristic model grids (urban, suburban, rural) were developed in accordance to real network parameters and network structures, provided by the company Wien Energie Stromnetz GmbH.

In the last part the developed model grids were then modeled and simulated with Neplan[®] and the simulation results evaluated with MathWorks[®] MATLAB[®].

The following research questions were addressed in this document:

- Is it possible to create distinctive and generally valid generic model grids, which reflect the main characteristics of common supply areas?
- Which network parameters have the most significant effects onto the developed model grids?
- What is the possible feed-in capacity for distributed micro-generation within the developed model grids?
- Which measures can be taken into consideration to increase the possible feed-in capacity for an existing grid and how practical and effective are they?

2. Fundamentals

The following chapter summarizes the basic fundamentals, forming the background of this thesis. The basic functionality of common photovoltaic generators, and especially the components of residential photovoltaic systems, including photovoltaic modules and inverters are explained. Furthermore principle network structures, which were used to develop characteristic model grids, are outlined and discussed. In addition, this section offers a derivation of the effects upon the supply voltage level in distribution grids, caused by load currents due to normal load flow conditions and also due to distributed generation. A simple way to estimate possible voltage rises, resulting from generator infeeds is shown as well as some measures against these rises, including their implementation for the performed simulations. Finally, this chapter also states the basic guidelines and standards, which were used to assess the simulation results in this thesis. These guidelines represent the constraints for all following considerations.

2.1. Photovoltaic Basics

The main principle of all crystalline photovoltaic elements is based on the photoactive p-n junction, found in silicon semiconductors. If light is irradiated onto the semiconductor, the photons are absorbed. Due to this absorption, the energy level of electrons from the valence band is raised. Within the crystal structure of the semiconductor, electrons from the conduction band can move freely. This results in an electrical current caused by the light irradiation and is called the "photoelectric effect" [12].

By inserting a crystal impurity, the conductance can be influenced and an extrinsic semiconductor is formed. Depending on the achieved conductance, compared to the crystal conductance without insertion of impurities, the result is an n-type conductivity if the conductivity is raised, and a p-type conductivity if it is lowered. The combination of p- and n-type conductors creates a p-n junction which also develops a diffusion voltage U_d at the barrier layer as seen in figure 2.1.1.a. Figure 2.1.1.b shows the electrical characteristics of the p-n junction. The external current through the semiconductor, also called diode current is represented by I_d . The current I_s stands for the saturation current against the barrier layer.

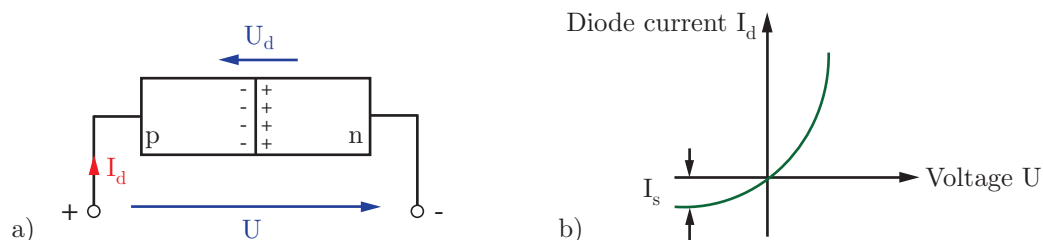


Figure 2.1.1.: Principle structure of semiconductor p-n junction a), and its characteristic b) [12].

If an external voltage is applied to the p-n junction it behaves like a diode, resulting in the characteristic in figure 2.1.1.b. Irradiation of the p-n junction with photons on the other hand, raises electrons from the valence band into the conduction band. The resulting potential gradient within the space-charge

region causes an electric current, flowing through an external circuit. The generated photo current I_{ph} acts against the direction of the diffusion current and is directly proportional to the irradiation intensity. The current, generated by the solar cell can be calculated as followed [12]:

$$I = I_{ph} - I_s \cdot \left[\exp\left(\frac{U}{U_T}\right) - 1 \right]. \quad (2.1.1)$$

The thermodynamic voltage $U_T = \frac{kT}{e}$ (25,7 mV at 25 °C) and the saturation current I_s are shown in figure 2.1.1.b. If short-circuited, the resulting short-circuit current I_{sc} is equal to:

$$I = I_{sc} = I_{ph}. \quad (2.1.2)$$

In case of an open-circuit the resulting open-circuit voltage U_0 is calculated as follows:

$$U = U_0 = U_T \cdot \ln\left(1 + \frac{I_{ph}}{I_s}\right). \quad (2.1.3)$$

The current in case of an short circuit I_{sc} is equal to the photo current I_{ph} , thus making it directly proportional to the irradiation. The open circuit voltage U_0 however shows a logarithmic characteristic. Due to the temperature dependency of the thermodynamic voltage U_T , the open circuit voltage U_0 is also influenced by the temperature of the solar cell. A rising temperature results in a lower power output from the cell and therefore in a lower efficiency. Figure 2.1.2 indicates the design of photovoltaic elements based on silicon semiconductors.

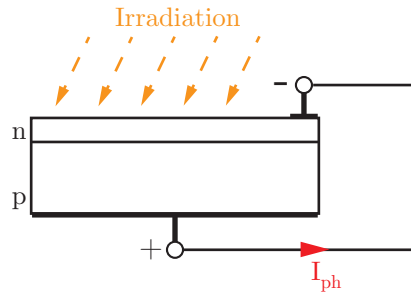


Figure 2.1.2.: Irradiated solar cell [12].

The characteristic of a real solar cell as a derivation of the standard diode characteristic curve is depicted in figure 2.1.3. Changes in the irradiation onto the cell result in changes in the characteristic. The maximum power for the available irradiation can be achieved at the point MPP which is called maximum power point. In this point, the cell is operated with the optimum values for the cell current I_{opt} and voltage U_{opt} . A simplified equivalent circuit shown in figure 2.1.4 can be used to analyze and explain the characteristics of solar cells.

The current source in figure 2.1.4 represents the photo current, generated by the irradiation of photons. A serial resistance R_s covers possible resistive connection losses. Leakage losses, which also cannot be avoided, are represented through a parallel resistance R_p . The resistance of the p-n junction is rep-

represented by the diode resistance R_d . An idealization of the diode characteristics, defined by the diode resistance R_d and the diffusion voltage U_d , helps to estimate the influence of the serial resistance R_s and the parallel resistance R_p upon the maximum power point (MPP).

The open circuit range of the characteristics can be approximated with the straight S1 defined as $U = U_0 - \left(R_s + \frac{R_p \cdot R_d}{R_p + R_d}\right) \cdot I$. The short circuited range of the characteristics can be approximated with the straight S2 with $U = (R_p + R_s) \cdot (I_{sc} - I)$ while $I_{sc} = \frac{R_p}{R_p + R_s} \cdot I_{ph} \approx I_{ph}$. The two straights meet in the theoretical power point P'.

Further examinations show that the ideal voltage at the maximum power point is only slightly depending on the irradiation. In addition the ideal current is only slightly affected by the cell temperature [12].

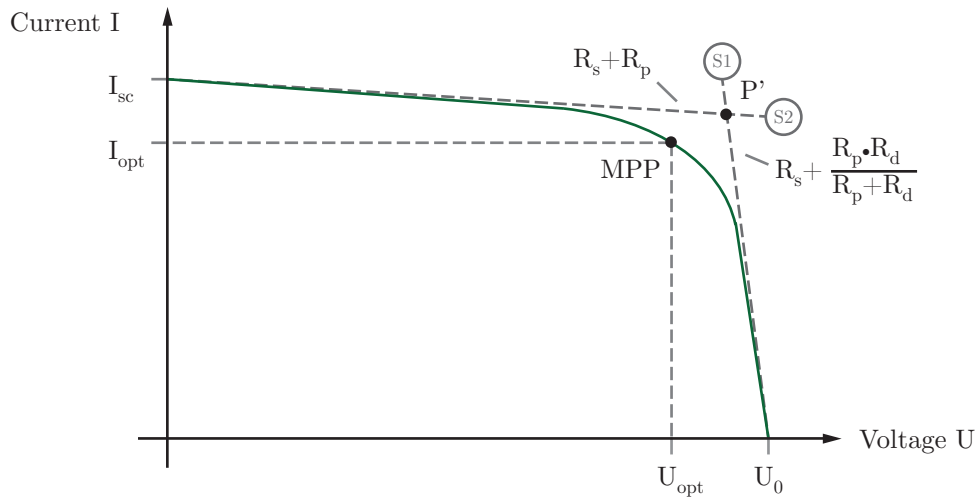


Figure 2.1.3.: Current/Voltage characteristic of a real solar cell [12].

To rate different photovoltaic cells, their power at the maximum power point is stated in Watt-peak (W_p). This power output is the result from standardized tests with an irradiation of 1000 W/m^2 at a cell temperature of 20°C with a defined spectral power distribution [6].

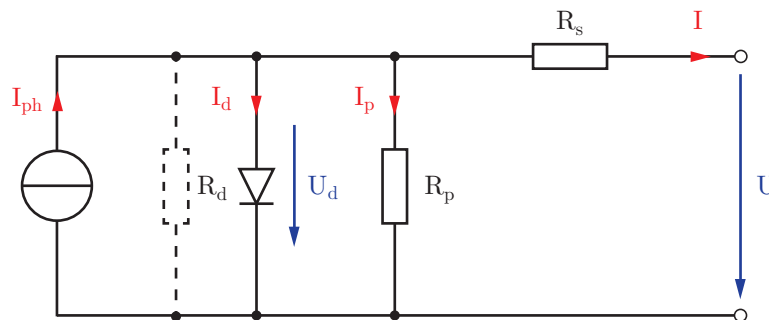


Figure 2.1.4.: Equivalent network of a basic solar cell [12].

In reality, the cell temperature increases significantly due to the irradiation, which results in a lower efficiency in standard condition installations.

2.2. Photovoltaic Modules

The serial connection of single solar cells creates a solar module. Depending on the used solar cell technology and the number of interconnected cells respectively the module size, the resulting output power reaches values from 50 Wp up to 250 Wp for a single module. The use of so called bypass diodes is essential to eliminate the risk of possible damages of shadowed cells, by the current from other cells, connected in series.

A solar generator is represented by the serial or parallel interconnection of solar modules. If serial connections are chosen, bypass diodes prevent the modules from damages due to back currents. The resulting interconnection of cells is often referred as string. Serial interconnection increases the output voltage of modules and the parallel connection of these strings increases the possible output current.

Crystalline silicon is the state of the art material for photovoltaic solar cells. There are currently two main technologies in use for manufacturing these cells:

1. Mono-crystalline silicon - Cut from cylindrical ingots, these cells have the highest achievable efficiency but are expensive in the production process.
2. Poly-crystalline silicon - Silicon is melted, casted into blocks and cooled to solidify. This technique makes the production less expensive but also results in lower module efficiencies.

Table 2.2.1 represents the efficiencies of the 10 mono-crystalline photovoltaic modules with the highest efficiencies available at the moment.

Table 2.2.1.: The 10 world's most efficient mono-crystalline photovoltaic modules (8. Jul. 2011) [2].

	Manufacturer	Module Efficiency	Module Type
1.	Sunpower	20.40%	E20 / 333 SOLAR PANEL
2.	AUO	19.50%	PM318B00
3.	Sanyo Electric	19.00%	HIT-N240SE10
4.	Jiawei	18.30%	JW-S100
5.	Crown Renewable Energy	18.30%	Summit 100LM
6.	JA Solar	16.84%	JAM5(L)-72-215/SI
7.	Trina Solar	16.40%	TSM-210DC80
8.	CNPV Solar	16.20%	CNPV-105M
9.	Yingli Solar	16.20%	Panda 265 Series
10.	Jetion	16.20%	JT315SAc

However, regarding the high prices of these modules, especially for the residential use of photovoltaic systems, lower average efficiencies are common. Therefore cheaper poly-crystalline modules are also often used for rooftop installation. The top 10 of the available efficiencies for poly-crystalline modules are shown in table 2.2.2.

Table 2.2.2.: The 10 world's most efficient poly-crystalline photovoltaic modules (12. Dec. 2011) [3].

	Manufacturer	Module Efficiency	Module Type
1.	Solland Solar	16.00%	Sunweb
2.	Siliken	15.70%	SLK72P6L-305
3.	LDK Solar	15.67%	LDK-200P-24(s)
4.	Vikram	15.63%	Eldora 280 (300)
5.	Wiosun	15.54%	E300P
6.	A2peak	15.50%	P3-235-60 (250)
7.	CNPV solar	15.40%	CNPV-300P
8.	Latitude Solar	15.30%	Latitude P6-60/6 (250)
9.	JA Solar	15.29%	JAP6-60-250
10.	China Sunergy	15.24%	CSUN295-72P

Another example of photovoltaic cells are so called thin-film solar cells. To reduce the production costs and material usage, very thin layers of possible material for the photoelectric effect is applied on a substrate. Commonly the material is evaporated onto metal sheets. The resulting cells have a lower efficiency, which results in larger system sizes for the same power output.

Some possible materials used for thin-film solar cells are [12]:

- Crystalline silicon Si
- Amorphous silicon Si
- Gallium-arsenide GaAs
- Cadmium-telluride CdTe
- Copper-indium-diselenid CuInSe_2

For all the calculation within this document an average module efficiency of 15% is chosen in accordance with [6]. With an average irradiation of 1000 W/m^2 for the area of Austria, this results in a maximum power output of 150 Wp/m^2 .

2.3. Photovoltaic Inverters

Photovoltaic inverters convert the direct current, produced by the photovoltaic modules, into alternating current with appropriate voltage amplitude and frequency. To ensure the maximum possible output power of the modules, the inverters can include a maximum power point tracker (MPPT). As mentioned in section 2.1, the output power is highly affected by the solar irradiation, the cell material and the cell temperature. The maximum power point tracker adjusts the inverters apparent resistance to meet the voltage at the point of maximum power output. This can also be seen at the point MPP in figure 2.1.3. Due to manufacturing tolerances, even solar cells of the same type may have slightly different power points, reducing the possible power output caused by the power point tracker, when serial interconnected modules are supplied by single inverters with a single tracker for all modules.

Depending on whether the photovoltaic system is realized as an islanded or grid connected generator, the inverter can also include safety devices to protect the system, and guarantee the personal safety and the protection of attached devices. In case of a threshold violation of the output voltage according to the

relevant grid code, or a loss of mains, the distributed generator is separated from the connected loads or the grid. This can also include an anti-islanding protection, which disconnects the inverter in case of a separation to prevent the operation as an islanded system. Special precautions must be considered when the system is connected to a public power supply grid, which are stated by additional guidelines and the system operator of the grid.

Module inverters are small inverters, sometimes also referred as micro-inverters, attached directly to the photovoltaic module. The result is an AC photovoltaic module[1] which can power consumer loads directly. Figure 2.3.1 shows the principle structure of an AC module. Other AC modules can be connected to the consumer in the same way, thus making an extension of the existing system easier and simplifying the interconnection between the modules. The issues of shadowing and problems with faulty modules do not affect the whole system anymore. Maximum power point trackers can operate at the power point, which is best for the corresponding module, improving the output power furthermore. As a result, module inverters allow the design of very modular and non-sensitive photovoltaic systems. The disadvantage of module inverters are higher investment costs.

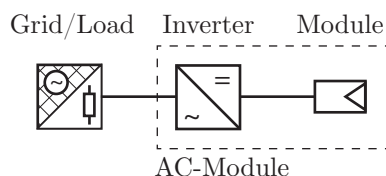


Figure 2.3.1.: AC-Module photovoltaic system including module inverter [1].

String inverters are the most commonly used photovoltaic inverters for residential applications. The basic structures, including the photovoltaic modules and the attached string inverter can be seen in figure 2.3.2. Several photovoltaic modules are connected in series to reach a sufficiently high direct output voltage. The DC output power of this string of modules is converted to AC power. Advantages of string systems may be lower initial costs, however error detection gets more complicated and a system expansion produces higher costs, mostly including the exchange of the inverter. Also the losses due to shadowing and line resistances increase with higher photovoltaic array sizes, influencing the overall system performance. Table 2.3.1 shows the efficiencies of the worlds ten most efficient photovoltaic string inverters.



Figure 2.3.2.: Single string photovoltaic system including string inverter [1].

Table 2.3.1.: The 10 world's most efficient string inverters (<5 kW) (02. Jan. 2012) [4].

	Manufacturer	Inverter Efficiency	Inverter Model
1.	Steca	98.60%	StecaGrid 3600
2.	Sunways	97.80%	NT5000
3.	Fronius	97.70%	IG TL 5.0
4.	Diehl AKO	97.70%	4800 TL
5.	Voltwerk	97.70%	VS 5
6.	Solaredge	97.60%	SE4000
7.	Mastervolt	97.50%	SunMaster ES4.6
8.	Mitsubishi Electric	97.50%	PV-S4200
9.	Solutronic	97.40%	Solplus 50
10.	Refu	97.40%	Refusol 500K

Multi-string inverters are an advanced form of string inverters, adding the possibility to convert the DC current from multiple strings. An example for an multi string photovoltaic system with the multi string inverter and two module strings is shown in figure 2.3.3. The separated strings feed a DC intermediate circuit through a DC/DC converter. Another inverter converts the energy from the intermediate circuit and supplies the attached grid or consumer loads. In general, every string is controlled by it's own maximum power point tracker, which helps to increase the output power for shady conditions and higher different cell characteristics of the used modules.

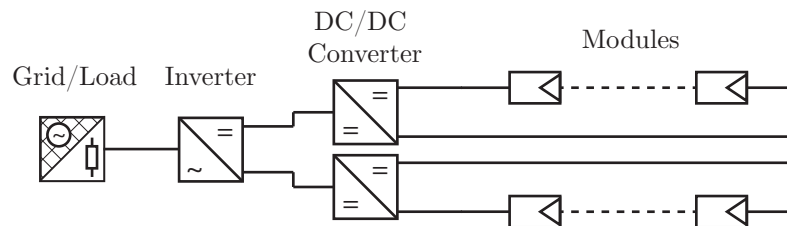


Figure 2.3.3.: Multi-string photovoltaic system including multi-string inverter [1].

Central inverters simplify the module arrangement and interconnection. Therefore they are often used for large photovoltaic arrays with high power ratings. In this case, the central inverter replaces several distributed inverters, thus improving the serviceability and also the overall system efficiency. String-diodes are essential to prevent the flow of balancing currents through the strings in case of module failures or shady conditions.

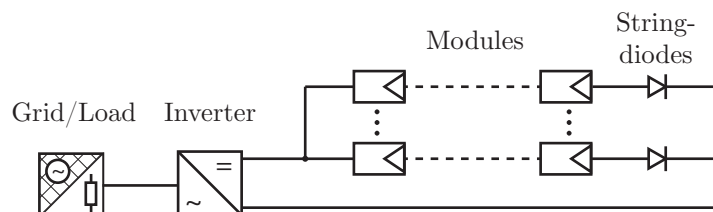


Figure 2.3.4.: Centralized photovoltaic system including central inverter [1].

Hybrid inverters have the main purpose to use more than only photovoltaic as an energy source. Possible secondary generators could for example be present in form of wind turbines or diesel generators. Furthermore, hybrid inverters can include batteries to store energy during times of higher production rates. The used photovoltaic system can be kept smaller in size and output power, because peak loads are supplied by the additional sources of energy or by the energy stored in the battery.

2.4. Photovoltaic Systems

Photovoltaic modules are interconnected to larger arrays, forming a so-called photovoltaic generator. The DC output of the module array is then converted into an AC output system with the appropriate phase voltage amplitudes and frequencies through inverters, to meet the requirements of the consumer loads. Conventional photovoltaic systems can be divided into self-contained island systems and grid-connected systems, which are based on the synchronous connection to existing public grids.

2.4.1. Islanded Systems

For small loads, an islanded photovoltaic system, also called off-grid system, can be a practical and economic energy supply. Especially for remote applications, photovoltaic generators represent an alternative to conventional combustion engine based generators.

The basic components of a photovoltaic islanded system can be seen in figure 2.4.1. A battery is charged with the help of a charge regulator by the output DC current of the attached photovoltaic modules. The energy, stored in the battery, can be used to supply DC loads directly. More common is the conversion of the DC power from the battery into AC power with the help of an inverter in order to supply ac loads.

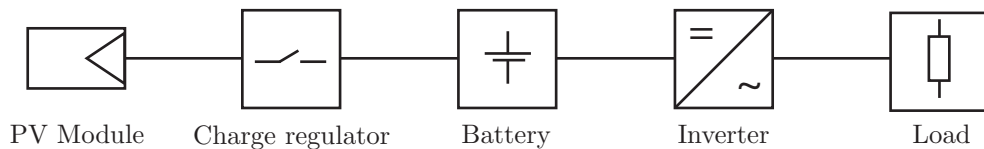


Figure 2.4.1.: Basic components of a simple islanded photovoltaic system [12].

Hybrid inverters gain increasing interest for the use in island systems. With their help, additional sources of energy production can be used which helps to compensate the fluctuating generation furthermore, thus making it possible to use smaller batteries to achieve the same security of supply. The photovoltaic generator can be paired with a wind generator. The resulting hybrid system charges the battery also in times without solar irradiation. Diesel generator sets or biogas generators can supply the system in times of very high consumer loads.

Often lead-acid batteries are used to store the energy in island systems. The size of the battery depends on the expected consumer load and the achievable generator output. It is therefore also depending on the location of the system and meteorological circumstances. Great efforts during the planning of island systems are necessary to find the right battery size. The attached charge regulator protects the battery from deep discharge or overloading and ensures higher lifespans.

2.4.2. Grid-Connected Systems

Grid-connected photovoltaic systems present a simple structure, compared to islanded systems. The connected grid supplies balancing energy in times, in which the generator cannot supply the attached consumer loads on its own, and therefore also replaces the function of the battery. The principle structure of a grid connected photovoltaic system is shown in figure 2.4.2. In comparison to islanded systems, the connection to public electricity networks requires special inverters with included safety devices to protect the system and the grid from dangerous network conditions and to separate the system from the grid in case of a failure, or a loss of mains. The inverters output voltage frequency is directly linked to the grid frequency.

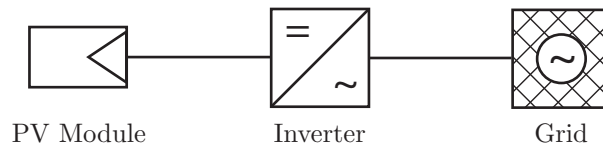


Figure 2.4.2.: Basic components of a grid connected photovoltaic system [12].

The thresholds for valid system frequencies and phase voltages are defined in the grid code of the particular country, in which the system is connected to the grid. An example for a set of guidelines can be seen in the grid code in section 2.7. Depending on the rated output power of the inverter, the connection can be realized monophase for small inverters or polyphase from a certain output power upwards. The connection depends on the respective grid code and is also affecting the voltage unbalance. The irregular connection of several monophase inverters at the same phase conductor could lead to invalid differences between the phase voltages.

2.5. Grid Structures

Table 2.5.1 includes the commonly used voltage levels for transmission and distribution grids in the area of Central Europe. From special interest for distributed generators are voltage levels with the purpose of energy distribution.

Table 2.5.1.: Most common voltage levels in Central Europe for transmission and distribution purpose in public electricity grids.

Identification	Abbreviation	Nominal Voltage U_n	Application
Extra-High Voltage	HV	380 kV	Transmission
		220 kV	
High Voltage		110 kV	Transmission / Distribution
Medium Voltage	MV	20 kV	Distribution
		10 kV	
Low Voltage	LV	0,4 kV	

The 110 kV voltage level is sometimes also referred as distribution level. However, the currently installed capacities of distributed generation facilities have no relevant effect upon the high voltage grid in Austria. Therefore the simulations in this document focus on the influences of high penetrations of distributed generators onto the medium and low voltage distribution grid. The main network structures for these two voltage levels are explained in detail in the following sections.

2.5.1. Distribution Grid Structures - Medium Voltage Level

Medium voltage distribution grids are used to supply energy from the high voltage transmission grid to their underlaid low voltage grids. In open-air switchyards or indoor gas insulated substations the high voltage is stepped down mostly by regulating transformers. Power rating for these substations lies usually between 20 MVA and 50 MVA [9]. Industrial loads can be directly connected to the medium voltage grid. Common voltage levels reach from 10 kV to 30 kV depending on the load density, reasons of insulation and historical causes. In urban areas a cable network is usually used to supply the low voltage substations. Due to the low transmission distance, 10 kV is a wide spread nominal voltage for urban areas. In areas with increasing line lengths, higher voltage levels help to reduce line losses. Medium voltage overhead lines might be used instead of cable lines to reduce costs and increase serviceability.

In general medium voltage grids are operated as ring networks with open joints. In case of a fault at one network section, the joint can be closed to cover the supply of the affected substations. The faulty part is disconnected at the adjacent substations. In order to increase service security the grid can be supplied by several feeders. Another way to create a higher intrinsic safety is the implementation of interconnecting lines between different medium voltage substations, connected with open joints in normal operation. To maintain a moderate short-circuit power, the degree of meshing and the number of feeders for the medium voltage grid is kept low [9].

2.5.2. Distribution Grid Structures - Low Voltage Level

In general there are 4 possible structures for low voltage distribution networks. In all these structures the distribution grid is fed through substations with distribution transformers from the medium voltage distribution grid. Common values for the rated power of the transformers average between 250 kVA and 800 kVA. In a similar manner the medium voltage distribution grid is supplied by the high voltage transmission grid. The transformation between the high voltage grid and the medium voltage grid is done by regulating transformers with a typical rating power between 20 MVA and 50 MVA. One factor for the application of a structure in a supply area is the existing load density.

For Areas with low load densities like rural areas, radial network structures are preferred. Several distributed network stubs are fed by one single substation. One example for this structure can be seen in figure 2.5.1. The disadvantage in this configuration can easily be seen in the service security. A single failure within the substation can lead to a blackout for the whole region, supplied by the grid.

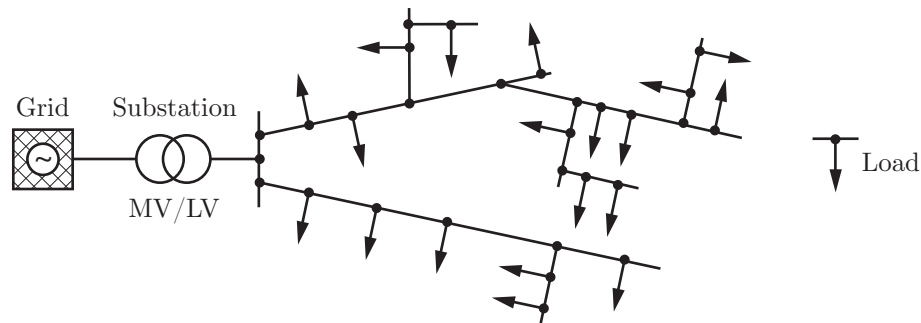


Figure 2.5.1.: Radial network structure of a low voltage distribution grid [9].

Another problem with branched distribution lines is the voltage drop along the lines because of the low cross sections and long distribution distances, which are common in rural areas. Especially when distributed generators are connected, this could lead to voltage rise problems at distant coupling points. A possible solution for the voltage rise issues could be a grid reinforcement of the affected area.

While overhead lines prevail cable lines in rural areas, cable lines more and more replaced them if the load density increases and transmission distances decrease. Therefore the network structures aren't extensively branched anymore. It is possible to plan connection lines between the single branches in order to increase service security.

An example for an open ring network structure, common in suburban areas, can be seen in figure 2.5.2. This could be represented by two lines along both sides of a street, which can be connected at the end. In case of an fault on one line, the affected line elements or households are disconnected at the building connection columns or cable distribution cabinets. Afterwards the open joint between the branches can be closed, which reassures the energy supply for the other households on the branch, which connection points lie after the isolated part. This results in a higher security of supply [9]. However the loading of the equipment, which takes over the supply, is increased. This possible higher load must be considered in the planning phase and during normal system operation.

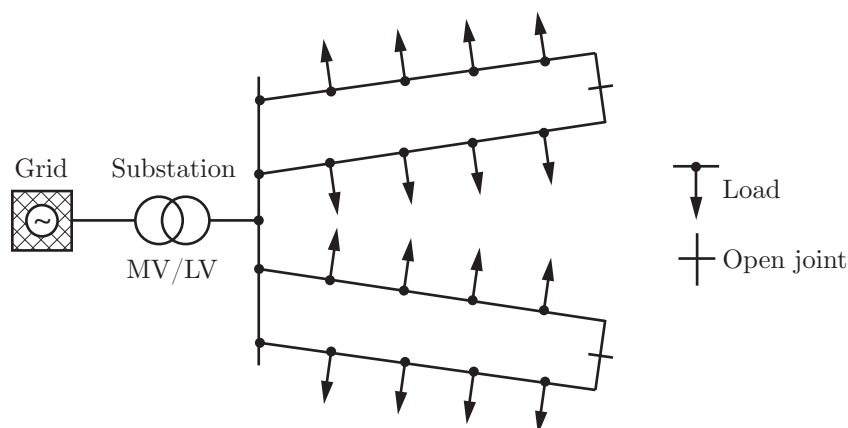


Figure 2.5.2.: Ring network structure of a low voltage distribution grid [9].

With a higher degree of intermeshing between the branches, the security of supply can be increased. However, any form of intermeshing within the distribution grid results in a complex protection concept. The branched ring network in figure 2.5.3 results in a high service security without creating a meshed network structure. In the event of several simultaneous faults, open joints at different locations can be closed to ensure the energy supply in the network.

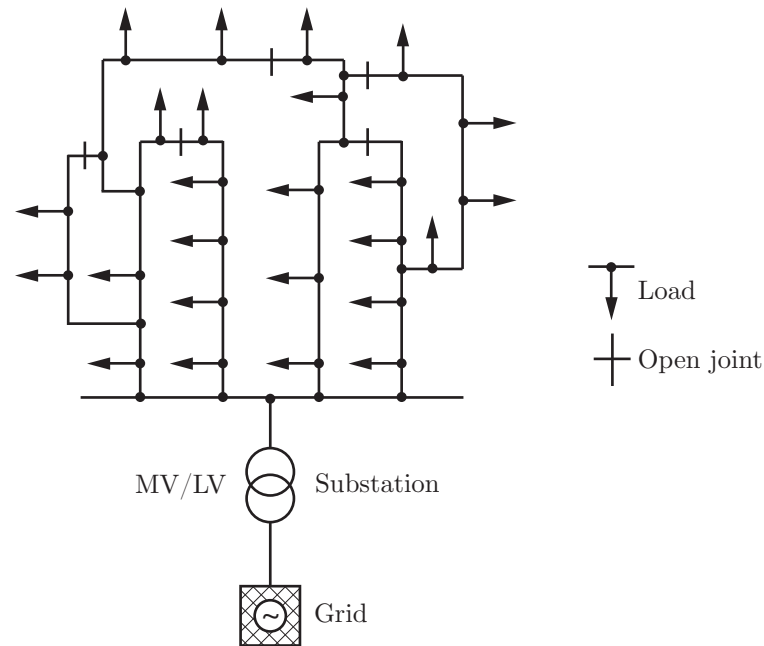


Figure 2.5.3.: Branched ring network structure of a low voltage distribution grid [9].

Figure 2.5.4 shows the principle structure of a meshed network with several infeeds and intermeshed network branches. This network structure represents the highest possible security of supply. It requires a high load density (>5 MVA/km² [9]), and a special protection concept.

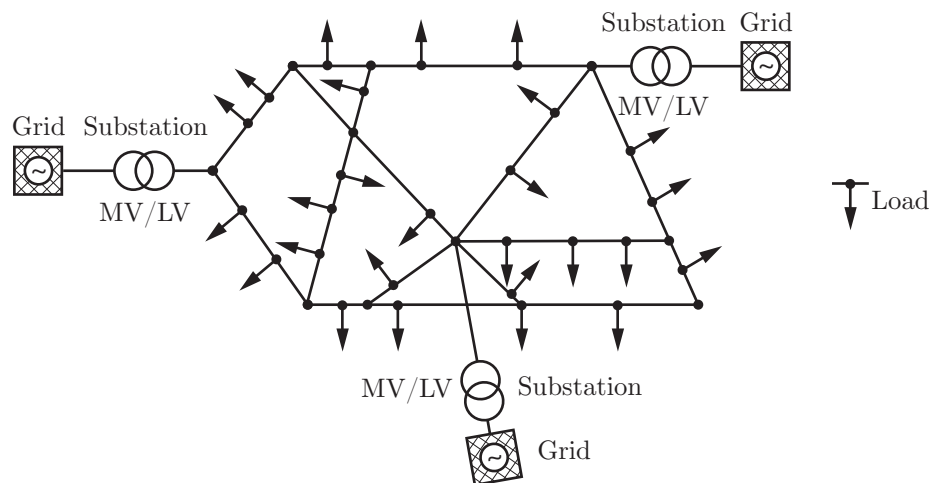


Figure 2.5.4.: Meshed network structure of a low voltage distribution grid [9].

2.6. Influence of Distributed Generator Infeeds on Distribution Systems

The following section should explain the principle steps to determine the influence of distributed generation onto the operation voltage at the point of common coupling in a radial network configuration. Figure 2.6.1 shows the basic vector diagram for the transport of electrical energy along lines with inductive characteristics.

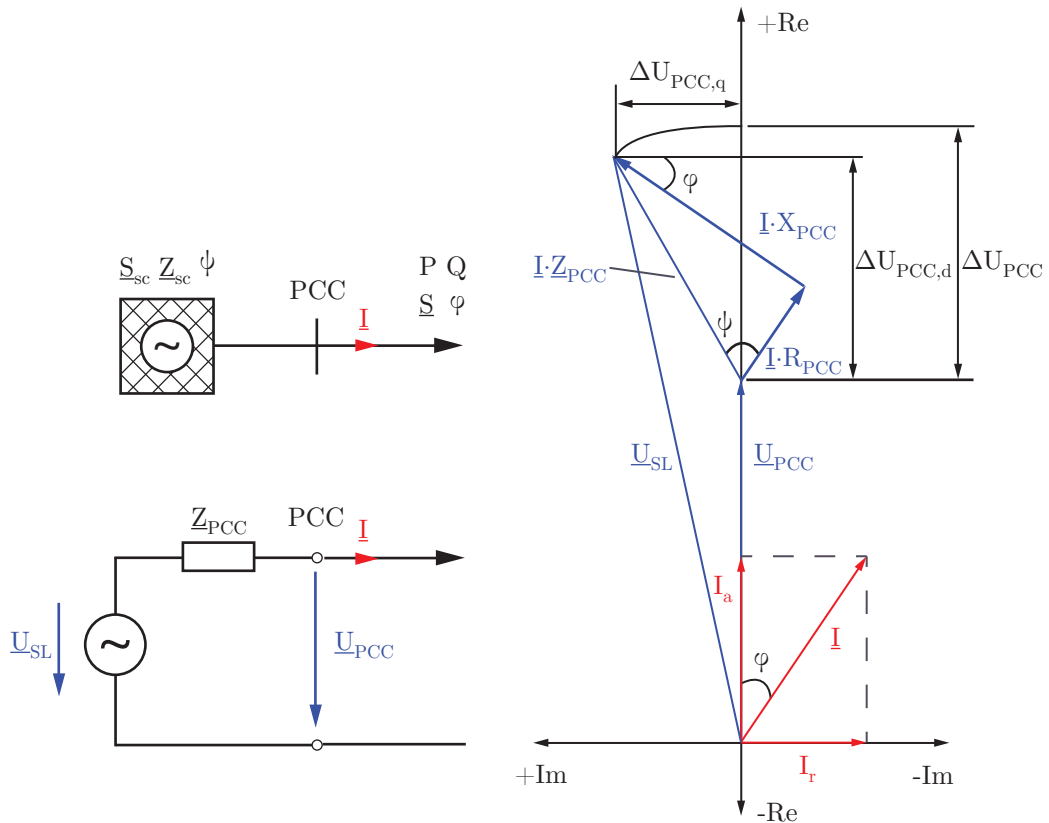


Figure 2.6.1.: Vector diagram, illustrating the voltage change at a given network node [11].

PCC	Point of common coupling
\underline{S}	Connected load at the PCC (active power P, reactive power Q)
φ	Power factor at the PCC
\underline{Z}_{sc}	Network short-circuit impedance
\underline{S}_{sc}	Network short-circuit apparent power
ψ	Network impedance angle
ψ_{PCC}	Network impedance angle at the PCC
\underline{Z}_{PCC}	Network impedance at the PCC ($\underline{Z}_{PCC} = R_{PCC} + jX_{PCC}$)
\underline{I}	Load current (I_a - active part, I_r - reactive part)
\underline{U}_{SL}	Voltage at the slack node
\underline{U}_{PCC}	Voltage at the PCC
ΔU_{PCC}	Difference in voltage at the PCC (direct component $\Delta U_{PCC,d}$, quadrature component $\Delta U_{PCC,q}$)

The network short-circuit impedance at the point of common coupling (PCC) \underline{Z}_{PCC} is equal to:

$$\underline{Z}_{PCC} = R_{PCC} + jX_{PCC} = Z \cdot e^{j\psi_{PCC}} \quad (2.6.1)$$

The connected load at the PCC results in:

$$\underline{S} = P + jQ = S \cdot e^{j\varphi} \quad (2.6.2)$$

The voltage drop along the line ΔU_{PCC} results out of the difference between the voltage at the PCC \underline{U}_{PCC} and the slack node voltage \underline{U}_{SL} :

$$\Delta U_{PCC} = \underline{U}_{PCC} - \underline{U}_{SL} \quad (2.6.3)$$

$$\underline{U}_{SL} = \underline{U}_{PCC} - \Delta U_{PCC} \approx \underline{U}_{PCC} + \Delta U_{PCC,d} \quad (2.6.4)$$

The mesh equation for the PCC results in:

$$\underline{U}_{SL} = \underline{U}_{PCC} + \underline{I} \cdot \underline{Z}_{PCC} = \underline{U}_{PCC} + \underline{I} \cdot R_{PCC} + \underline{I} \cdot jX_{PCC} \quad (2.6.5)$$

The direct voltage drop along the line $\Delta U_{PCC,d}$ is equal to:

$$\begin{aligned} \Delta U_{PCC,d} &= \underline{I} \cdot R_{PCC} \cdot \cos\varphi + \underline{I} \cdot X_{PCC} \cdot \sin\varphi = I_a \cdot R_{PCC} + I_r \cdot X_{PCC} \\ &= \frac{P}{\underline{U}_{PCC}} \cdot R_{PCC} + \frac{Q}{\underline{U}_{PCC}} \cdot X_{PCC} \end{aligned} \quad (2.6.6)$$

The same can be applied for the quadrature voltage drop $\Delta U_{PCC,q}$:

$$\Delta U_{PCC,q} = -\underline{I} \cdot R_{PCC} \cdot \sin\varphi + \underline{I} \cdot X_{PCC} \cdot \cos\varphi = -\frac{Q}{\underline{U}_{PCC}} \cdot R_{PCC} + \frac{P}{\underline{U}_{PCC}} \cdot X_{PCC} \quad (2.6.7)$$

Thus making the relative direct voltage drop based on the infeed voltage U_L :

$$\Delta u_{PCC,d} = \frac{\Delta U_{PCC,d}}{\underline{U}_{SL}} = \frac{P}{\underline{U}_{PCC} \cdot \underline{U}_{SL}} \cdot R_{PCC} + \frac{Q}{\underline{U}_{PCC} \cdot \underline{U}_{SL}} \cdot X_{PCC} \quad (2.6.8)$$

For all these calculations it is assumed that there is no initial load at the PCC, which makes P and Q also the relative change in active and reactive power ΔP and ΔQ at this point. If this is not the case, the relative values differ and also the relative change in the load current ΔI is needed for the evaluation of the relative change in the voltage:

$$d_d = -\frac{U_d}{\underline{U}_{SL}} = -\left(\frac{\Delta P}{\underline{U}_{PCC} \cdot \underline{U}_{SL}} \cdot R_{PCC} + \frac{\Delta Q}{\underline{U}_{PCC} \cdot \underline{U}_{SL}} \cdot X_{PCC} \right) \quad (2.6.9)$$

With equation 2.6.4 the relative voltage drop d equals in:

$$d = -\frac{\Delta U_{PCC}}{\underline{U}_{SL}} \approx -\left(\frac{\Delta P}{\underline{U}_{SL}^2} \cdot R_{PCC} + \frac{\Delta Q}{\underline{U}_{SL}^2} \cdot X_{PCC}\right) \quad (2.6.10)$$

Another way to estimate the voltage change at the node can be seen in [11]. The short-circuit impedance of the network at the PCC can also be derived from the short-circuit apparent power:

$$\underline{Z}_{PCC} = \frac{U_{PCC}^2}{\underline{S}_{PCC}} \quad (2.6.11)$$

The consumer load, given as apparent power, can be divided into active and reactive power P and Q :

$$\Delta P = S \cdot \cos\varphi \quad (2.6.12)$$

$$\Delta Q = S \cdot \sin\varphi \quad (2.6.13)$$

With this, the resulting change in voltage can be calculated as followed:

$$\Delta u_{PCC,d} = \frac{P}{\underline{S}_{PCC}} \cdot \cos\psi + \frac{Q}{\underline{S}_{PCC}} \cdot \sin\psi = \frac{S}{\underline{S}_{PCC}} \cdot \cos(\psi - \varphi) \quad (2.6.14)$$

$$d \approx -\Delta u_{PCC,d} = -\frac{S}{\underline{S}_{PCC}} \cdot \cos(\psi - \varphi) \quad (2.6.15)$$

2.6.1. Voltage Rises due to Distributed Generation

In every node of a network, the voltage rise is a result of the active and reactive power of consumer loads and generators. The second influencing factor is the network short-circuit impedance and the network short-circuit apparent power at any considered network node. For an evaluation, the voltage condition without the particular generator and the voltage condition after the connection of the generator to the grid is important. The influence of several distributed generators within the same network can be calculated with the principle of superposition after Helmholtz.

Equation 2.6.16 and 2.6.17 represent an approximation of the voltage rise at the point of common coupling (PCC) due to change in the connected power of one or more consumer loads or generators [7].

$$\Delta u_{PCC} = \frac{S_{DGmax}}{S_{sc}} \cdot \cos(\Psi_{PCC} - \varphi_{DG}) \quad (2.6.16)$$

$$\Delta u_{PCC} = \frac{\Delta P_{PCC} \cdot R_{PCC} + \Delta Q_{PCC} \cdot X_{PCC}}{U_{PCC}^2} \quad (2.6.17)$$

Δu_{PCC}	Relative change in voltage at the PCC
S_{sc}	Network short-circuit apparent power at the PCC
S_{DGmax}	Maximum output power of the distributed generator at the PCC

Ψ_{PCC}	Network impedance angle at the PCC
φ_{DG}	Power factor of the distributed generator infeed
ΔP_{PCC}	Change in active power at the PCC
ΔQ_{PCC}	Change in reactive power at the PCC
R_{PCC}	Network resistance at the PCC
X_{PCC}	Network reactance at the PCC
U_{PCC}	Phase voltage at the PCC

Equation 2.6.17 is separated into the influence of active and reactive feed-in power and can therefore be used to examine the effects of reactive power provision onto the voltage rise.

One simplification for this approach is the disregard of the medium voltage lines. To simplify matters, the distributed generators are supposed to be connected directly to the transformers main distribution board. No resistances and reactances between the transformer busbar and the generators have to be considered.

$$\Delta u_T = \frac{S_{DGmax}}{S_{scT}} \cdot \cos(\Psi_T - \varphi_{DG}) \quad (2.6.18)$$

$$\Delta u_T = \frac{\Delta P_{PCC} \cdot R_T + \Delta Q_{PCC} \cdot X_T}{U_T^2} \quad (2.6.19)$$

Δu_T	Relative change in voltage at the transformer (secondary)
S_{scT}	Network short-circuit apparent power at the transformer (secondary)
S_{DGmax}	Maximum output power of the distributed generator at the PCC
Ψ_T	Network impedance angle at the transformer (secondary)
φ_{DG}	Power factor of the distributed generator infeed
ΔP_{PCC}	Change in active power at the PCC
ΔQ_{PCC}	Change in reactive power at the PCC
R_T	Network resistance at the transformer (secondary)
X_T	Network reactance at the transformer (secondary)
U_T	Phase voltage at the transformer (secondary)

The equation 2.6.19 furthermore leads to the voltage rise due to the sum of all distributed generators within the supplied network of a transformer at its secondary busbar:

$$\Delta P_{sum} = \sum_1^K \Delta P_{PCC,k} \quad \text{with } k = 1 \dots K \quad (2.6.20)$$

$$\Delta Q_{sum} = \sum_1^K \Delta Q_{PCC,k} \quad \text{with } k = 1 \dots K \quad (2.6.21)$$

$$\Delta u_T = \frac{\Delta P_{sum} \cdot R_T + \Delta Q_{sum} \cdot X_T}{U_T^2} \quad (2.6.22)$$

ΔP_{sum}	Sum of active power variation in the network
ΔQ_{sum}	Sum of reactive power variation in the network
$\Delta P_{\text{PCC},k}$	Change in active power at the PCC k
$\Delta Q_{\text{PCC},k}$	Change in reactive power at the PCC k
K	Sum of generators

If different kinds of distributed generating facilities are present, the corresponding simultaneity factor should be taken account of. The resistive part of the network impedance at the transformer busbar is insignificant low. Due to the prevailing network reactance, the reactive power has a higher effect for the voltage change than the active power [7].

Equations 2.6.23 and 2.6.24 combine the preceding calculations and offer a simplified way to estimate the voltage rise at any given connection point within an network, due to the sum of all connected generators.

$$\Delta u_{PCC,k} = \sum_{i=1}^k \frac{S_{DGmax,i} \cdot \cos(\Psi_{PCC,i} - \varphi_{DG,i})}{S_{sc,i}} + \sum_{i>k}^n \frac{S_{DGmax,k} \cdot \cos(\Psi_{PCC,k} - \varphi_{DG,i})}{S_{sc,k}} \quad (2.6.23)$$

$$\Delta u_{PCC,k} = \sum_{i=1}^k \frac{\Delta P_{PCC,i} \cdot R_{PCC,i} + \Delta Q_{PCC,i} \cdot X_{PCC,i}}{U_{PCC,i}^2} + \sum_{i>k}^n \frac{\Delta P_{PCC,i} \cdot R_{PCC,k} + \Delta Q_{PCC,i} \cdot X_{PCC,k}}{U_{PCC,k}^2} \quad (2.6.24)$$

$\Delta u_{\text{PCC},k}$	Relative change in voltage at the PCC k
$S_{sc,i}$	Network short-circuit apparent power at the PCC i
$S_{DGmax,i}$	Maximum output power of the distributed generator at the PCC i
$\Psi_{\text{PCC},i}$	Network impedance angle at the PCC i
$\varphi_{DG,i}$	Power factor of the distributed generator infeed at the PCC i
$\Delta P_{\text{PCC},i}$	Change in active power at the PCC i
$\Delta Q_{\text{PCC},i}$	Change in reactive power at the PCC i
$R_{\text{PCC},i}$	Network resistance at the PCC i
$X_{\text{PCC},i}$	Network reactance at the PCC i
$U_{\text{PCC},i}$	Phase voltage at the PCC i

Figure 2.6.2 depicts a basic radial network stub with distributed generator infeeds. From special interest is the effect of the different generators, connected at the nodes $i=1\dots n$, upon the voltage at the node k.

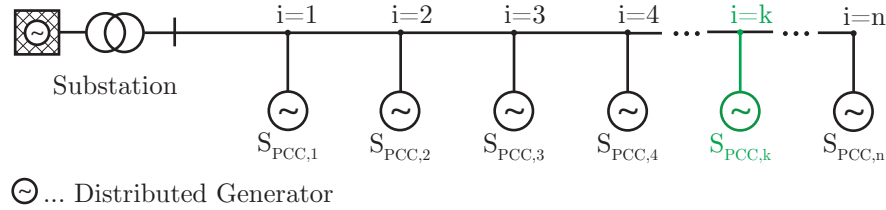


Figure 2.6.2.: Low voltage stub with distributed loads.

The index i starts at the transformer busbar with the number 1 and increases into the direction of distant coupling points. For the evaluation of complex network topologies [7] suggests the use of a power flow simulation tool.

2.6.2. Approximation of the Voltage Rise

One simplification for low voltage grids is the assumption of a evenly distributed load. This simplification leads to more accurate results if the number of considered loads is increased. For residential consumer loads the reactive power can be neglected due to the lack of highly inductive loads. With a remaining transmission of mere active power along the lines, also the line reactance can be disregarded.

With these assumptions ($Q = 0$, $X_{sc} = 0$), the equation 2.6.10 can be written as:

$$d = -R_{PCC} \cdot \frac{P}{U_{SL}^2} \quad (2.6.25)$$

If only the resistance of the line is considered, the short circuit resistance at the coupling point can be derived from the specific electric conductance of the used line material and the cross section:

$$R_{PCC} = \frac{L}{\gamma \cdot A} \quad (2.6.26)$$

In equation 2.6.26, L represents the length between the infeed point and the coupling point. In an equally distributed network, the length of one line element L can be multiplied with the number of the considered node to get the respective short circuit resistance. Figure 2.6.3 shows the distributed load structure of a single low voltage branch with equal distribution lengths.

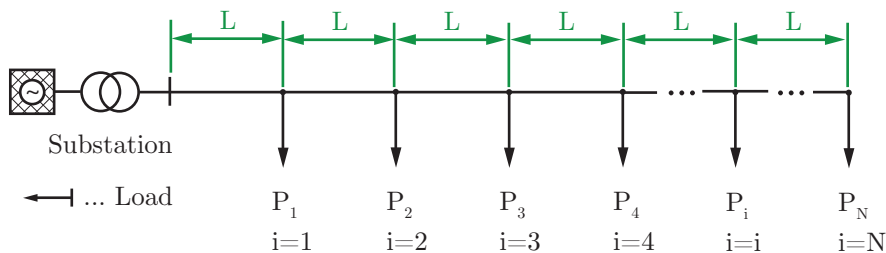


Figure 2.6.3.: Low voltage stub with distributed loads [11].

- L Average line length
 γ Specific conductance
A Cross section of conductor
 U_N Nominal voltage
 P_N Node power
n Number of equal nodes with the distance L
i, k Node number

This calculation method can be used to examine the effects of power infeeds onto the network. With the use of the principle of superposition after Helmholtz, the influence of single distributed generators, or the influence of all installed generators together, can be estimated. This implies equally distributed active feed in powers of same size. If the relative change in voltage is related to the supply voltage at the feeder U_N it can be written in % of the nominal voltage [11]:

$$d_{i(i)} = -\frac{P_N}{U_N^2} \cdot \frac{i \cdot L}{\gamma \cdot A} \cdot 100 \quad (2.6.27)$$

The resistance at the considered node can be simplified as element resistance of one line element $R_L = \frac{L}{\gamma \cdot A}$ multiplied with the node number i. With the help of equation 2.6.27, the influence at any specific node within the simplified network can be calculated:

$$d_{i(i)} = -\frac{P_N}{U_N^2} \cdot (R_L \cdot i) \cdot 100 \quad (\text{Change in voltage at node i due to node i})$$

$$d_{i(k)} = -\frac{P_N}{U_N^2} \cdot (R_L \cdot k) \cdot 100 \quad (\text{Change in voltage at node i due to node k for } i \geq k)$$

$$d_{i(k)} = -\frac{P_N}{U_N^2} \cdot (R_L \cdot i) \cdot 100 \quad (\text{Change in voltage at node i due to node k for } i < k)$$

$$d_i = -\frac{P_N}{U_N^2} \cdot (R_L \cdot i) \cdot \left[n - \frac{i}{2} + \frac{1}{2} \right] \cdot 100 \quad (\text{Change in voltage at node i due to sum of all nodes})$$

$$d_N = -\frac{P_N}{U_N^2} \cdot \frac{1}{2} \cdot R_L \cdot [n^2 + n] \cdot 100 \quad (\text{Change in voltage at remotest node due to sum of all nodes})$$

These equations follow the considerations in [11]. The maximum achievable voltage rise, occurs at the remotest network node as a result of the feed-in power of all distributed generators $d_{max} = d_N$.

2.7. Applied Grid Codes and Standards

As mentioned in section 2.6, every load or generator creates a change in the phase voltage when connected to the grid. This change in voltage does not only effect the corresponding coupling point but also all the other coupling points within the network. For the purpose of this document, the voltage rise resulting from distributed generation is the most important factor for valuation. However for the operation of grid connected generators, more factors have to be considered [7]:

- Voltage rise
- Switching-borne changes in voltage
- Flicker
- Harmonics
- Commutation notches
- Unbalance
- Reactive power compensation
- Influences on devices for the signal transmission through electric power systems

The constraints for every single point have to be met by the distributed generator. Limiting thresholds and maximum values differ in various countries. The constraints for the connection of distributed generators at the medium and low voltage level for Austria are given in [7]. The evaluation of the voltage rise is discussed in section 2.6.1.

In addition to the special guidelines for grid connected distributed generators, also the normal guidelines for the voltage characteristics of electricity supplied by public distribution systems, stated in the European standard EN 50160 [5] have to be satisfied.

2.7.1. Power Frequency

The frequency of the operating voltage for the European integrated grid is 50 Hz (ENTSO-E network code). During normal operating conditions the 10 s average values of the base frequency should stay within the following range [5]:

Synchronous grids:	50 Hz \pm 1%	(i.e. 49,5 Hz to 50,5 Hz) during 99,5% of one year
	50 Hz \pm 4% / \pm 6%	(i.e. 47,0 Hz to 52,0 Hz) during 100,0% of all time
Asynchronous grids:	50 Hz \pm 2%	(i.e. 49,0 Hz to 51,0 Hz) during 95,0% of one year
	50 Hz \pm 15%	(i.e. 42,5 Hz to 57,5 Hz) during 100,0% of all time

2.7.2. Voltage Magnitude Variations

From special concern for the operation of distributed generators and to estimate valid load states for the following simulations are the constraints for voltage magnitude variations [5]:

Medium voltage grid:	$\Delta u = \pm 10\%$ for 95% of 10 min RMS values of a week
Low voltage grid:	$\Delta u = \pm 10\%$ for 95% of 10 min RMS values of a week

2.7.3. Rapid Voltage Changes

Rapid voltage changes are mainly caused by load changes and switching operations. As a threshold for these changes [5] states:

Medium voltage grid:	$\Delta u = \pm 4\%$ under normal operating conditions and $\pm 6\%$ infrequently
Low voltage grid:	$\Delta u = \pm 5\%$ under normal operating conditions and $\pm 10\%$ infrequently

2.7.4. Supply Voltage Unbalance

The 10 min average effective component of the negative sequence for the operating voltage must not exceed 2 % during a measuring interval of 1 week and normal operating conditions. The corresponding effective positive sequence component must stay within a threshold of 95 %. A voltage unbalance up to 3 % at the coupling point may occur in areas with single-phase and two-phase consumer facilities [5].

2.7.5. Voltage Rise Constraints for Distributed Generators

Following the constraints in [7], the resulting voltage rise due to the sum off all distributed generators within the particular network must not exceed the following thresholds:

Medium voltage grid:	$\Delta u = +2\%$
Low voltage grid:	$\Delta u = +3\%$

2.7.6. Reactive Power Management

The Austrian grid code does not include any guidelines for the reactive power output of distributed generators at the medium and low voltage grid. Therefore the power factor values from the German standard VDE-AR-N 4105 [13], which deals with the technical requirements for distributed generators in parallel operation with the low voltage distribution grid, are stated here. The German standard requires distributed generators to participate in the static voltage maintenance.

1) Generator apparent power:	$S_{DG} \leq 3,68 \text{ kVA}$	$\cos\varphi = 0,95(\text{lag.}) - 0,95(\text{lead.})$
2) Generator apparent power:	$3,68 \text{ kVA} < S_{DG} \leq 13,80 \text{ kVA}$	$\cos\varphi = 0,95(\text{lag.}) - 0,95(\text{lead.})$
3) Generator apparent power:	$S_{DG} > 13,80 \text{ kVA}$	$\cos\varphi = 0,90(\text{lag.}) - 0,90(\text{lead.})$

Generators with rated output powers below 3,68 kVA may also be operated with a power factor different to 1,00 (in the range of 0,95(lagging) - 0,95(leading)). However the network operator is not allowed to demand the stated values. Generator rated powers in the ranges from 2) and 3) may require the generator to follow a special characteristics for the power factor in relation to the output power. This characteristic may be defined by the network operator, regarding the existing grid circumstances.

2.8. Measures to Decrease the Voltage Rise

The resistive character of low voltage power supply lines results in serious voltage drops due to the current flow caused by the connected consumer loads. As mentioned in chapter 2.6, distributed generators cause a voltage rise because of the same effect. Whereas in the first case, the power transmission causes a voltage drop for the connected consumers, in the second case, the local production of electric energy exceeds the local consumption, thus reversing the power flow, resulting in a voltage rise at affected coupling points. Some measures to decrease the rise in the phase voltage are discussed in the following section. Their effects onto possible feed-in capacities of the developed model grids are examined in the performed simulations.

2.8.1. Line Impedance

Electric power lines for the medium voltage level consist of a resistive part resulting in the normal line losses, and a reactive part, caused not only by the inductive character of power lines, but also by line capacities. Especially cable lines show an increased capacity reactance, which in theory lead to voltage rises at open line ends. However, with real cable parameters and the observed line lengths, this effect is insignificant and can be neglected. In the low voltage distribution level however, the resistive part of the line impedance dominates. For simple calculations it is therefore possible to neglect the reactive part completely.

The developed model grids in section 3 show increased line lengths in the low voltage sections compared to the lengths of the developed medium voltage section. Together with the extended grid structure of the low voltage distribution system, this results in a mostly resistive character of the complete grid. This behavior can also be observed in real distribution grids.

Thus, the line resistance is the most important factor when considering distributed generation in a low voltage power system. Resulting effects onto the voltage level can be explained with the calculations in section 2.6, which are based on the behavior of real power lines with resistive and reactive components. The voltage rise due to distributed generation is therefore the main limiting factor for the feed-in capacity considering grids with high impedance values.

The dominating resistance depends on three factors:

- Line length
- Line cross section
- Specific resistance of the used conductor material

The length can be represented by the line element length L . The cross section is mostly referred to as A . For the resistance of the conductor material two descriptions are possible. It can be given as the specific resistance ρ , or the specific conductance γ with $\gamma = \frac{1}{\rho}$. The specific conductance is $\gamma = 0,0178 \frac{\text{S}}{\text{m}}$ for copper and $\gamma = 0,0287 \frac{\text{S}}{\text{m}}$ for aluminium (54 Cu, 45 Ni, 1Mn) at a conductor temperature of 20°C [10].

With these three factors the resistance of the line element R_L can be calculated:

$$R_L = \frac{L}{\gamma \cdot A} \quad (2.8.1)$$

At the same time, these three factors can be changed to reduce the resulting voltage rise caused by distributed generators. However, the line lengths are predefined by the allocation of the supplied consumers and can only be changed on a very small scale with improved line routing. The replacement of existing power lines is the only possible way to effectively decrease the line resistance. Due to cost factors the change from aluminium conductors to copper conductors is unusual. The only remaining factor is therefore the use of higher cross sections, achievable by a complete exchange of existing lines or by parallel laying of new lines. Also the transition from overhead lines to cable lines is common. While the resistive part nearly stays the same if cross section and conductor material are kept similar, the inductive reactance part decreases significantly with the use of cable lines instead of overhead lines.

Another possibility to influence the network impedances at the observed coupling points, is the meshing of the network structure.

2.8.2. Decentralized Reactive Power Management

The new proposal for the German grid code requires the participation of grid connected distributed generators in the reactive power management. Therefore, the distributed generators have to be able of four-quadrant operation. Figure 2.8.1 shows the possible states of the generators or consumers apparent power S . The phase angle between active power P and reactive power Q , also known as power factor, is represented by $\cos\varphi$. In this special case consumed power is defined to be positive and produced power is by definition negative. The same is applied for the reactive power.

Distributed generators, coupled to the grid with inverters are capable of providing reactive power in the same way, they produce active power. The maximum output current limited by the power electronics determines the possible output apparent power. With a power factor of 1, the maximum active output power is reached. Every deviation in the power factor of 1 however, reduces the possible active power output in favor of reactive power provision. Therefore a reactive power provision means a loss of active power output for the operator of the inverter-based generator.

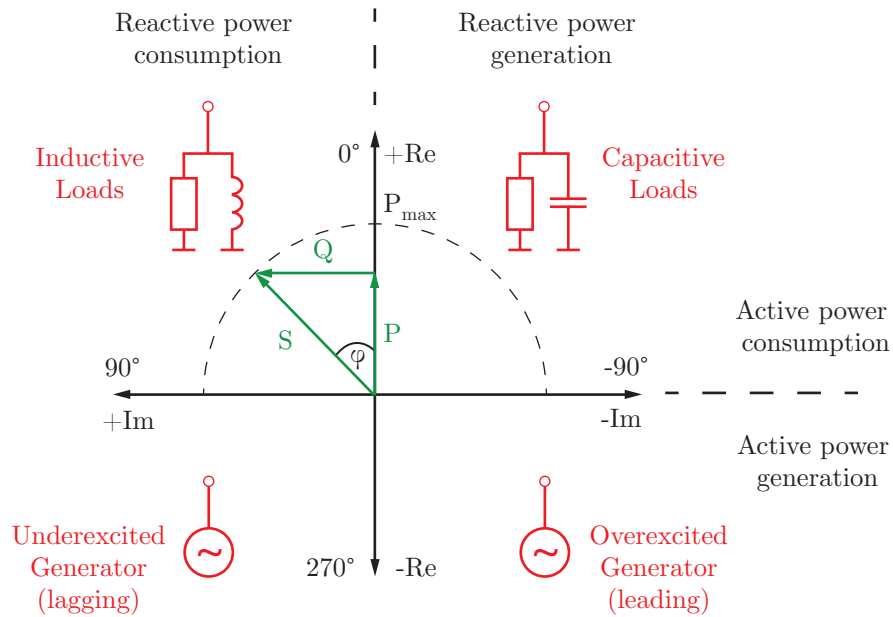


Figure 2.8.1.: Exemplary vector diagram illustrating the four-quadrant operation.

Figure 2.8.2 shows the influence of a lagging power factor onto the phase voltage at the corresponding point of common coupling at which the distributed generator is connected to the grid. The lagging power factor of the generator means, it supplies active power but at the same time also draws inductive reactive power from the grid. Due to the inductive characteristic of the grid, this results in a decreasing voltage drop along the line, thus causing a lower voltage rise at the PCC, compared to a distributed generation with a power factor of 1.

The vector diagram in figure 2.8.2.a represents the infeed of active power at the point of common coupling. Due to the inductive character of the power line between this point and the slack grid, a phase shift Ψ_{PCC} can be observed between the generators voltage U_{PCC} and the slack node voltage \underline{U}_{SL} . This phase shift is caused by the network impedance at the PCC \underline{Z}_{PCC} , and includes therefore also the network impedance angle Ψ .

For the vector diagram in figure 2.8.2.b a power factor of 0.95 (lagging) was chosen for the output power of the generator. The changed phase shift for the generators output current \underline{I} , now composed of an active part I_a and a reactive part I_r , together with the inductive line characteristics, leads to a decreased magnitude for the voltage U_{PCC} . This is a consequence of the voltage vector addition, depicted in figure 2.8.2.b.

However, the decreasing voltage at the point of common coupling results in a slight increase of the generators output current. To maintain the same power output, when the voltage level drops, the generator has to raise the output current. The higher current flow across the power lines, leads to increased voltage drops, which partly counteract the previous mentioned effects.

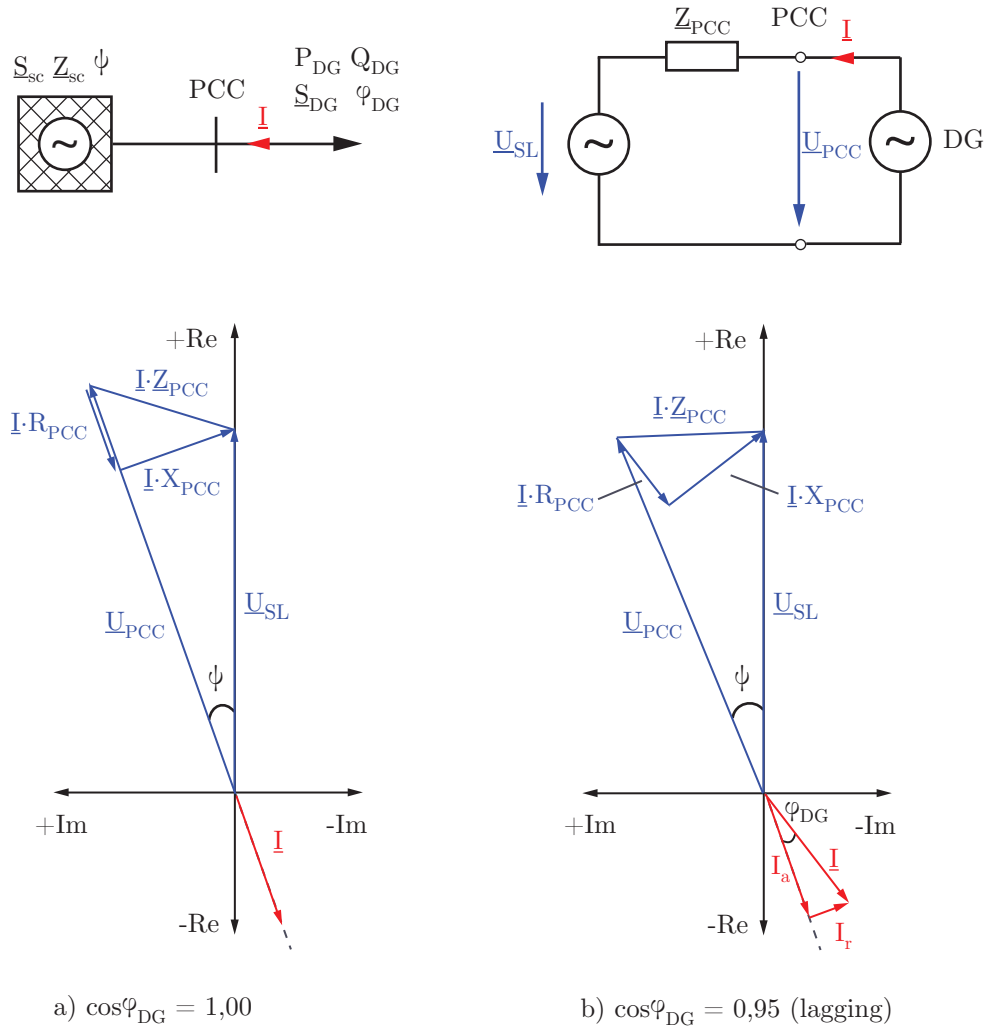


Figure 2.8.2.: Exemplary vector diagram illustrating the influence of a lagging power factor.

PCC	Point of common coupling
\underline{S}_{sc}	Network short-circuit apparent power at slack node
\underline{S}_{DG}	Output apparent power of the distributed generator at the PCC
P_{DG}	Output active power of the distributed generator at the PCC
Q_{DG}	Output reactive power of the distributed generator at the PCC
Z_{sc}	Network short-circuit impedance at slack node
Z_{PCC}	Network impedance at PCC ($Z_{PCC} = R_{PCC} + jX_{PCC}$)
Ψ	Network impedance angle at slack node
Ψ_{PCC}	Network impedance angle at the PCC
φ_{DG}	Power factor of the distributed generator infeed
\underline{U}_{PCC}	Phase voltage at the PCC
\underline{U}_{SL}	Phase voltage at the slack node

→ $\cos\varphi$ leading $\hat{=}$ overexcited operation of synchronous generator

→ $\cos\varphi$ lagging $\hat{=}$ underexcited operation of synchronous generator

In conventional low voltage distribution grids, reactive power is not produced locally, and must therefore be drawn from the medium and high voltage grid. Thus the participation in the reactive power management by distributed generators causes additional apparent power transmissions across the affected power lines and therefore additional losses.

On the other hand it offers an effective and cheap possibility to decrease the phase voltage at the connection points of distributed generators.

2.8.3. Centralized Reactive Power Management

Power factor correction is often applied in electrical power grids with high inductive loads like in industrial grids with increased numbers of electric motors. Due to the use of special capacitor based compensation systems, the reactive power exchange in the particular grids can be reduced and minimized.

However, the reactive power compensation unit introduced in this document follows a different approach. The principle function is based on the decentralized reactive power management explained in section 2.8.2. Instead of capacitor based compensation systems, an inductive, coil based compensation unit is installed at any desired node within a medium or low voltage grid.

A lagging power factor represents the consumption of inductive reactive power by the generator. The resulting change in the output currents phase angle, together with the line impedance characteristics decreases the voltage at the corresponding coupling point, as mentioned before.

The same effect can be achieved with the use of concentrated inductive loads. Figure 2.8.5 shows the possible arrangement of one compensation unit, represented by an inductive load, connected directly at the distribution transformers secondary busbar.

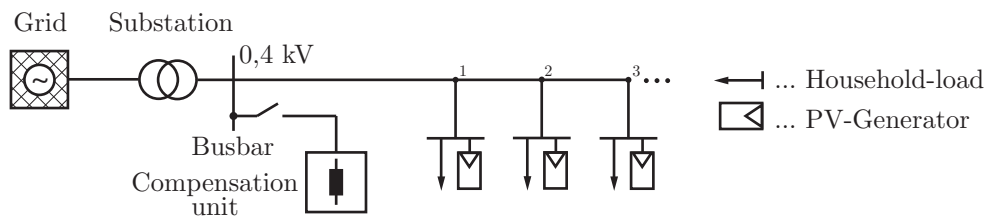


Figure 2.8.3.: Possible arrangement of a low voltage compensation system.

The resulting inductive load leads to a decrease of the voltage at the busbar, thus lowering the voltage levels at all coupling points in the supplied low voltage grid. In times of high voltage levels due to increased distributed generation, the compensation unit is connected to the busbar. For the simulations in this document, the following three choke coils with an ideal three phase reactive power consumption Q where exemplary chosen:

- 50 kvar
- 100 kvar
- 150 kvar

Resistive losses are neglected to simplify the simulations. The resulting ideal coils are represented by three phase reactive power consumers with the consumption values, stated above.

2.8.4. Regulating Distribution Transformers

Regulating transformers, which can change their transmission ratio without disrupting the supply, represent another possibility to actively influence the voltage level for the connected consumers. This so called on-load tap-changers are commonly used to supply medium voltage grids with energy from the high voltage level, while maintaining the appropriate operation voltage. Smaller versions of these transformers can be used for distribution purposes, in order to keep the operation voltage at the low voltage distribution level at a set value during different load, and infeed states. However, regulating distribution transformers with on-load tap-changers are currently not state of the art. The following assumptions for a working implementation of such a system are based on current research projects and testing facilities as seen in [8].

Two possible control concepts can be used to regulate the voltage at the secondary busbar of the transformer, and thus keeping the voltage in the grid within the allowed levels stated in the applied standards [8]:

Base control - The phase voltage at the secondary busbar is measured and compared with a set value. The difference value is used by the controller, influencing the tap-changer, according predefined control rules. The modified voltage level at the busbar causes the phase voltages at the corresponding coupling points to change their magnitudes depending on the control rule. A simple structure of a base control operated regulating distribution transformer is shown in figure 2.8.4. The simplicity of the controller components and the lack of data communication equipment can be seen as advantage of this system.

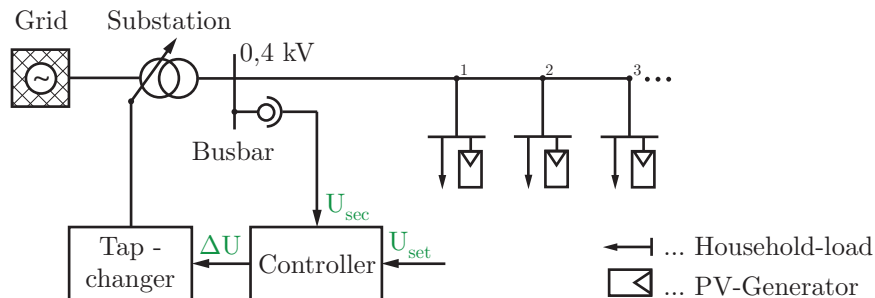


Figure 2.8.4.: Regulating distribution transformer with basic control concept [8].

However, the phase voltage magnitudes at the remote coupling points are unknown to the regulator, making it complicated to find appropriate control rules in order to achieve suitable voltage levels at the end of the supplied distribution lines (compensation).

Multivariable control - The phase voltage at a chosen remote point within the supplied network is measured and compared with a set value. Following a customized control rule, the controller changes the tap of the regulating transformer, according the voltage difference between busbar and remote connection point. Figure 2.8.5 shows an example for a regulating distribution transformer based on a multivariable control system.

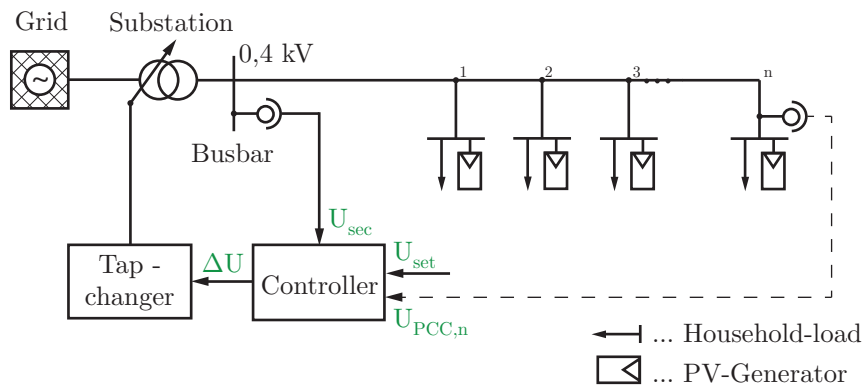


Figure 2.8.5.: Regulating distribution transformer with multivariable control concept [8].

Besides the busbar voltage at the low voltage side of the transformer, also the phase voltage at one or more remote coupling points is measured and used by the controller to adjust the tap-changer. Therefore additional communication equipment and a voltage measurement system is needed. The control rules for the transformer regulation are specifically adjusted for the supplied grid.

For the simulations in this document, a regulating distribution transformer with the following discrete on-load tap-changer configuration was used:

- Number of steps: 5 (step 0 ± 2)
- Step size Δu : 1,25 %
- Multivariable control

A higher number of steps can furthermore improve the behavior of the system voltage during times of intense distributed generation, and can also decrease the voltage drop in the grid, which is common in times of high consumer loads. Smaller step sizes can reduce the permanent voltage difference between the set value and the actual phase voltage, achievable with the current tap position. The power rating and the loading thresholds, following the allowed load currents, was left unchanged for the respective distribution transformer.

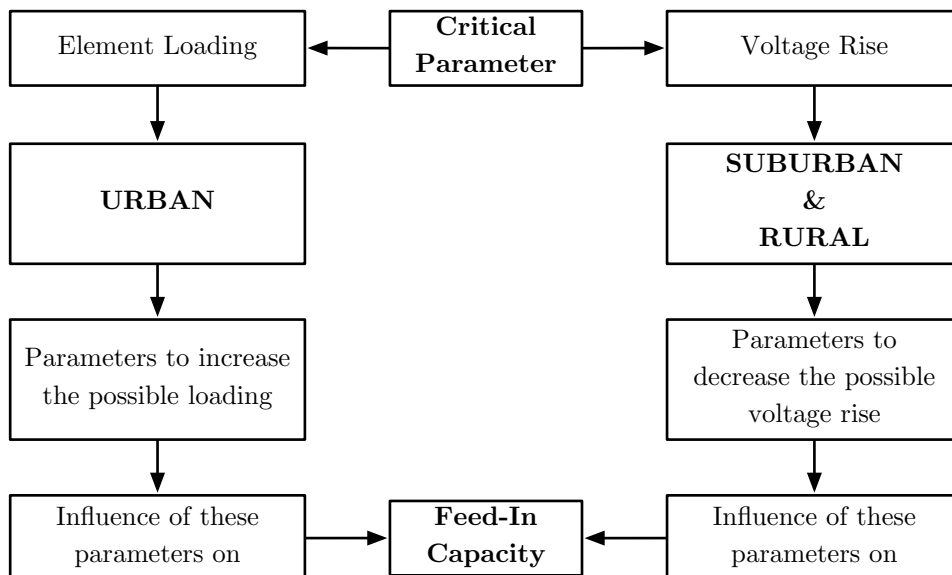
3. Model Grid Development

This chapter explains the basic steps in developing the model grids, used for the simulations. Section 2.7 includes the compulsory general requirements to connect decentralized generation facilities to the medium voltage, and low voltage grid. The given voltage thresholds and maximum equipment loadings which have to be kept to ensure service security, result in an upper limit for the nominal power of distributed generators within an analyzed medium or low voltage grid area. The objective of this thesis is to create several generic model grids in order to determine their characteristics and the consequences of clustered distributed generators onto the network operation.

Therefore three different model grid types were chosen:

1. **Urban model grid**
2. **Suburban model grid**
3. **Rural model grid**

These three typical network structures can be grouped, regarding their capabilities for analyzing the different restricting factors for the achievable feed-in power of decentralized generation units:



Due to the low line lengths, the use of cable lines and their comparatively high cross sections, electricity distribution networks with urban characteristics do not show extensive voltage problems. Thus making it

possible to achieve a high feed-in capacity. However, an increasing number of distributed generators with a high nominal output power can lead to equipment loadings near the given thresholds. Therefore the urban model grid was chosen to determine how distributed generators influence the equipment loading and which possible measures can decrease the loading.

Suburban grids on the other hand show a mixed usage of cable lines and overhead lines. Together with lower cross sections and longer line lengths this results in higher voltage drops along the lines. Therefore the influence of distributed generators on the supply voltage is significantly higher in suburban areas, making a suburban model grid perfect for analyzing voltage rise problems. With the help of this model grid, different actions to prevent extensive voltage excursions at the coupling points can be evaluated. It is also suitable to analyze the possibilities and effects of exchanging existing overhead lines with cable lines. Finally with increasing feed-in powers and the use of different measures to maintain the supply voltage level (line reinforcements, reactive power management and regulating distribution transformers, as seen in section 2.8), also the upper limits for the equipment loadings are reached.

The contemplated rural grids mostly consist out of overhead lines with high line lengths. Equipment loadings do not affect the feed-in capacity of such network structures. The influence of the distributed generators onto the supply voltage on the other hand is very crucial. The increasing line resistance due to the long distribution lines produces higher voltage drops, which restrict the possible generator capacity. The rural model grid is therefore suitable for analyzing the effects of different line lengths onto the feed-in capacity.

The principle steps in the model grid development process can be seen in figure 3.0.1. The urban, suburban and rural model grids were developed, based on general parameters from the distribution grid of the Wien Energie Stromnetz GmbH, together with averaged network structures for the three chosen regions mentioned before.

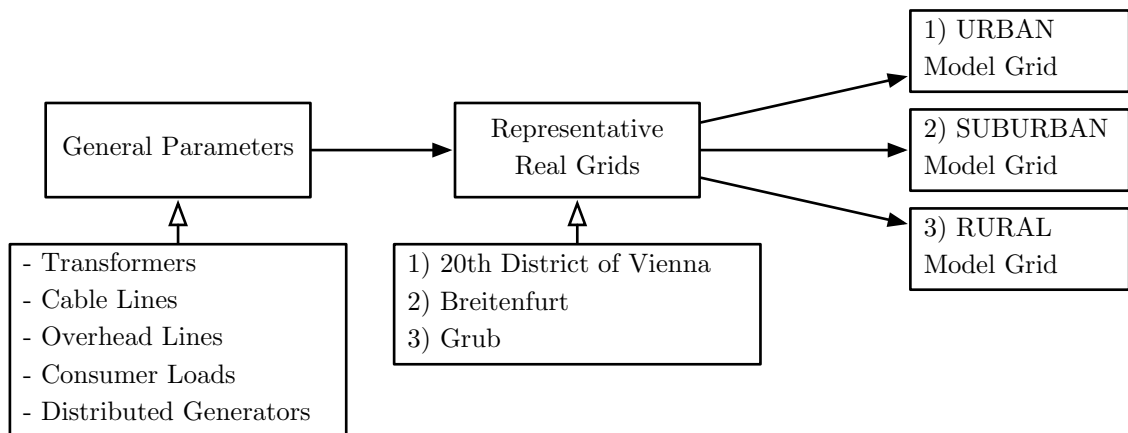


Figure 3.0.1.: Model grid development.

The basic parameters of the developed model grids are shown in table 3.0.1. The values represent the standard configuration for every single model grid, including the rated power of the used distribution transformer S_{Tr} and the used line lengths and conductor materials.

Table 3.0.1.: Comparison of the developed model grid parameters in standard configuration.

	Urban	Suburban	Rural
U_{MV} in kV	10	20	20
U_{LV} in kV	0,4	0,4	0,4
MV-Line type	cable	cable	cable / overhead line
MV-Line material	Al	Cu	Cu / StAlu
MV-Line cross section in mm ²	240	150	150 / 95
LV-Line type	cable	cable / overhead line	overhead line
LV-Line material	Al	Al / StAlu	StAlu
LV-Line cross section in mm ²	150	150 / 95	95
MV-Length in km	0,422	0,422	0,840 / 0,280
LV-Length in km	0,025	0,035	0,288
Number of substations	9	9	19/39
S_{Tr}	630 kVA	400 kVA	400 kVA
Number of feeders	5	2	1
Loads / Generators at feeder	5	20	10

3.1. General Model Grid Parameters

Several global parameters, like the operation voltages can be applied to all model grids. Furthermore the parameters of the supplying slack node for the medium voltage grid and the used regulating transformer stays the same for all simulations. The upper limit for the equipment loading of all used cable lines, overhead lines and transformers was set to 60% of the equipment's rated power. This should assure the possibility to take over the consumer load of faulty grid sections.

As a slack node for all simulations served a 110 kV high voltage grid with a short circuit apparent power of 3,5 GVA. Table 3.1.1 includes the set operation voltages for the on-load tap-changer and the slack node.

Table 3.1.1.: Nominal and operation voltages for the used voltage levels.

Nominal Voltage U_n	Operation Voltage U
110 kV	115,0 kV
20 kV	20,4 kV
10 kV	10,2 kV

3.1.1. Transformers

All medium voltage grids in the simulations were supplied by a 40 MVA regulating transformer, represented by an on-load tap-changer. Due to the voltage regulation of this transformer, the voltage levels of 10,2 kV and 20,4 kV in the particular grids were kept near the set value at all occurring static load conditions.

The following characteristic parameters are applied for the transformation to both required voltage levels (10 kV and 20 kV).

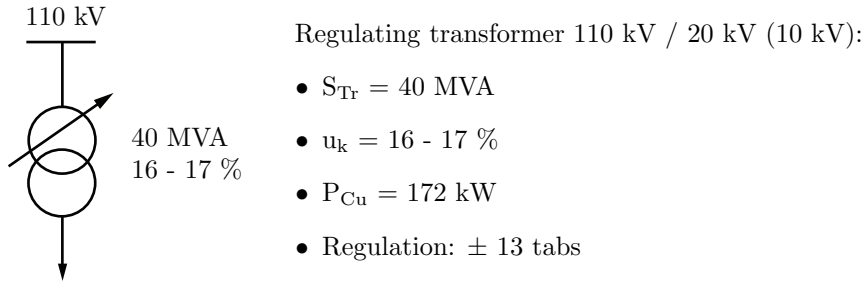


Table 3.1.2 contains the values for the relative impedance voltage u_k and the copper losses P_{Cu} of the used distribution transformers with the corresponding rated apparent power S_{Tr} . The iron losses P_{Fe} were disregarded for all transformers in the simulations. The values represent transformers, actually used in the Vienna electricity supply network by the company Wien Energie Stromnetz GmbH. However, transformers with increased rated powers of 1000 kVA and 1250 kVA are not yet in use, because current substations don not offer the ability to house these sizes. Their abilities to influence the feed-in capacity of the urban model grid were examined in the following simulations.

Table 3.1.2.: Parameters of the used distribution transformers (source: Wien Energie Stromnetz GmbH).

S_{Tr}	160 kVA	250 kVA	400 kVA	630 kVA	800 kVA	1000 kVA	1250 kVA
u_k	4%	5,5 %	6 %	6 %	6%	6%	6%
P_{Cu}	2,0 kW	4,0 kW	5,0 kW	5,0 kW	7,0 kW	10,0 kW	11,0 kW

3.1.2. Cable Lines

The specific impedance values of the used medium and low voltage cable lines and their thermal limiting currents I_{th} can be seen in table 3.1.3. The values represent the most common cable types within the medium and low voltage distribution system of the Wien Energie Stromnetz GmbH. The capacitances were included in the simulations as far as they were available for the particular cable type.

Table 3.1.3.: Parameters of the used cable types (source: Wien Energie Stromnetz GmbH).

	Medium Voltage		Low Voltage		
	150 mm ²	240 mm ²	50 mm ²	95 mm ²	150 mm ²
Material	Cu	Al	Al	Al	Al
r' in $\frac{\Omega}{km}$	0,124	0,125	0,641	0,321	0,207
x' in $\frac{\Omega}{km}$	0,104	0,074	0,063	0,082	0,080
c' in $\frac{\mu F}{km}$	0,250	0,440	-	-	-
I_{th} in A	403	340	141	211	300

3.1.3. Overhead Lines

Table 3.1.4 contains the impedance values for the used overhead lines and their thermal limiting currents I_{th} . The values were chosen in accordance to the most common overhead lines used by the company Wien

Energie Stromnetz GmbH in the distribution grids, and consequently also in the developed model grids. For the simulations the line capacitances were considered if they were available for the used line type.

Table 3.1.4.: Parameters of the used overhead lines (source: Wien Energie Stromnetz GmbH).

	Medium Voltage		Low Voltage	
	95 mm ²	10 mm ²	50 mm ²	95 mm ²
Material	StAlu	StAlu	StAlu	StAlu
r' in $\frac{\Omega}{\text{km}}$	0,319	1,790	0,641	0,320
x' in $\frac{\Omega}{\text{km}}$	0,370	0,095	0,079	0,075
c' in $\frac{\mu\text{F}}{\text{km}}$	-	-	0,250	0,240
I _{th} in A	350	60	125	185

3.1.4. Consumer Loads

All single households were defined as inductive loads with a power factor of $\cos\varphi = 0,97$ (lagging). The consumer load was set to 0,5 kW for every household. This value follows analyses of the H0 load profile and an averaging of measured consumer loads. The data for the measured consumer loads has been obtained from Wien Energie Stromnetz GmbH.

Figure 3.1.1 illustrates the voltage profiles of two different consumer loads along the same radial low voltage stub starting at the distribution transformers busbar with the relative voltage u_{Tr} . A variation in the attached consumer loads at every PCC changes the characteristics of the voltage profile and the final voltage drop at the end of the stub. The voltage rise Δu , resulting from distributed generation and restricted by thresholds stated in standards and network operation guidelines in section 2.7 however, depends on the feed-in power of the generators at their respective coupling points. For the purpose of this document, the maximum voltage rise Δu_{max} , caused by distributed generation, is 3% in accordance with [7].

The voltage rise at the coupling points is a result of the load current and the line impedance. Therefore the voltage does not directly affect it. Nevertheless, the generators output currents increase when the voltage in the connection point decreases and the output power has to be kept. Thus, also the voltage drop along the lines, caused by the output current, and consequently the voltage rise at the coupling points is increased indirectly.

In the urban supply area, examined for the grid development, apartment buildings with several households prevailed. Therefore a model apartment building was defined for further calculations. One model building included 20 identical model households. This number was also near the result of averaged values from STATISTICS AUSTRIA, Statistik Wien (Magistratsabteilung 23 - Wirtschaft, Arbeit und Statistik) and Wien Energie Stromnetz GmbH. Every model household within the building had its own average consumer load of 0,5 kW, which summed up to a total load of 10 kW for the complete model apartment building.

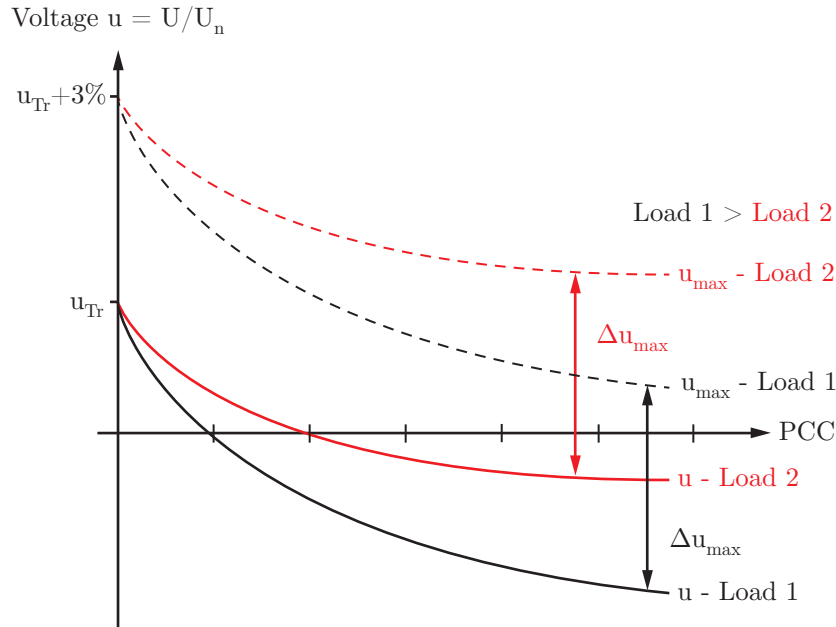


Figure 3.1.1.: Influence of different consumer loads onto the voltage profile.

The suburban and rural supply areas which, were analyzed, showed a different average building structure and consumer load density. Therefore detached houses were chosen as typical consumer loads. Every detached house represented a single average household consumer load of 0,5 kW.

3.1.5. Residential Photovoltaic System Configuration - Distributed Generator

The distributed generator used in all simulations was defined as residential roof top photovoltaic system. In suburban and rural areas, also the application of freestanding systems would be possible. These systems are not restricted by existing roof sizes and can therefore easily reach high rated output powers. For the performed simulations however, it was irrelevant how the distributed energy was generated. Every type of distributed generator produces the same effects onto the distribution grid when feeding in. Therefore the simulations can be applied onto all forms of decentralized energy production facilities (photovoltaic systems, wind turbines, micro gas turbines,...). Differences can arise due to the different abilities of distributed generators to provide reactive power, their frequency control and the control of their active power output.

For the examination of photovoltaic systems as generators, the influence of the inverter efficiency is disregarded. To calculate the rooftop area, needed to achieve the possible feed-in power, only the module efficiency was used. In chapter 2.2 the module efficiency was defined as 15%. The difference between the average and the real module efficiency as well as the assumption of a maximum irradiation may lead to a higher value for the required rooftop areas if modules with lower efficiencies are used. Modules with higher efficiency values on the other hand can lead to a smaller needed rooftop area. A common simplification assumes a maximum solar energy production of 150 W/m^2 as a result of an efficiency of 15% and an irradiation of 1000 W/m^2 [6].

3.2. Representative Real Grids

To determine and assess the impacts of distributed generation in medium and low voltage distribution grids, different supply areas with miscellaneous load densities have been chosen beforehand. For the purpose of this document urban, suburban and rural grid structures with the corresponding load densities were selected. Distinctive and generally valid model grids have been developed, representing the main characteristics of these three regions. Therefore three special regions from the whole service area of the company Wien Energie Stromnetz GmbH, which represented the desired load densities and network structures, were used:

- Urban model grid → *20th district of Vienna*
- Suburban model grid → *Breitenfurt near Vienna*
- Rural model grid → *Grub near Vienna*

After the separation into the three regions, stated above, representative network parts were picked from each one of them to form the base for the model grid development. Important network parameters from these parts, like the number of distribution transformers or the complete length of all medium and low voltage lines and their conductor materials and cross sections, were then investigated furthermore and averaged, in order to get the main parameters for the model grids.

The structures for the model grids were derived from the network structures, present in the real network parts of the observed regions. Some specific grid attributes, like the number of substations or the branching in the medium voltage section, were altered to achieve the desired characteristics, which were observed in real networks.

During the development of the low voltage sections, several grid parameters were specifically chosen and modified to point out important influencing factors, regarding distributed generation. These modifications should improve the possibilities to examine the different expected effects of distributed generators and the investigated voltage rise counter measures.

3.2.1. Urban Model Grid

The urban model grid was developed based on real grid parameters of the 20th district of Vienna. The resulting medium voltage structure contained 9 substations. All of them were allocated at the medium voltage line within the same distances. The averaging of several representative medium voltage networks resulted in a medium distance between the Stations of 422 m. Every single substation included one distribution transformer which supplied one low voltage distribution grid. For the medium voltage grid, aluminum cable lines with a cross section of 240 mm² were used. The considered medium voltage feeder was supplied by a 40 MVA regulating transformer, stepping down the high voltage from the 110 kV slack node. The nominal voltage for the medium voltage grid in Vienna was 10 kV, which is common for urban areas. The resulting structure is depicted in figure 3.2.1.

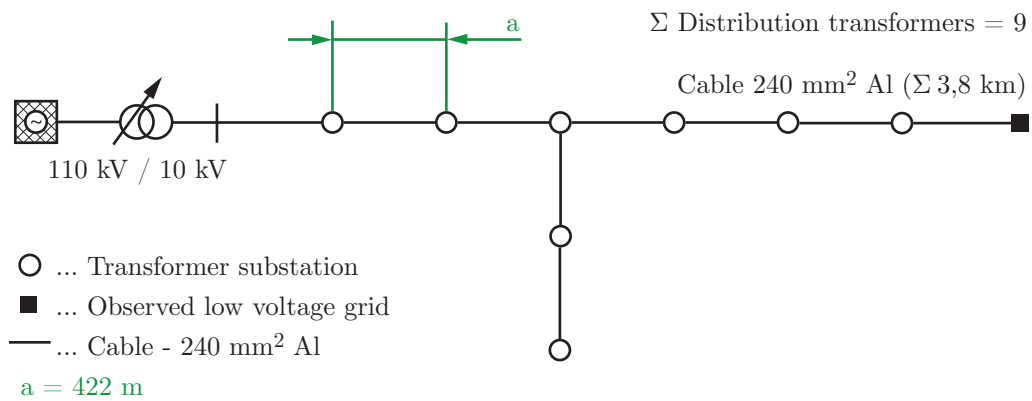


Figure 3.2.1.: Medium voltage structure of the urban model grid.

Figure 3.2.2 shows the structure of the developed low voltage grid. The average transformer power rating resulted in 630 kVA, which was the most common transformer size within the examined urban grids. Based on the five transformer feeders (F1-F5), four low voltage stubs (F1-F4) of the same structure and one single load at the fifth feeder (F5), were supplied. The four equal stubs contained five model apartment houses, mentioned in chapter 3.1.4, arranged in constant distances of $b = 25$ m. The single load at the fifth feeder was also represented by a model apartment house. However this load was also determined to be used as a infeed point for a combined heat and power plant (CHP), or another distributed generator with a higher power rating. For the low voltage distribution lines, aluminum cable lines with a cross section of 150 mm² were used.

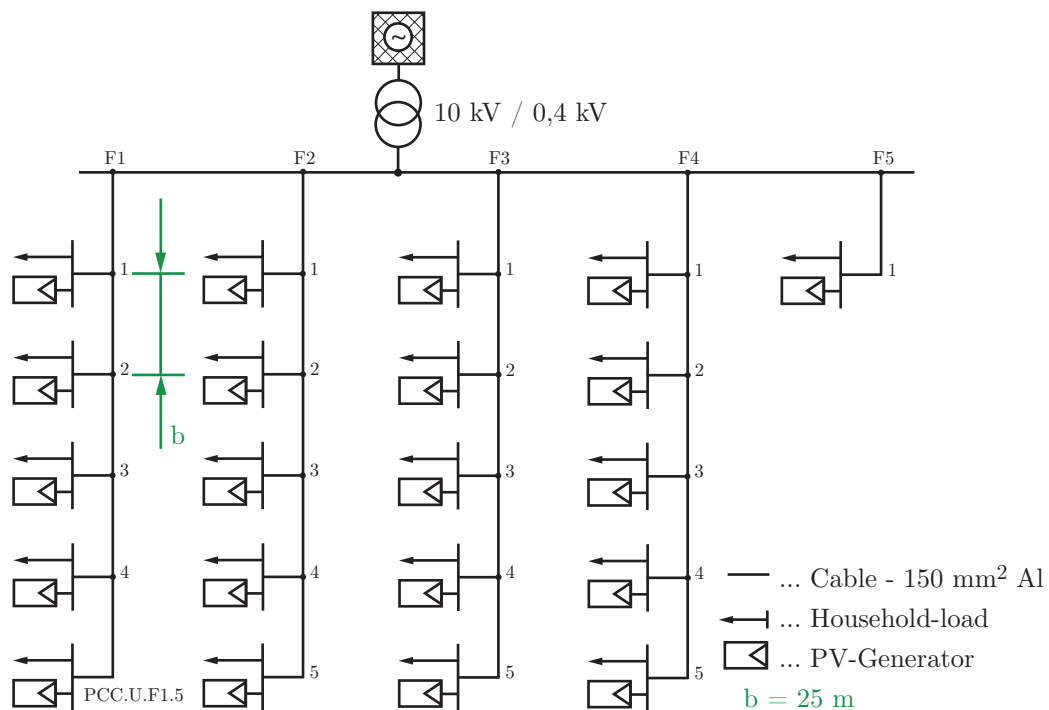


Figure 3.2.2.: Low voltage structure of the urban model grid.

Every single model apartment house contained 20 model households (HH) with a defined consumer load of 0,5 kW. In addition to the consumer loads, every house also included a rooftop photovoltaic generator (PV) which fed in the produced energy at the particular point of common coupling.

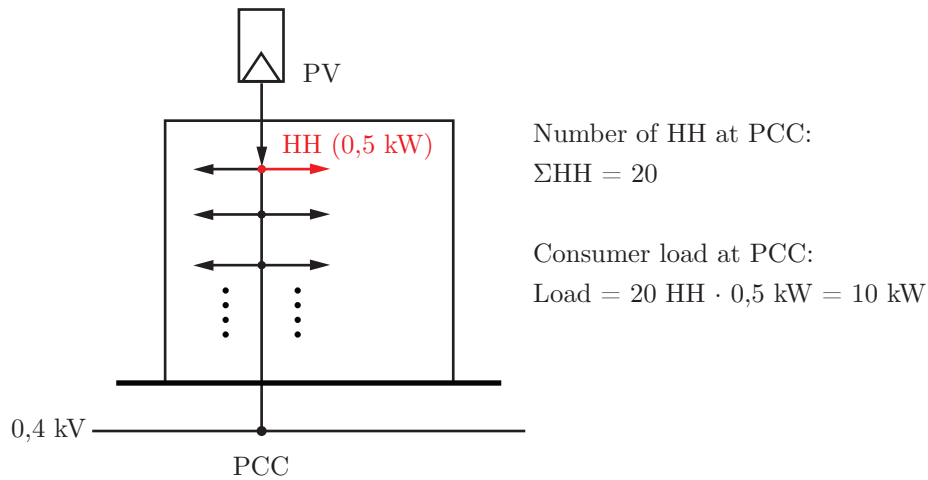


Figure 3.2.3.: Model apartment building, including the consumer loads and PV generator.

3.2.2. Suburban Model Grid

The suburban model grid was developed with the help of representative network structures from the area Breitenfurt near Vienna. The final structure of the medium voltage section can be seen in figure 3.2.4. Due to the substation arrangements and similar attributes of these networks, the medium voltage structure of the urban model grid, seen in section 3.2.1, was adopted for the suburban grid. The average distances between the substations were adjusted to meet the lengths of the urban grid. This was acceptable because of the negligible difference between these two structures.

However, the nominal voltage in the suburban area was 20 kV. Therefore copper cable lines with a cross section of 150 mm² were used for the medium voltage level instead of the aluminum cable lines with a cross section of 240 mm². The low voltage grids were supplied by 400 kVA distribution transformers.

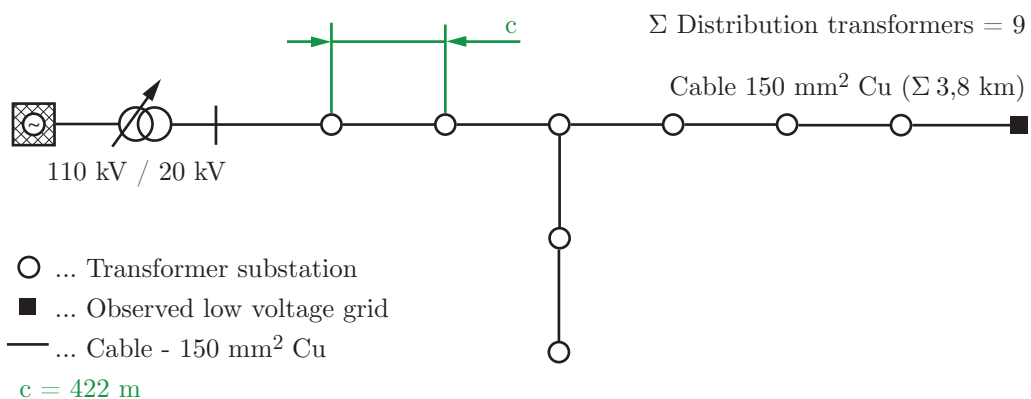


Figure 3.2.4.: Medium voltage structure of the suburban model grid.

The distribution transformer of the suburban low voltage grid, depicted in figure 3.2.5, had two feeders (F1,F2) which supplied two low voltage branches of equal arrangement. Every low voltage stub included two line sections.

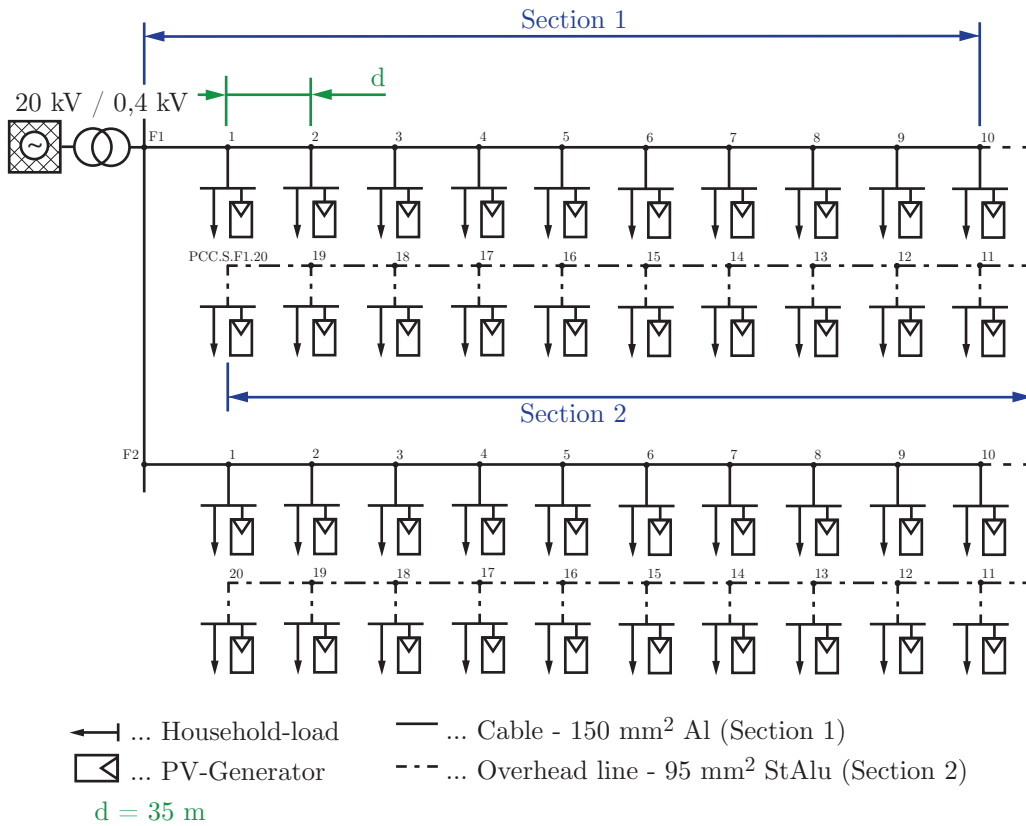


Figure 3.2.5.: Low voltage structure of the suburban model grid.

The first section was represented by 10 detached houses, each containing one single household load. Aluminium cable lines with a cross section of 150 mm² were used to connect the houses, represented by their coupling points with the attached loads and distributed generators. Section two also included 10 houses. The connection of the houses in section two was however realized with overhead lines. The steel reinforced aluminum cable had a cross section of 95 mm² for this special grid. In both cases, the distances between the houses were specified to be $d = 35$ m.

The configuration for the developed detached model houses in the suburban low voltage grid can be seen in figure 3.2.6. Every PCC contained one single detached house with a defined consumer load of 0,5 kV. The distributed generators, represented by rooftop photovoltaic systems, were connected for every single detached house at the corresponding coupling point.

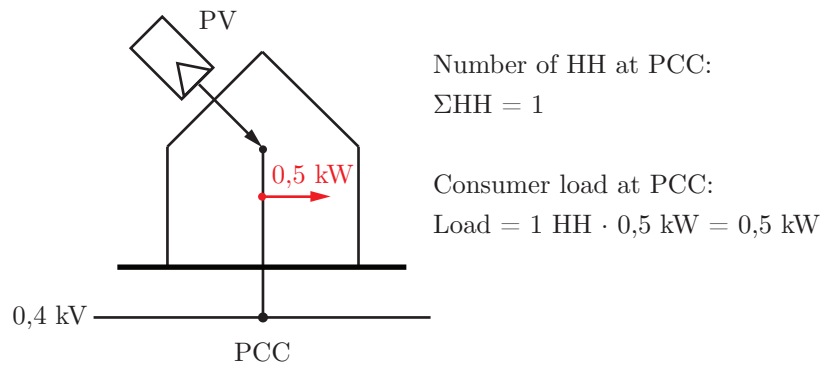


Figure 3.2.6.: Detached model house, including the consumer load and PV generator.

3.2.3. Rural Model Grid

The rural model grid was adapted from medium and low voltage grid structures of the region Grub near Vienna. The medium voltage grid was divided into two line-sections. Section 1 included 19 substations, which were connected with 150 mm² aluminum cable lines. The 39 substations present in section 2 were connected with medium voltage 95 mm² steel reinforced aluminum overhead lines. Distances between the substations varied from $e = 840$ m in section 1 to $f = 280$ m in section 2. The resulting structure is depicted in figure 3.2.7. A regulating transformer, with an installed capacity of 40 MVA, stepped down the voltage from the high voltage level, represented by the 110 kV slack node, to a medium voltage of 20 kV, used to supply the medium voltage grid.

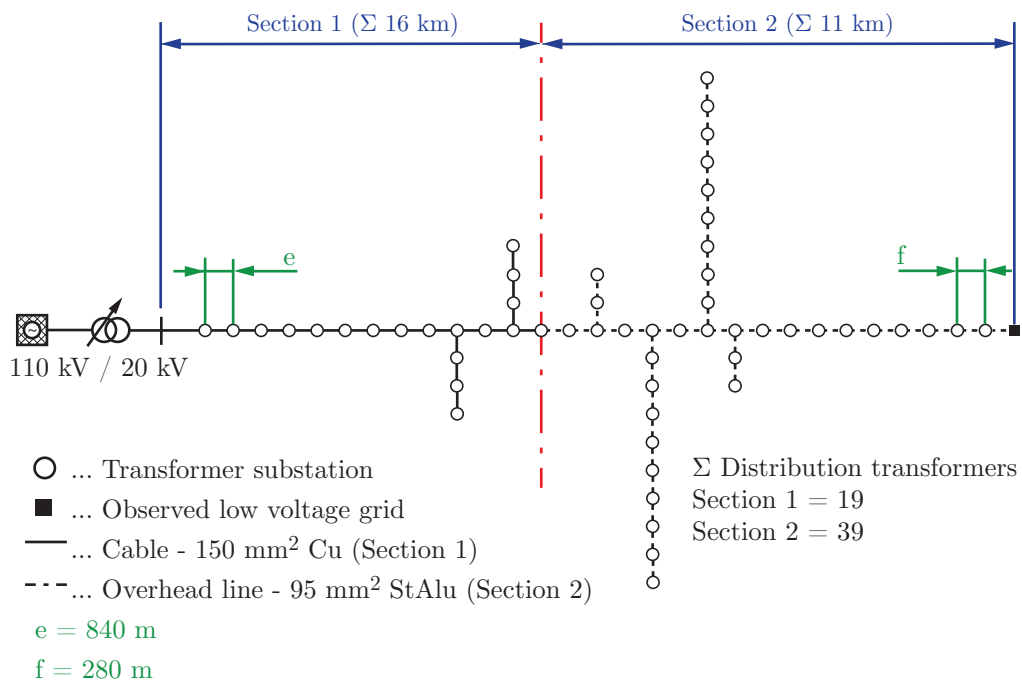


Figure 3.2.7.: Medium voltage structure of the rural model grid.

Figure 3.2.8 shows the low voltage model grid structure used in the simulations for the rural area. Based on real network structures a 400 kVA distribution transformer was selected to supply one single low voltage stub on feeder F1. On this stub 10 detached houses with 10 single consumer loads were evenly distributed with an average distance of $g = 288$ m between them. These relatively high lengths showed the worst possible case in distribution distances. For the simulations the length was varied in the favor of shorter values. A steel reinforced aluminum overhead line with a cross section of 95 mm^2 was used as distribution line for the low voltage level. Every household had its own rooftop photovoltaic generator which fed in electrical energy at the corresponding coupling point.

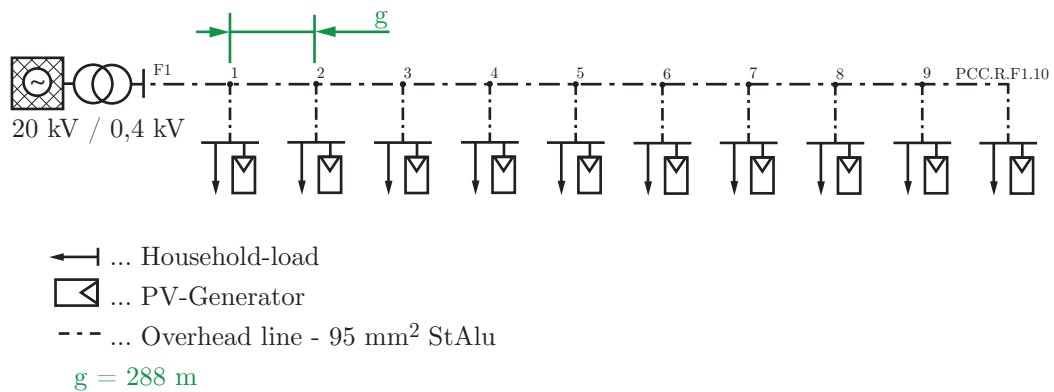


Figure 3.2.8.: Low voltage structure of the rural model grid.

The configuration for the developed detached model houses in the rural low voltage grid can be seen in figure 3.2.9. Every PCC contains one single detached house with a defined consumer load of $0,5 \text{ kW}$.

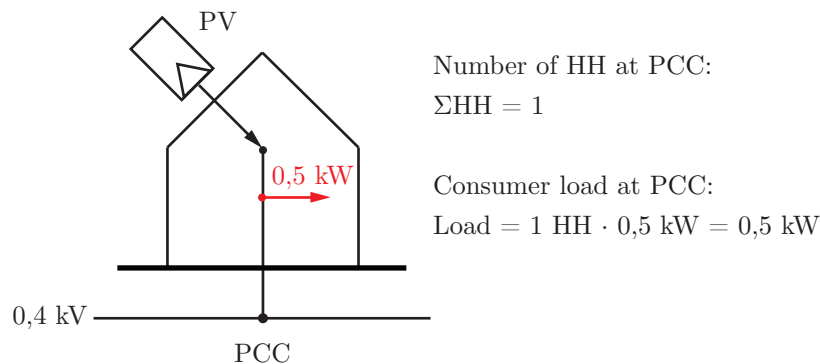


Figure 3.2.9.: Detached model house, including the consumer load and PV generator.

The distributed generators, represented by rooftop photovoltaic systems, were connected for every single detached house at the corresponding coupling point. This load distribution was already used for the suburban low voltage model grid in the same configuration.

4. Simulations

The characteristic model grids developed in chapter 3 were implemented in the power flow simulation program Neplan[®] by BCP Busarello + Cott + Partner AG in order to perform simulations of the chosen load states. The following chapter includes the used parameters for these simulations, which were performed in the same order, given in chapter 3. Common parameters were taken from section 3.1. As solver algorithm for the power flow calculations the Extended Newton Raphson method was used. The Evaluation of the simulation results was done with MathWorks[®] MATLAB[®].

The performed simulations and parameter variations, stated in this chapter, are structured as seen in figure 4.0.1. Beginning with the three developed model grids (urban, suburban, rural), basic power flow simulations were performed with the respective grid configurations, in order to determine their feed-in capacities under the different circumstances (exchange of transformers, different low voltage line lengths). In addition, further parameter and equipment variations were performed with the standard configuration of the three model grids.

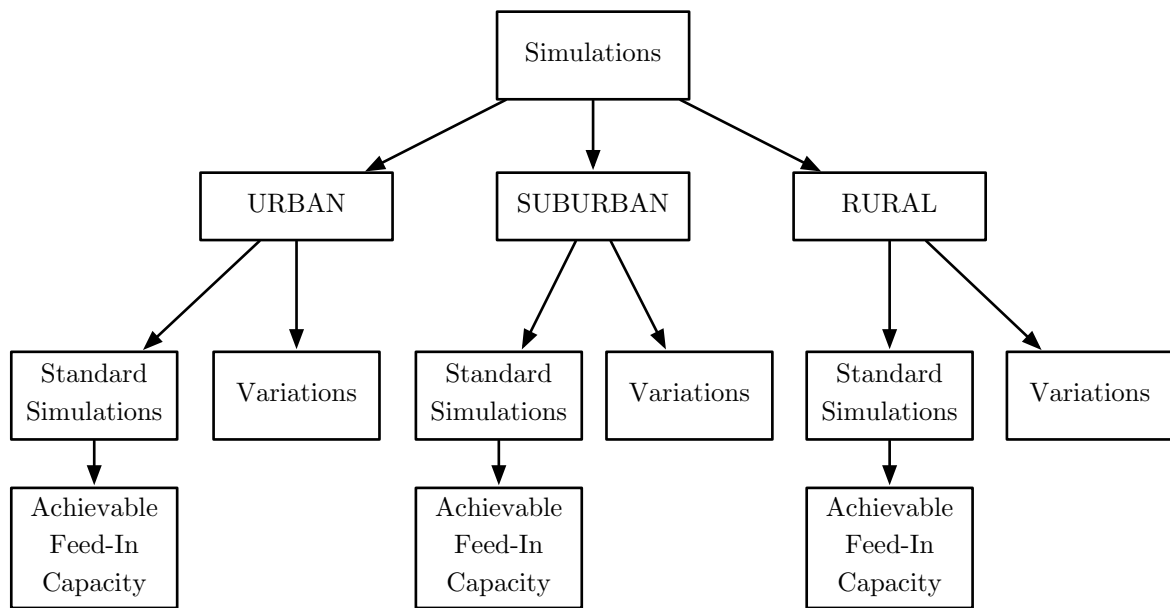


Figure 4.0.1.: Structure of the performed simulations and variations for the model grids.

The resulting voltage profiles along one of the symmetric low voltage network stubs of the observed low voltage model grids, stating the supply voltage at every point of common coupling are listed in the appendix A for the urban model grid, appendix B for the suburban model grid and appendix C for the rural model grid.

4.1. Urban Model Grid

First, simulations were performed for the urban model grid. As mentioned before, the upper limits for the equipment loading represented the major restricting factor for the possible decentralized power generation in areas defined by the present grid structure and load density. Therefore the general feed-in capacity for distributed generation of the medium and low voltage grid at higher penetration levels was analyzed first. Figure 4.1.1 shows the low voltage network structure for the urban model grid, developed in section 3.2.1.

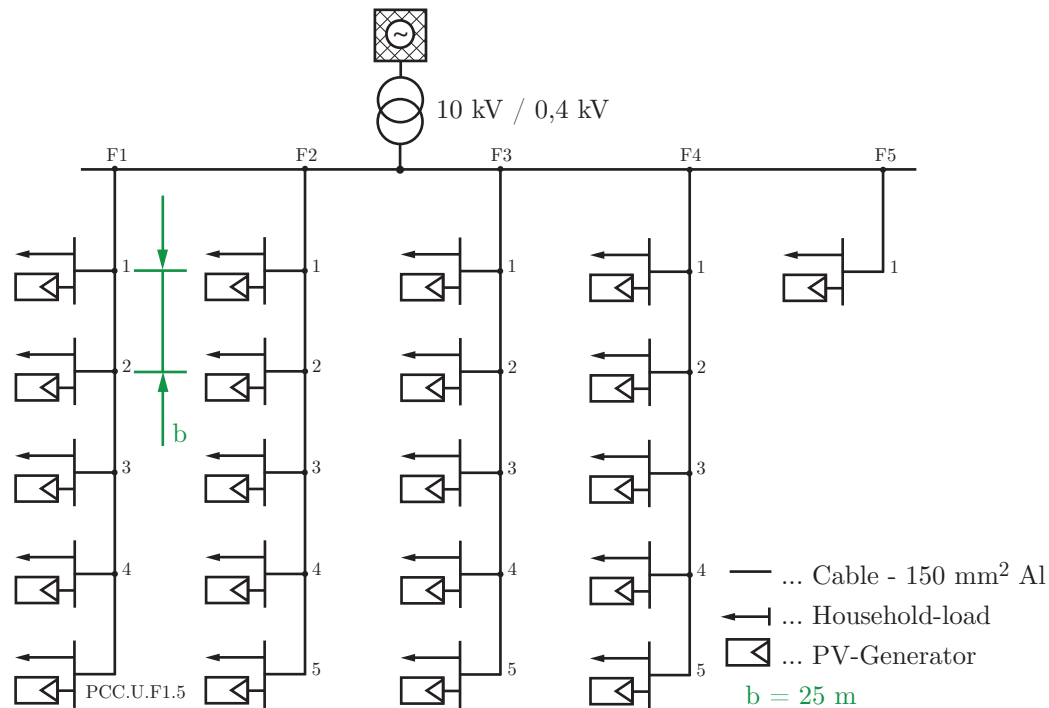


Figure 4.1.1.: Low voltage structure of the urban model grid.

Subsequently advanced simulations were performed in which the lines and transformers, with the highest loading due to the increased energy transport, were varied in their transmission capacity. These variations should help to illustrate the connection between the equipment loading thresholds and the resulting maximum feed-in power for the combination of all distributed generators within the examined low voltage and medium voltage model grid.

The problem of resulting voltage rises at the coupling points due to the additional power generation had to be analyzed separately. Different measures, like reactive power provision by the distributed generators or the exchange of distribution transformers, had to be taken to decrease the resulting voltage levels at the remote coupling points.

Figure 4.2.2 shows the structure of the performed simulations regarding the urban model grid. Standard power flow simulations with three distribution transformer configurations (630 kVA, 800 kVA and 1000 kVA) were performed to determine the grids feed-in capacity. To increase the feed-in capacity, simulations with reactive power provision by the distributed generators were included with all three transformer configurations.

A sensitivity analysis for the standard grid configuration with a 630 kVA distribution transformer should

illustrates the general grid behavior, towards changes in the characteristic grid parameters.

Further equipment variations were performed with the standard grid configuration, altering transformer rated powers and cable cross sections, to examine their effects upon the achievable feed-in capacity.

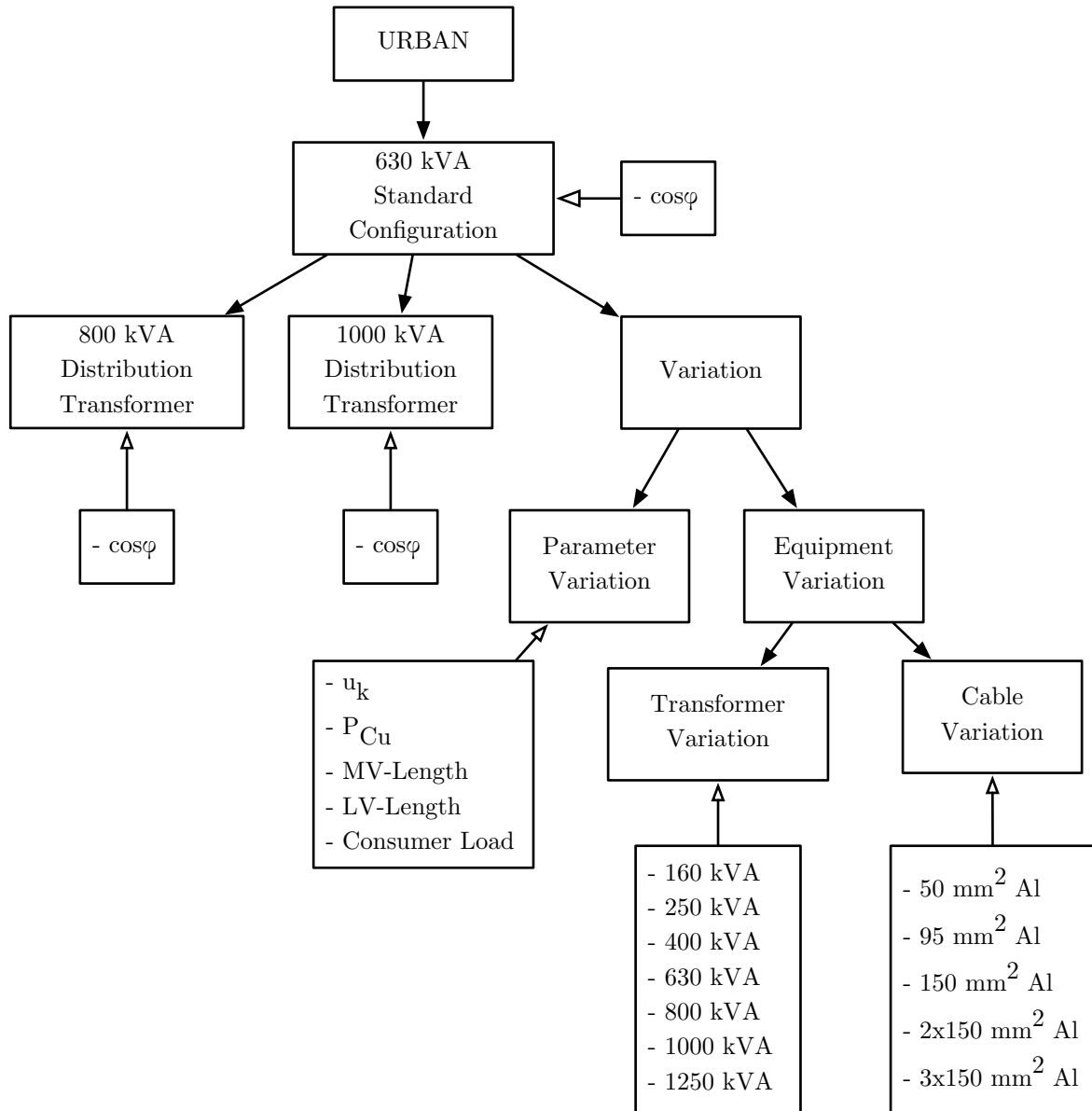


Figure 4.1.2.: Performed simulations for the urban model grid.

4.1.1. Simulation Parameters

The following general parameters were applied to all simulations performed with the urban model grid. For all simulations, the voltage regulation of the feeding tap-changer was activated (110 kV / 10 kV). Therefore the voltage at the secondary busbar of the transformer was kept near the set operation voltage. The discrete voltage steps of the tap-changer resulted in a permanent differential voltage.

Table 4.1.1.: Simulation parameters for the urban model grid.

Transformer regulation (110 kV / 10 kV)	active
Operating voltage (10 kV)	10,2 kV
Maximum equipment loading	60%
Consumer load at PCC	$20 \times 0,5$ kW
Node with highest voltage rise	PCC.U.F1.5

An average consumer load of 0,5 kW for every single household was chosen for the performed simulations. This meant a total load of 10 kW for every model apartment building with 20 identical households at the corresponding coupling point.

The low voltage feeders 1 to 4 supplied 5 model apartment buildings each, and were therefore carrying a load of 50 kW. The fifth feeder supplied one single apartment building with the equal load and feed-in power. This resulted in a total consumer load of 210 kW for the whole low voltage grid.

The distributed generators were represented by residential rooftop photovoltaic systems. For the simulations the output power of these generators was varied in discrete 1 kW steps. Due to the chosen urban building structure, the size of the distributed photovoltaic systems, installed in real conditions, is limited by the available roof areas. This fact was disregarded in the simulations.

At the chosen network structure, the highest voltage rise was observed at the remotest coupling point of the remotest low voltage grid within the modeled medium voltage stub, depicted as PCC.U.F1.5 in figure 4.1.1. Therefore the voltage changes due to distributed generators were evaluated at this point for all performed simulations.

Due to the structure of the medium voltage section, with its low line lengths and high cross sections, the voltage rise in the medium voltage level was never about to reach its threshold of $\Delta u = +2\%$ [7] during all states of the attached consumer loads and distributed generation. The evaluation of the voltage rise at the medium voltage level could therefore be disregarded.

The first four low voltage feeders were symmetrically arranged which resulted in the same voltage profile on each one of them. The fifth feeder however, only supplied one single apartment house with the respective consumer load and feed-in power of the photovoltaic system. Because of the low line length, it was possible to neglect the voltage rise at the affected point of common coupling. The feed-in power at this point however, influenced the overall loading of the distribution transformer, and was therefore important for evaluations regarding the equipment loading.

4.1.2. Simulation Sequence

All performed simulations were carried out in the following order. The corresponding feed-in power of the distributed generators and the purpose of the simulation can be seen in table 4.1.2. The tables in section 4.1.3 include the results of the simulations.

Table 4.1.2.: List of simulations for the urban model grid.

Standard Configuration			
Simulation #	PV in kW	S_{Tr} in kVA	Simulation title
1	0,0	630	Idle state, load only (Reference)
2 - 6	5,0 - 25,0	630	PV is increased (5 kW steps)
7	26,0	630	Max PV ($\Delta u = +3\%$ voltage rise reached)
8	28,0	630	Upper limit for transformer loading is reached
9	28,0	630	Reactive power provision for # 8
10	0,0	800	Idle state, load only (Reference)
11	25,0	800	PV is increased (5 kW steps)
12	27,0	800	Max PV ($\Delta u = +3\%$ voltage rise reached)
13	30,0	800	PV is increased
14	30,0	800	Reactive power provision for # 13
15	33,0	800	Upper limit for transformer loading is reached
16	33,0	800	Reactive power provision for # 15
17	0,0	1000	Idle state, load only (Reference)
18	25,0	1000	PV is increased (5 kW steps)
19	28,0	1000	Max PV ($\Delta u = +3\%$ voltage rise reached)
20	30,0	1000	PV is increased
21	30,0	1000	Reactive power provision for # 20
22	39,0	1000	Upper limit for transformer loading is reached
23	39,0	1000	Reactive power provision for # 22

630 kVA - Distribution Transformers

Beginning with the standard network configuration and a 630 kVA distribution transformer, the feed-in power of every single model apartment house, supplied by the low voltage grid, was consistently increased in 5 kW steps. The other low voltage grids within the medium voltage stub were set to the same values for the consumer loads and the feed-in power of the distributed generators.

The reference value for the voltage levels and equipment loadings, with the chosen load state and without distributed generation, was represented by the simulation number 1. All simulations with the same network configuration and the same distribution transformer were compared with these results.

Voltage rises and equipment loadings were evaluated referring to the constraints in chapter 2.7. With a distributed feed-in power of 26 kW for the generator of every apartment house and coupling point, the possible upper limit for the voltage rise of $\Delta u = +3\%$ was reached.

The related results for the equipment loading can be seen in simulation number 7. Therefore this value represents the possible capacity for distributed generation within the observed model grid and with the chosen load and generator allocations.

Figure 4.1.3 illustrates the voltage profiles along the low voltage stub of the urban model grid for the simulations 1, 7 and 9.

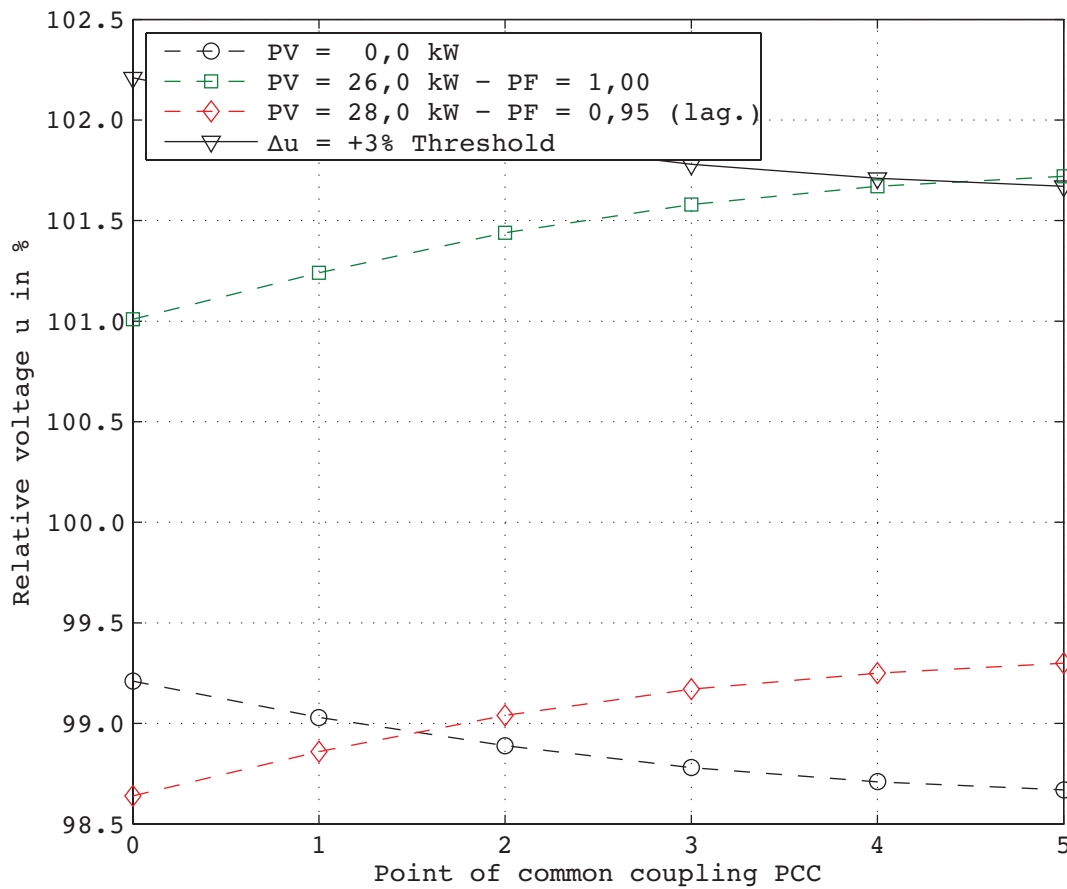


Figure 4.1.3.: Voltage profile of the suburban model grid (630 kVA Distribution Transformers, reactive power provision).

In simulation 8 the feed-in power was further increased until the loading threshold of 60% for the distribution transformer was reached. To decrease the improper voltage rise, the power factor of the distributed generators was changed in simulation 9.

With a power factor of 0,95 lagging, inductive power was drawn by the generators, thus reducing the voltage at the corresponding coupling point due to the effects discussed in section 2.6. As a result, the voltage rise could be kept within the allowed limits. However, the obtained inductive power is not generated locally within the low voltage grid and must therefore be transported across the distribution transformer and the medium voltage grid. This additional power transmission increased the equipment loading furthermore, which led to the exceedance of the given loading threshold.

800 kVA - Distribution Transformers

The simulations 10 to 16 include the results for the same procedure stated above, but for distribution transformers with a rated power of 800 kVA. Starting with a consumer load of 10 kW for one model apartment house (0,5 kW / HH) and without distributed generation as reference value, it was possible to increase the feed-in power up to a maximum value of 27 kW. Then the upper limit for the voltage rise

of $\Delta u = +3\%$ was reached.

In the simulations 13 to 16, the feed-in power was increased furthermore and the voltage rise was decreased due to reactive power provision by the distributed generators. At a feed-in power of 33 kW for every coupling point and the same 10 kW consumer load, the loading threshold of 60% for the 800 kVA distribution transformer was reached, thus making 33 kW the upper limit for the feed-in capacity, regarding the equipment loading of this transformer.

1000 kVA - Distribution Transformers

The simulation 17 to 23 followed the same approach. The network structure was kept the same, however the power rating of the distribution transformers was increased to 1000 kVA. The corresponding transformer parameters can be seen in table 3.1.2. The reference value without distributed generation was represented by simulation number 17.

The maximum feed-in capacity was reached in simulation 19 with a feed-in power of 28 kW for every single generator. This value led to a voltage rise of $\Delta u = +3\%$. The upper limit for the feed-in capacity regarding the transformer loading was 39 kW, reached in simulation 22.

With participation in the reactive power management by the distributed generators, it was possible to decrease the resulting voltage rise to meet the constraints. However the increasing transport of reactive power exceeded the allowed loading thresholds.

4.1.3. Simulation Results

Table 4.1.3.: Simulation results for the urban model grid (voltage levels at PCC.U.F1.5 and distribution transformer loading, for the three transformer configurations 630 kVA, 800 kVA and 1000 kVA including reactive power provision by the distributed generators).

630 kVA - Distribution Transformer						
#	Load in kW	PV in kW	u max in %	Δu in %	Distribution Transformer I in A (sec.)	Distribution Transformer Loading in %
1	20 × 0,5	0,0	98,7	-	316,0	34,8
2	20 × 0,5	5,0	99,3	+0,6	171,0	18,8
3	20 × 0,5	10,0	99,9	+0,9	76,0	8,4
4	20 × 0,5	15,0	100,5	+1,8	169,0	18,6
5	20 × 0,5	20,0	101,1	+2,4	310,0	34,0
6	20 × 0,5	25,0	101,6	+2,9	455,0	50,0
7	20 × 0,5	26,0	101,7	+3,0	484,0	53,2
8	20 × 0,5	28,0	101,9	+3,2**	542,0	59,6
9	20 × 0,5	28,0 ($\cos\varphi = 0,95$)	99,3	+0,6	657,0	72,2*

800 kVA - Distribution Transformer						
#	Load in kW	PV in kW	u max in %	Δu in %	Distribution Transformer I in A (sec.)	Distribution Transformer Loading in %
10	20 × 0,5	0,0	98,8	-	316,0	27,3
11	20 × 0,5	25,0	101,6	+2,8	455,0	39,4
12	20 × 0,5	27,0	101,8	+3,0	513,0	44,4
13	20 × 0,5	30,0	102,1	+3,3**	600,0	52,0
14	20 × 0,5	30,0 ($\cos\varphi = 0,95$)	99,5	+0,7	718,0	62,2*
15	20 × 0,5	33,0	102,4	+3,6**	687,0	59,5
16	20 × 0,5	33,0 ($\cos\varphi = 0,95$)	99,5	+0,7	812,0	70,4*

1000 kVA - Distribution Transformer						
#	Load in kW	PV in kW	u max in %	Δu in %	Distribution Transformer I in A (sec.)	Distribution Transformer Loading in %
17	20 × 0,5	0,0	98,9	-	315,0	21,8
18	20 × 0,5	25,0	101,6	+2,7	455,0	31,5
19	20 × 0,5	28,0	101,9	+3,0	542,0	37,5
20	20 × 0,5	30,0	102,1	+3,2**	600,0	41,6
21	20 × 0,5	30,0 ($\cos\varphi = 0,95$)	99,9	+1,0	715,0	49,6
22	20 × 0,5	39,0	103,0	+4,1**	860,0	59,6
23	20 × 0,5	39,0 ($\cos\varphi = 0,95$)	100,0	+1,1	998,0	69,1*

* Loading threshold of 60% exceeded

** Voltage threshold of +3% exceeded

Table 4.1.4.: Simulation results for the urban model grid (line loading of the first medium voltage line at the 40 MVA medium voltage feeder and the first low voltage line at the feeder F1, for the three transformer configurations 630 kVA, 800 kVA and 1000 kVA including reactive power provision by the distributed generators).

630 kVA - Distribution Transformer						
#	Load in kW	PV in kW	1. MV-Line		1. LV-Line	
			I in A	Loading in %	I in A	Loading in %
1	20 × 0,5	0,0	113,0	27,7	75,0	25,1
2	20 × 0,5	5,0	60,0	14,7	41,0	13,5
3	20 × 0,5	10,0	25,0	6,0	18,0	6,0
4	20 × 0,5	15,0	60,0	14,6	40,0	13,4
5	20 × 0,5	20,0	111,0	27,2	74,0	24,6
6	20 × 0,5	25,0	163,0	40,0	108,0	36,0
7	20 × 0,5	26,0	174,0	42,6	115,0	38,4
8	20 × 0,5	28,0	195,0	47,8	129,0	43,0
9	20 × 0,5	28,0 ($\cos\varphi = 0,95$)	235,0	57,6	156,0	52,1

800 kVA - Distribution Transformer						
#	Load in kW	PV in kW	1. MV-Line		1. LV-Line	
			I in A	Loading in %	I in A	Loading in %
10	20 × 0,5	0,0	113,0	27,6	75,0	25,1
11	20 × 0,5	25,0	163,0	40,0	108,0	36,1
12	20 × 0,5	27,0	184,0	45,2	122,0	40,7
13	20 × 0,5	30,0	216,0	52,9	143,0	47,6
14	20 × 0,5	30,0 ($\cos\varphi = 0,95$)	258,0	63,1*	171,0	57,0
15	20 × 0,5	33,0	247,0	60,6*	164,0	54,5
16	20 × 0,5	33,0 ($\cos\varphi = 0,95$)	292,0	71,5*	193,0	64,5*

1000 kVA - Distribution Transformer						
#	Load in kW	PV in kW	1. MV-Line		1. LV-Line	
			I in A	Loading in %	I in A	Loading in %
17	20 × 0,5	0,0	113,0	27,6	76,0	25,0
18	20 × 0,5	25,0	163,0	40,0	108,0	36,1
19	20 × 0,5	28,0	195,0	47,8	129,0	43,0
20	20 × 0,5	30,0	216,0	52,9	143,0	47,6
21	20 × 0,5	30,0 ($\cos\varphi = 0,95$)	258,0	63,1	170,0	56,8
22	20 × 0,5	39,0	310,0	76,0*	205,0	68,2*
23	20 × 0,5	39,0 ($\cos\varphi = 0,95$)	360,0	88,3*	237,0	79,1*

* Loading threshold of 60% exceeded

4.1.4. Achievable Feed-In Capacity

The upper limit for the achievable feed-in power of every single distributed generator in the urban model grid, set by the $\Delta u = +3\%$ voltage threshold and the 60% loading threshold, can be seen in figure 4.1.4. The base value is defined by the standard grid configuration with a 630 kVA distribution transformer. To increase the possible generator size, the standard distribution transformers were exchanged with transformers including rated powers of 800 kVA and 1000 kVA. Other measures based on reactive power management, are discussed in the simulations for the suburban and rural model grid.

Regulating distribution transformers did not increase the feed-in capacity. The main limiting factor was the loading threshold of the transformer, which stays the same for distribution transformers with on-load tap-changers of the same rated power.

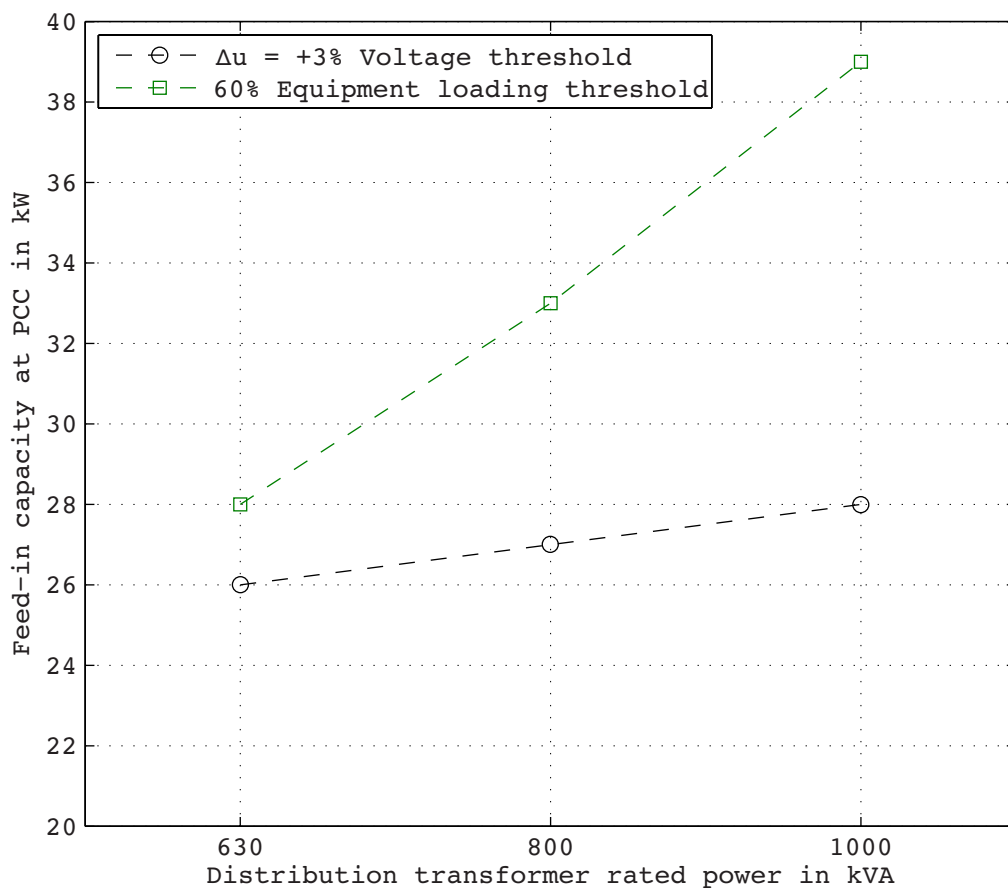


Figure 4.1.4.: Feed-In capacity of the urban model grid.

Part one of table 4.1.5 includes the possible feed-in capacity for one coupling point in accordance to the guidelines of the network operators and the grid code. The increasing possible feed-in powers at higher transformer ratings can be explained with the change in the respective transformer impedance. Depending on the used transformer, this impedance causes an additional series resistance. The resulting voltage drop changes not only the losses at the transformer but also the voltage level within the low voltage grid, thus increasing the possible feed-in capacity.

Table 4.1.5.: Upper limits for the feed-in power regarding the voltage rise and loading limits.

1) $\Delta u = +3\%$ Voltage Threshold			
Transformer rated power S in kVA	630	800	1000
Max PV at PCC in kW	26,0	27,0	28,0
2) 60% Loading Threshold			
Transformer rated power S in kVA	630	800	1000
Max PV at PCC in kW	28,0	33,0	39,0

Part two of Table 4.1.5 includes the upper limits for the feed-in capacities in case the voltage rise is neglected. The limiting factor is consequently defined by the highest possible loading of the applied distribution transformers. However, for higher feed-in powers also the line loading should be taken into consideration.

The simulations show, that distribution transformers with higher rated powers increase the possible distributed generation not only due to their higher transmission power but also by changing the supply voltage within the low voltage grid. However, the variation in the transformer impedance is only a side effect and has only a small impact on the systems behavior concerning distributed generation.

The loading of the used distribution transformers reached its maximum first when the output power of the distributed generators was increased to higher values. Shortly after reaching the threshold at the transformer, also the load of the first low voltage cable lines near the transformers feeder exceeded the given upper limit. Due to the homogenous arrangement of the low voltage grids along the medium voltage stub, and their identical feed-in power, also the medium voltage cable lines near the feeder of the network exceeded the loading limit shortly afterwards. Therefore the simulation results for the equipment loadings were most important to evaluate the effects of distributed generation upon grids with urban network characteristics.

4.1.5. Parameter Variation - Sensitivity Analysis

A sensitivity analysis of several network parameters was conducted to determine the overall behavior of the urban model grid. The resulting relations between the parameter variations and the change in the achievable output power of the distributed generators are shown in figure 4.1.5. Selected parameters for the variation were:

- Distribution transformer - related impedance voltage u_k
- Distribution transformer - copper losses P_{Cu}
- Length of medium voltage lines - MV-Length
- Length of low voltage lines - LV-Length
- Attached consumer load at PCC

The mentioned parameters were varied in a range from 0% to 200% of their initial values, independently from each other in steps of 50%. For every variation, the possible output power for all distributed generators at their coupling point was evaluated while keeping the voltage levels within the constraints

stated in section 2.7. Simulation number 7, performed in section 4.1.2, defines the initial state for the variations including following base values:

- $u_k = 5,5\%$
- $P_{Cu} = 6,0 \text{ kW}$
- MV-Length = 422 m
- LV-Length = 25 m
- Load = 10,0 kW

The resulting diagram shows, how each parameter influences the achievable feed-in capacity of the urban model grid. Due to the relation between the line resistance and the resulting voltage rise, the highest influence can be seen at the low voltage line length, followed by the medium voltage line length.

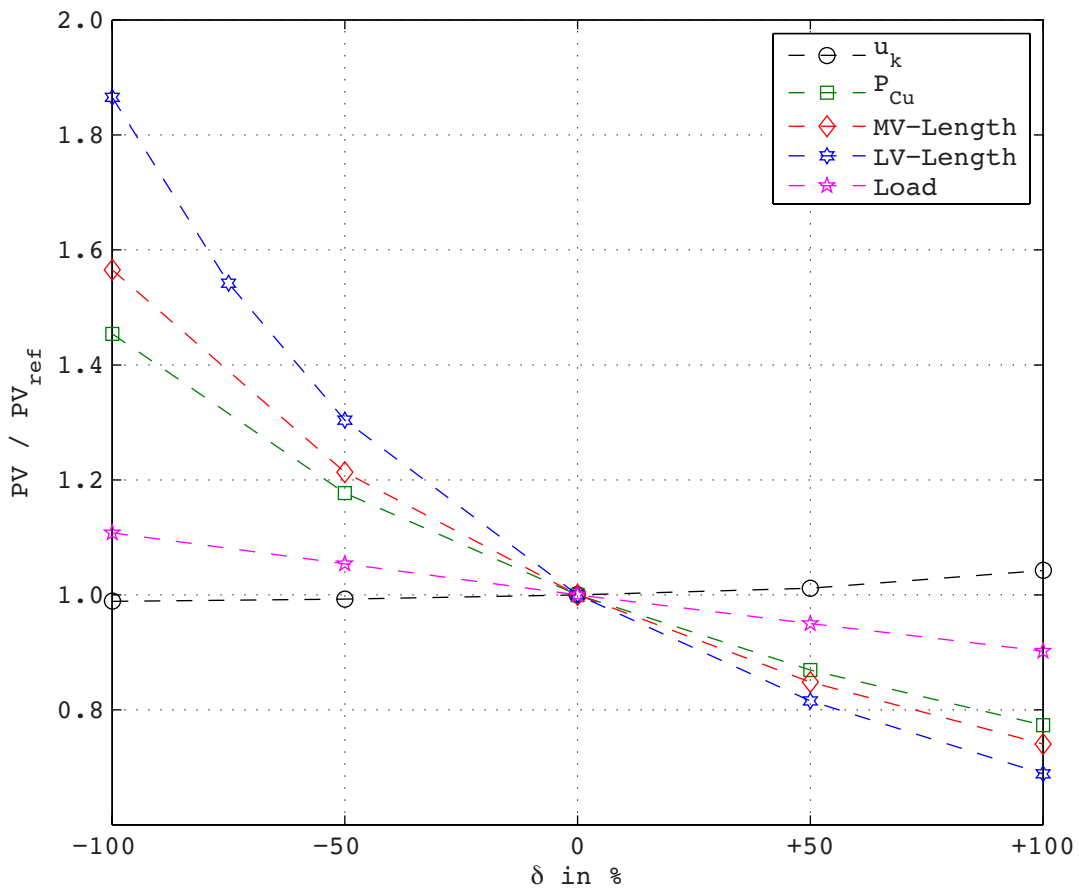


Figure 4.1.5.: Sensitivity analysis of the urban model grid (variation of: u_k , P_{Cu} , MV-Length, LV-Length, consumer load).

A line length of 0% from the initial value is represented by the direct connection of all distributed generators at the distribution transformer's secondary busbar. To emphasize the non-linear relation

between line lengths and the achievable feed-in capacity, an additional simulation was conducted for the low voltage line with 25% of its initial value. The highest voltage rise was observed at the remotest point of common coupling within the remotest supplied low voltage grid at the longest medium voltage stub PCC.U.F1.5.

4.1.6. Equipment Variation

In section 4.1.5, a steady variation of several important model grid parameters was performed. However, in real grids only few of these parameters allow a variation on a small scale, thus making it difficult to influence a real grid with them.

Therefore special equipment variations were performed for the urban model grid. The distribution transformers which step down the medium voltage from 10 kV to 0,4 kV, were altered in their rated powers from 160 kVA up to 1250 kVA, while retaining transformer parameters from real transformers, used in the distribution system of Wien Energie Stromnetz GmbH. In addition, also the low voltage cable lines were varied in their cross section from the lowest value of 50 mm² up to a parallel routing of 3 cable lines with a cross section of 150 mm². The used conductor material was aluminium for all performed simulations. The consumer load of 0,5 kW for a single household, resulting in a load of 10 kW at each point of common coupling was kept constant.

The main focus of the urban model grid was the observation of system restrictions due to equipment loadings. Thus, the voltage rise threshold was neglected for one part of the simulations. For the other part the loading of the affected lines and transformers was ignored in order to illustrate the possible capacities for distributed generation depending on the used cable lines and transformers, while keeping the resulting voltage rise within the given thresholds.

The resulting distribution transformer variation can be seen in figure 4.1.6. The maximum possible generator output power for a single coupling point was evaluated while keeping the loading of the transformer beneath the given threshold of 60% of its rated value. The diagram shows the expected linear relation between the transformer rated power and the possible feed-in capacity at every point of common coupling within the low voltage distribution grid.

Transformers with rated powers of 1000 kVA and above led to energy transports, which overloaded the affected low voltage lines. The diagram in figure 4.1.6 also includes the possible upper limit for the feed-in power at each coupling point regarding the aluminum cable cross section and the corresponding load current, set to 60% of its maximum value. The standard cross section for low voltage aluminum cable lines in the deployed model grid was 150 mm². With this cross section, transformers up to 800 kVA in rated power, represented the limiting factor for distributed generation. If transformers with higher rated powers were used, the feed in capacity was limited by the cable lines.

The smallest simulated cross section was 50 mm², which is still sufficient to transfer the maximum possible transmission power for distribution transformers up to 400 kVA, while still keeping an additional capacity of transmission power for the lines themselves. For distribution transformers with higher rated powers, the 150 mm² aluminium cable in single routing, showed insufficient loading thresholds and had to be reinforced.

Figure 4.1.7 follows the same approach. However, the voltage at the remotest point of common coupling within the low voltage section, which shows the highest rise, was used as evaluation base. The possible feed-in power of the distributed generators increased with higher transformer rating powers due to the changing transformer parameters. The same behavior can be observed at the parameter variation for the sensitivity analysis in figure 4.1.5. The equipment loading of the low voltage cable lines and distribution transformers was neglected during the simulations. The resulting figure shows how the used transformer indirectly influences the voltage levels during normal load conditions and in times of increased distributed generation.

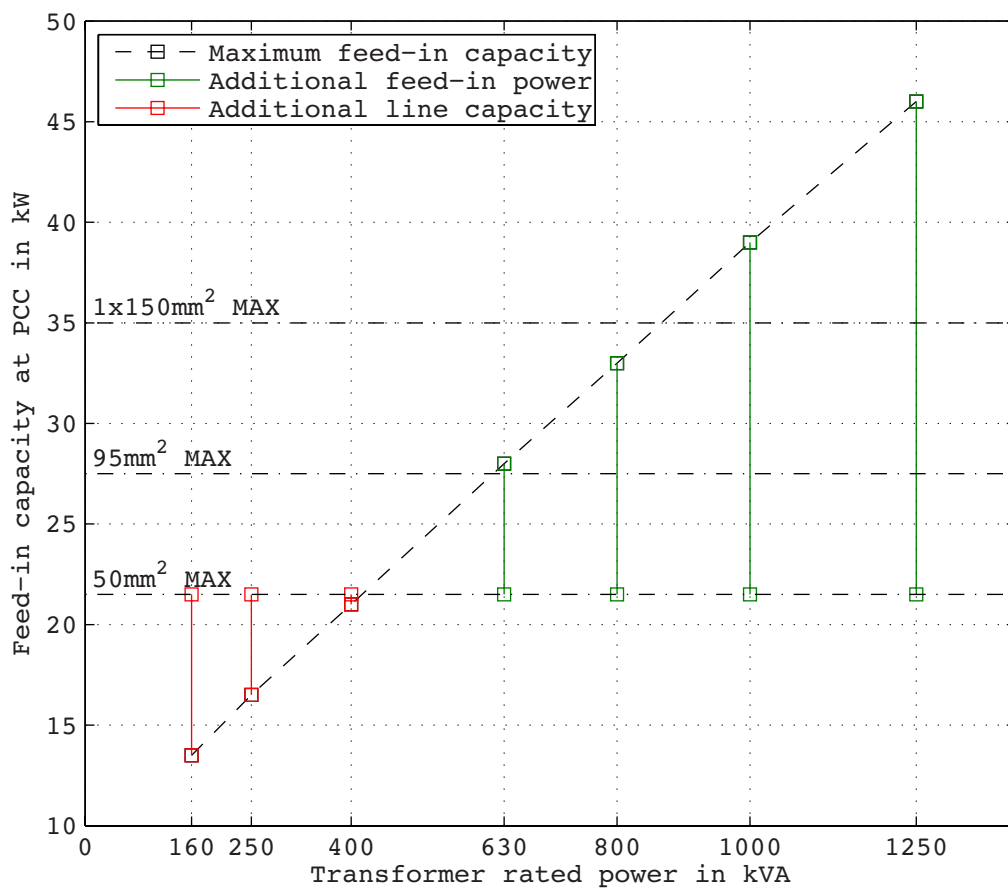


Figure 4.1.6.: Distribution transformer variation for the urban model grid (voltage threshold neglected).

Transformer rated power S in kVA	160	250	400	630	800	1000	1250
Max PV at PCC in kW	13,5	16,5	21,0	28,0	33,0	39,0*	46,0*

* Loading threshold of 60% at LV-Line exceeded

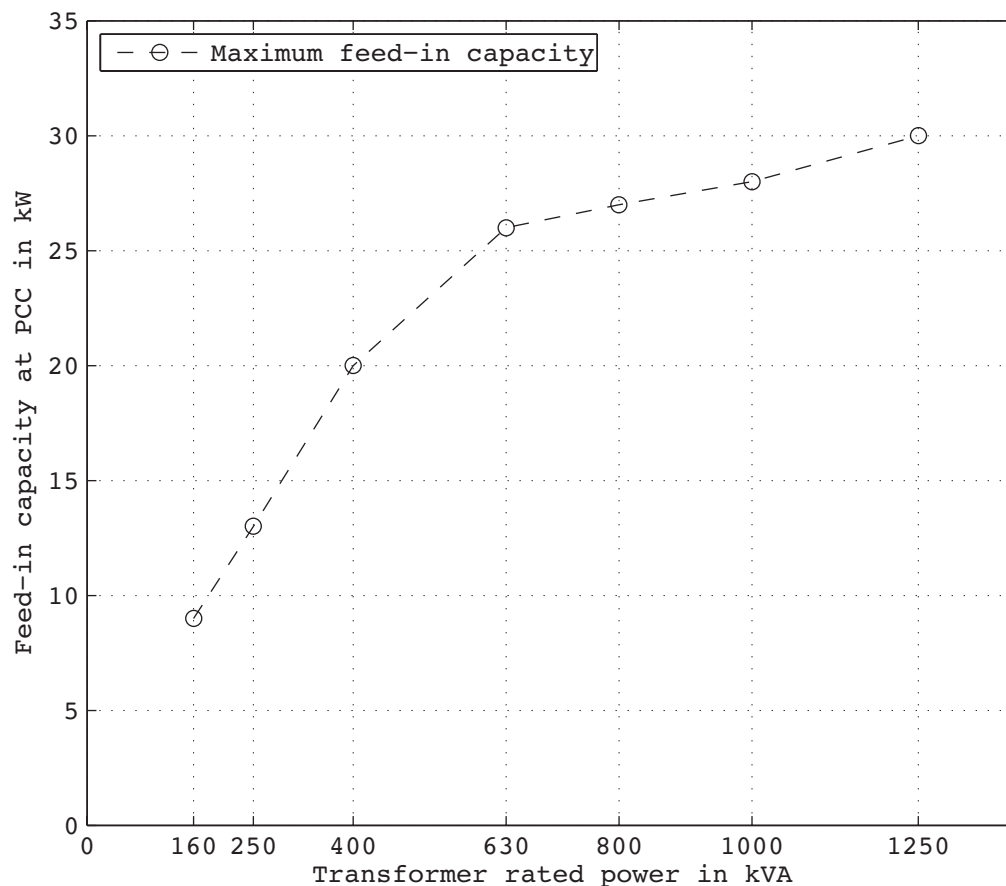


Figure 4.1.7.: Distribution transformer variation for the urban model grid (equipment loading neglected).

Transformer rated power S in kVA	160	250	400	630	800	1000	1250
Max PV at PCC in kW	9,0	13,0	20,0	26,0	27,0	28,0	30,0

To illustrate the relation between the cable cross section and the resulting loading thresholds, several simulations with different cross section values of real cable lines, stated in table 3.1.3, were conducted in figure 4.1.8. The loading thresholds for the specified transformers are also included in the graph. For the used distribution transformer with a rated power of 630 kVA in standard configuration, a cable cross section of 150 mm² was needed, in order to satisfy the upper limit for the resulting load currents due to the achievable feed-in power by the attached distributed generators. This cross section was also sufficient for the use of transformers with a rated power of 800 kVA. Transformers with higher rated powers required a grid reinforcement. The next step for the simulations was a parallel routing of 2 cable lines with a cross section of 150 mm² and aluminium as conductor material. Regarding the existing low voltage grid structure, a cross section of 50 mm² was able to supply the attached consumer loads and generators at all load conditions without any loading threshold violations, for distribution transformers with rated powers of 400 kVA and below.

Figure 4.1.9 shows the relation between the achievable feed-in power and the cable cross section, if only

the threshold of $\Delta u = +3\%$ for the resulting voltage rise is considered. All values lie below the maximum values for the loading threshold in figure 4.1.8. When the output power of the distributed generators was increased, the voltage threshold was reached before the loading threshold of the used cable lines for all observed cross sections. The non-linear influence can also be observed at the cable lengths variation in the sensitivity analysis shown in figure 4.1.5.

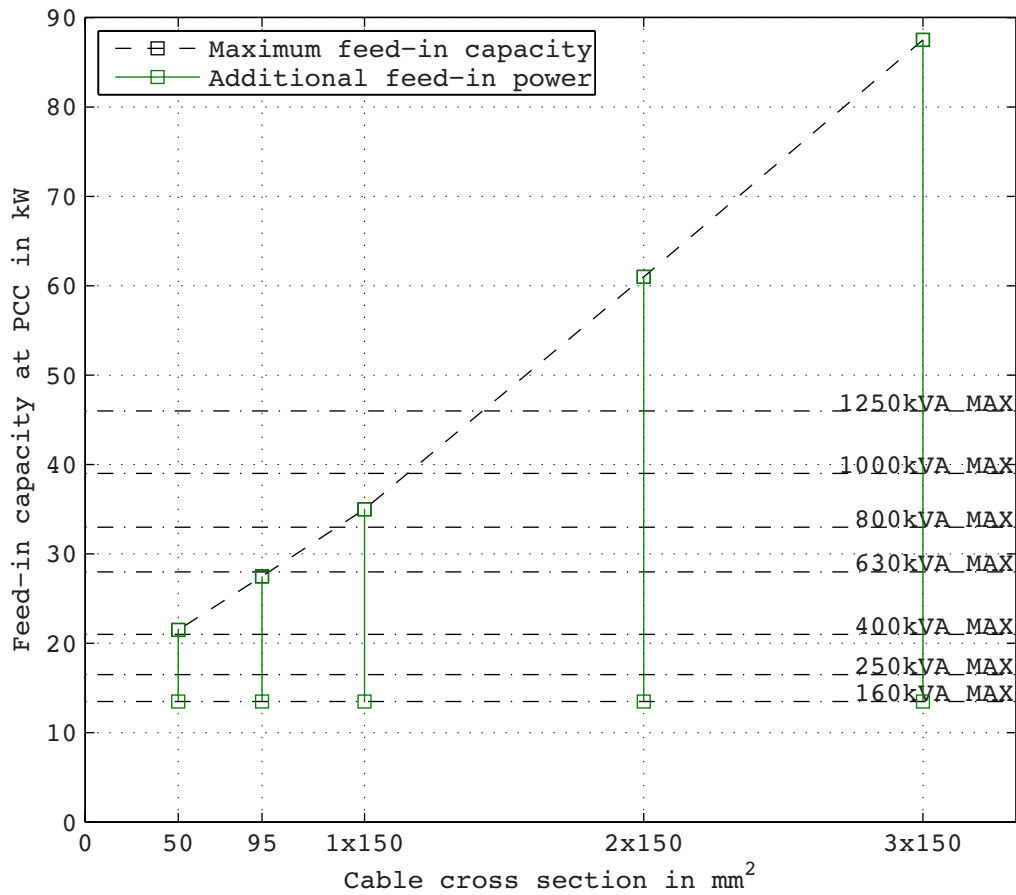


Figure 4.1.8.: Cable cross section variation for the urban model grid (voltage threshold neglected).

Cross Section in mm ²	50	95	150	2×150	3×150
Max PV at PCC in kW	21,5	27,5	35,0	61,0*	87,5*

* Transmission capacity of distribution transformer exceeded

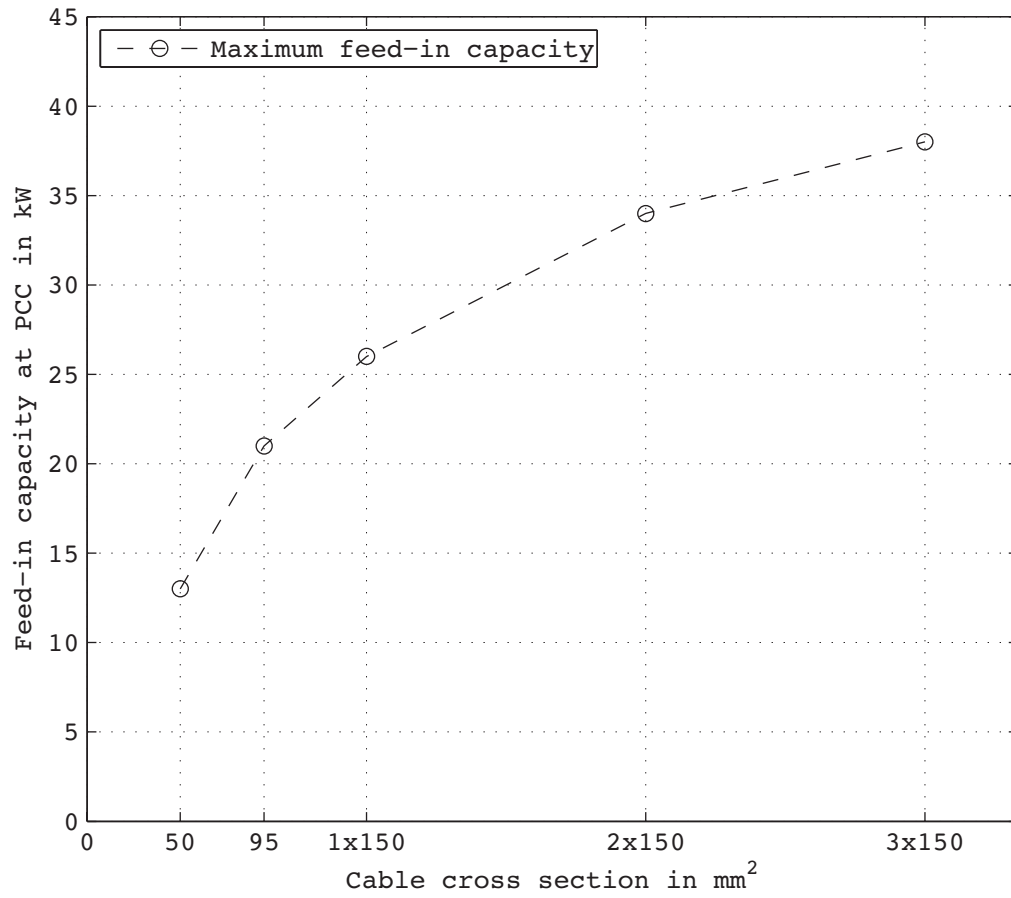


Figure 4.1.9.: Cable cross section variation for the urban model grid (equipment loading neglected).

Cross Section in mm ²	50	95	150	2×150	3×150
Max PV at PCC in kW	13,0	21,0	26,0	34,0	38,0

4.2. Suburban Model Grid

For the suburban model grid, the apartment buildings were replaced with detached single-family houses. In comparison to the urban model grid, the distances between the observed houses were increased which meant a slightly higher line length between the coupling points. Due to the higher number of coupling points supplied by one feeder, the total line length of a complete low voltage stub however increased significantly in comparison to the urban model grid. Overhead lines were used in the second low voltage section to supply the attached consumer loads, as a result of the real network parameters taken into consideration for developing the model grid. Figure 4.2.1 shows the low voltage network structure for the developed suburban model grid.

The line resistances increased due to the lower cross section of the overhead lines and the used material, leading to higher voltage drops, thus making the suburban model grid suitable for evaluating the effects of different network parameters onto the voltage rise. The limiting factor for distributed feed-in capacities was the allowed voltage rise, stated in chapter 2.7.

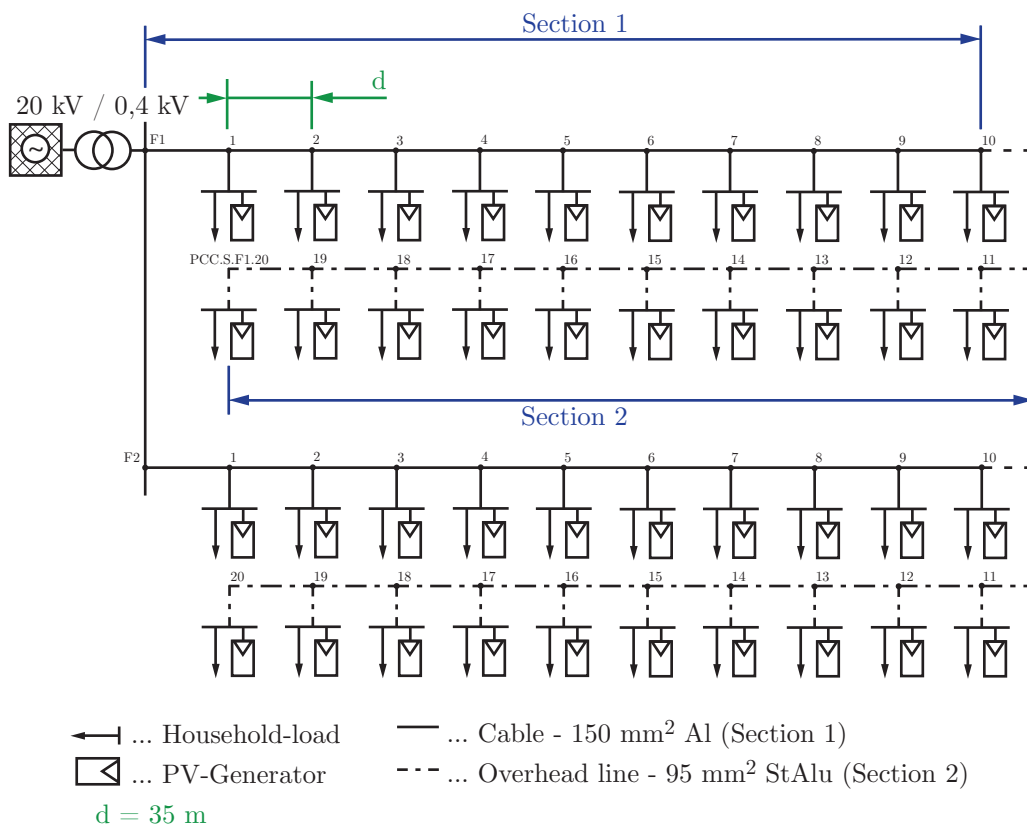


Figure 4.2.1.: Low voltage structure of the suburban model grid.

In chapter 3.2.2 a distribution transformer with a rated power of 400 kVA was determined to supply each low voltage grid connected to the modeled medium voltage stub. The resulting possible transformer loading, set to 60% of its maximum value, did not limit the possible feed-in capacities achievable in the suburban model grid. A comparatively high feed-in power at every coupling point was needed to reach considerable equipment loadings. However, in every observed case the voltage rise limit of $\Delta u = +3\%$ was reached first. To achieve the listed feed-in powers, different measures to decrease the voltage levels, like a

grid reinforcement, reactive power management or the use of regulating distribution transformers, had to be realized. With the help of these measures it was possible to increase the amount of distributed generation. However, depending on the chosen method, also the equipment loading was increased in most cases.

Figure 4.2.2 shows the structure of the performed simulations regarding the suburban model grid. Basic power flow simulations were performed for the standard grid configuration and 400 kVA distribution transformers. To increase the achievable feed-in capacity of the model grid, further simulations, including reactive power provision by the distributed generators, a grid reinforcement with cable lines instead of overhead lines, a centralized reactive power management and regulating distribution transformers, were conducted.

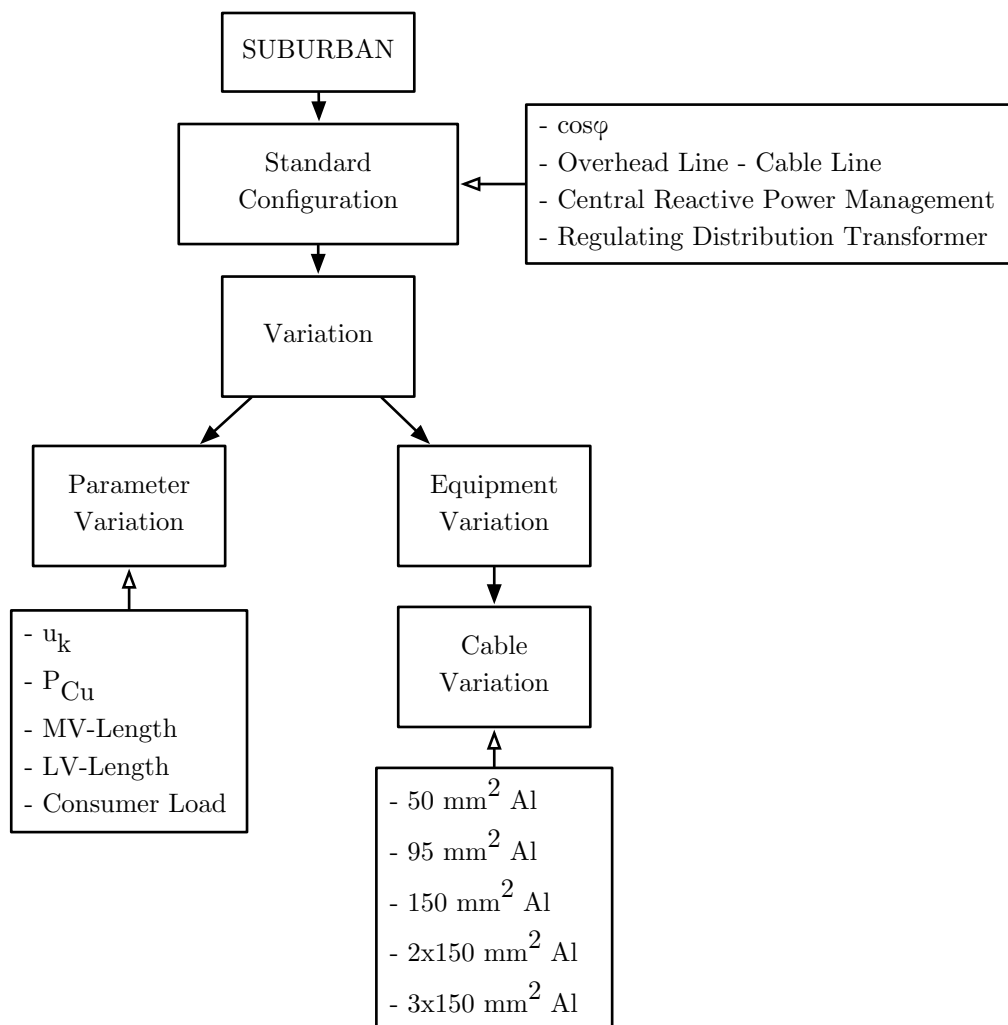


Figure 4.2.2.: Performed simulations for the suburban model grid.

To illustrate the general model grid behavior, towards changes in the characteristic grid parameters, a sensitivity analysis was performed with the standard grid configuration. For a detailed cable cross section variation, the overhead lines in the low voltage section were replaced with aluminium cable lines and their cross section was altered.

With the chosen grid structure and consumer load allocation, only a change from overhead lines to cable lines or the use of a regulating distribution transformer, did not lead to higher equipment loadings. Cable lines resulted in a lower voltage rise due to the reduced reactance values. In the following cases, also higher cross sections were used, which led to reduced resistance values and consequently to a further lowering of the voltage drop.

Regulating distribution transformers affected the voltage level of the complete low voltage grid supplied by them. With them it was possible to assure a voltage rise within the given thresholds even at high distributed generation powers.

Other measures, based on reactive power balance, depend on additional power transmissions from the overlaid medium voltage grid and therefore resulted in a higher cable and transformer loading.

4.2.1. Simulation Parameters

The following general assumptions were applied onto all simulations performed for the suburban model grid. The regulation of the tap-changer, stepping down the 110 kV from the slack node to the medium voltage, was activated for all simulations. In comparison to the urban model grid, the nominal voltage for the medium voltage level was 20 kV instead of the former 10 kV. The operation voltage was set to 20,4 kV, and was kept near this value automatically by the regulating transformer. As mentioned before, a possible remaining voltage difference was caused by the discrete voltage steps of the regulation. The higher voltage level, applied in the suburban area, should also help to reduce the transport losses resulting from the higher line lengths and lower cross sections. However the insulation efforts increase with higher voltage levels.

Table 4.2.1.: Simulation parameters for the suburban model grid.

Transformer regulation (110 kV / 20 kV)	active
Operating voltage (20 kV)	20,4 kV
Maximum equipment loading	60%
Consumer load at PCC	0,5 kW
Node with highest voltage rise	PCC.S.F1.20

During all simulations the consumer load for every single detached house was set to 0,5 kW. One low voltage stub supplied 20 detached houses, resulting in a total load of 10 kW for a single feeder. The used low voltage model grid contained two identical low voltage stubs. Every distribution transformer was therefore supplying a load of 20 kW. The distributed generators were once again defined as evenly allocated photovoltaic systems. Every coupling point represented by the corresponding house connection included one distributed generator, feeding in its produced electrical power at this point. Due to the lower possible generation capacity expected for the suburban grid, the photovoltaic output power was discretized within steps of 0,5 kW instead of the 1 kW steps, used for the urban grid.

The chosen suburban area offers the installation of freestanding photovoltaic systems. The actual possible photovoltaic system capacity is not limited by the available roof size of the selected house. This results in higher possible generator sizes for real applications.

With the present network structure, the highest voltage rise was achieved at the remotest point of common coupling in the remotest low voltage grid supplied by the observed medium voltage stub. This point

can be seen as PCC.S.F1.20 in figure 4.2.1. Therefore this coupling point was used for the evaluation of the performed simulations. Both low voltage stubs showed the same load and generator allocation. The two voltage profiles were therefore identical.

The medium voltage structure of the suburban model grid was already used for the urban model grid. With the lower resulting load currents due to the consumer loads and distributed generators, the resulting voltage rise in the medium voltage level was never about to reach the $\Delta u = +2\%$ threshold [7]. The evaluation of the voltage rise at the medium voltage level could therefore be disregarded.

4.2.2. Simulation Sequence

Table 4.2.2 shows in which order the simulations were performed, and the respective feed-in power together with the simulation title. The achieved voltage rises and equipment loadings for these simulations can be seen in section 4.2.3.

Table 4.2.2.: List of simulations for the urban model grid.

Standard Configuration		
Simulation #	PV in kW	Simulation title
1	0,0	Idle state, load only (Reference)
2	2,5	Max PV
3	3,5	Max PV (Reactive power provision)
Overhead Lines Exchanged With Cable Lines		
Simulation #	PV in kW	Simulation title
4	0,0	Idle state, load only (Reference)
5	2,5	Max PV
Regulating Transformer		
Simulation #	PV in kW	Simulation title
6	0,0	Idle state, load only (Reference)
7	5,5	Max PV
Central Compensation Unit		
Simulation #	PV in kW	Simulation title
8	3,0	Max PV - 50 kvar
9	4,0	Max PV - 100 kvar
10	4,5	Max PV - 150 kvar

Reactive Power Provision by the Distributed Generators

Simulation number 1 determined the basic reference values for the voltage rise and the transformer and cable loadings. Therefore the standard configuration of the low voltage grid with a standard 400 kVA distribution transformer was used. The simulation for the reference values included the consumer loads stated above but was performed without distributed generation. While the constraints in chapter 2.7 were satisfied, it was possible to achieve a feed-in power as high as 2,5 kW for every single generator without exceeding the $\Delta u = +3\%$ threshold of the voltage rise, thus making this value the feed-in capacity for the chosen model grid without additional measures. The respective results are included in simulation 2.

When the distributed generators took part in the reactive power management, it was possible to reach higher capacities. With a power factor of 0,95 lagging, as used in simulation 3, the output power of the generators could be increased to 3,5 kW, while still staying within the allowed voltage levels. Figure 4.2.3 shows the voltage profile of the observed low voltage stub in normal configuration and with reactive power provision by the attached generators. The voltage rise Δu at the remotest coupling point was kept at 3% in both cases. However, due to the reactive power provision it was possible to increase the feed-in power of every generator by 1 kW.

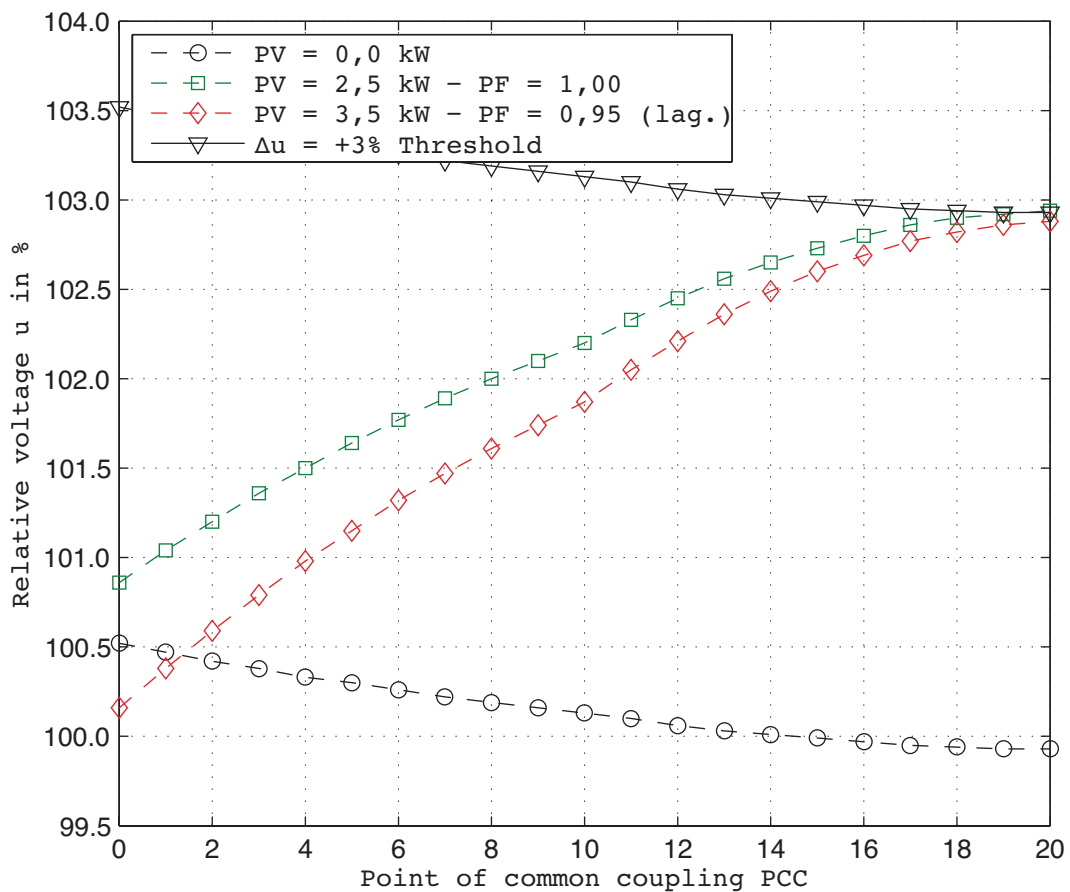


Figure 4.2.3.: Voltage profile of the suburban model grid (reactive power provision).

Replacement of Overhead Lines With Cable Lines

The simulations 4 and 5 should emphasize how the change from overhead lines to cable lines in section 2 of the low voltage grid, affects the voltage levels. Figure 4.2.4 depicts the change in the model grid configuration. Case A represents the standard grid configuration, whereas in Case B the overhead lines in section 2 where replaced with cable lines of the same material and cross section, as present in section 1. Simulation number 4 displays the reference values with the chosen consumer load and without active generation. The lower line impedance led to smaller voltage drops caused by the power transmission due

to distributed generators and thus decreased the resulting voltage rise. However, also with a continuous cable line between all coupling points it was not possible to rise the feed-in capacity to 3 kW, without exceeding a voltage rise of $\Delta u = +3\%$. The load currents in section 2 were too low to have a significant effect onto the voltage level within the range of the two different line impedances.

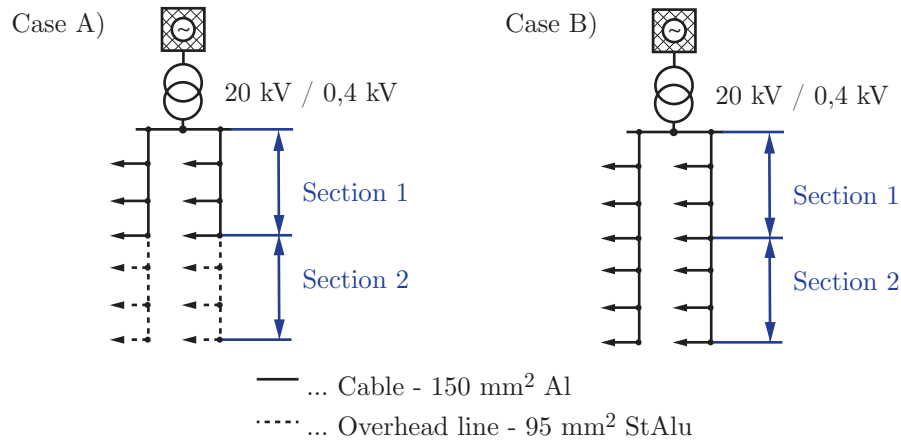


Figure 4.2.4.: Model grid configuration for the comparison between overhead lines and cable lines.

Regulating Distribution Transformers

When 400 kVA regulating transformers were used, which regulated their secondary busbar voltage according to a measurement value from the remotest coupling point, the feed-in capacities could be drastically increased. The default value for the regulation was set to 100% of the standard 0,4 kV phase-to-phase voltage. Simulation number 6 defines the reference values for the simulations performed with regulating transformers. Without distributed generators the power flow caused the voltage at the end of the line to drop beneath the supply voltage at the busbar. To keep the voltage at the set value, the regulation changed the transmission ratio of the transformer. As mentioned before, a small difference in the voltage was observed due to the discrete regulation steps. With this method, the total feed-in capacity for every coupling point was increased to 5,5 kW. Higher values were not possible due to the restriction of the resulting voltage rise. Another possible setup for the regulating transformer would have been the regulation of the busbar voltage according to a fixed value while measuring the busbar voltage instead of the voltage at a remote coupling point.

Central Reactive Power Management

In the simulations 8 to 10 the application of central reactive power compensation units within the low voltage grid is discussed. To reduce the voltage rise, compensation systems were installed at the transformers secondary busbar, which drew an inductive load in case of a high distributed energy generation. For the suburban model grid, the sizes of these systems were determined to be 50 kvar, 100 kvar and 150 kvar units. As a result, the generation capacity was increased from 2,5 kW without power factor correction up to 4,5 kW with the 150 kvar unit. However, the reactive power for the units was not produced within the low voltage grid. Therefore it had to be transported from the higher network levels to the low voltage busbar at the transformer, which caused additional losses and equipment loadings. In simulation 10 the upper loading limit of 60% was exceeded due to the additional energy transport.

4.2.3. Simulation Results

Table 4.2.3.: Simulation results for the suburban model grid (voltage levels at PCC.S.F1.20 and distribution transformer loading for 400 kVA transformers, including reactive power provision by the inverters, the exchange of overhead lines with cable lines, regulating transformers and a centralized reactive power management).

400 kVA - Distribution Transformer (Standard Configuration)							
#	Load in kW	PV in kW	u max in %	Δu in %	Distribution Transformer		
					I in A (sec.)	Loading in %	
1	0,5	0,0	99,9	-	30,0	5,1	
2	0,5	2,5	102,9	+3,0	113,0	19,6	
3	0,5	3,5 ($\cos\varphi=0,95$)	102,9	+3,0	185,0	32,0	
Overhead Lines Exchanged With Cable Lines							
4	0,5	0,0	100,0	-	30,0	5,1	
5	0,5	2,5	102,7	+2,7	113,0	19,6	
400 kVA - Regulating Distribution Transformer							
#	Load in kW	PV in kW	u max in %	Δu in %	Distribution Transformer		
					I in A (sec.)	Loading in %	
6	0,5	0,0	101,2	-	29,0	5,1	
7	0,5	5,5	104,0	+2,8	283,0	49,0	
Central Compensation Unit (50 kvar / 100 kvar / 150kvar)							
#	Load in kW	PV in kW	u max in %	Δu in %	Distribution Transformer		
					I in A (sec.)	Loading in %	
8	0,5	3,0	102,7	+2,8	163,0	28,2	
9	0,5	4,0	102,9	+3,0	252,0	43,6	
10	0,5	4,5	102,6	+2,7	324,0	56,1	

Table 4.2.4.: Simulation results for the suburban model grid (line loading of the first medium voltage line at the 40 MVA medium voltage feeder and the first low voltage line at the feeder F1, for 400 kVA transformers, including reactive power provision by the inverters, the exchange of overhead lines with cable lines, regulating transformers and a centralized reactive power management).

400 kVA - Distribution Transformer (Standard Configuration).						
#	Load in kW	PV in kW	1. MV-Line		1. LV-Line	
			I in A	Loading in %	I in A	Loading in %
1	0,5	0,0	7,0	1,8	15,0	5,0
2	0,5	2,5	21,0	5,1	57,0	18,9
3	0,5	3,5 ($\cos\varphi=0,95$)	31,0	7,7	92,0	30,8

Overhead Lines Exchanged With Cable Lines						
#	Load in kW	PV in kW	1. MV-Line		1. LV-Line	
			I in A	Loading in %	I in A	Loading in %
4	0,5	0,0	7,0	1,8	15,0	5,0
5	0,5	2,5	21,0	5,1	57,0	18,9

400 kVA - Regulating Distribution Transformer						
#	Load in kW	PV in kW	1. MV-Line		1. LV-Line	
			I in A	Loading in %	I in A	Loading in %
6	0,5	0,0	7,0	1,8	15,0	4,9
7	0,5	5,5	50,0	12,2	141,0	47,1

Central Compensation Unit (50 kvar / 100 kvar / 150 kvar)						
#	Load in kW	PV in kW	1. MV-Line		1. LV-Line	
			I in A	Loading in %	I in A	Loading in %
8	0,5	3,0	27,0	6,6	71,0	23,7
9	0,5	4,0	42,0	10,3	100,0	33,2
10	0,5	4,5	54,0	13,3	114,0	38,1

4.2.4. Achievable Feed-In Capacity

According to the different measures for reducing the voltage rise, certain distributed generation capacities were achieved without violating the $\Delta u = +3\%$ threshold. Figure 4.2.5 illustrates the effects of the explained methods onto the possible generator output power at each point of common coupling.

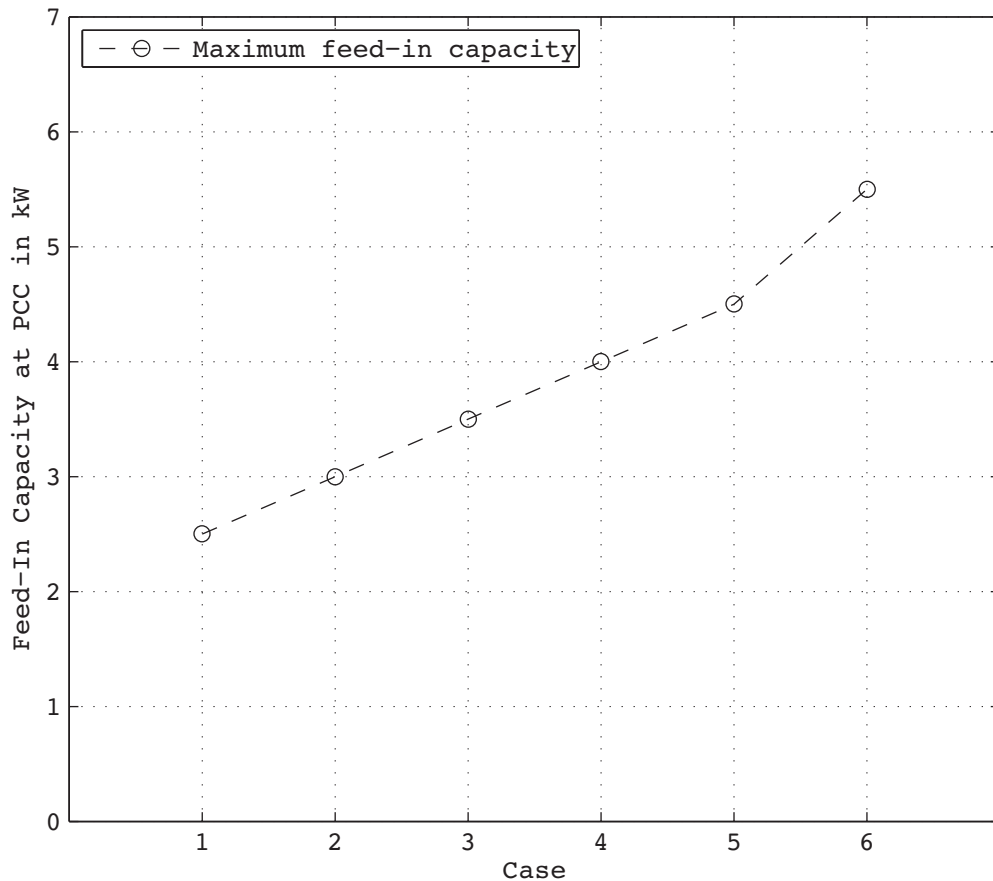


Figure 4.2.5.: Feed-In capacity of the suburban model grid.

The upper limits for the output power of the attached distributed generators at every single point of common coupling, and the measures realized to achieve it, are stated in table 4.2.5.

Table 4.2.5.: Upper limits for the feed-in power regarding the voltage rise.

Case	Simulation #	Max PV at PCC in kW	Measure to increase PV
1)	2, 5	2,5	$\cos\varphi = 1,00$, cable lines
2)	8	3,0	50 kvar compensation
3)	3	3,5	$\cos\varphi = 0,95$ (lagging)
4)	9	4,0	100 kvar compensation
5)	10	4,5	150 kvar compensation
6)	7	5,5	Regulating distribution transformer

For the existing grid structure, the feed-in capacity and the different methods to increase it, show a linear relation. The highest generator output power was realized with a regulating distribution transformer, as seen in point 6. Due to the low load currents, especially in the low voltage section 2 depicted in figure 4.2.1, the influence of the line resistance in this part had no distinct effect on the voltage rise for the simulated cases. In Simulation number 5, the overhead lines in section 2 were replaced with cable lines. However, the resulting lower resistance due to the higher cross section did not lower the voltage level enough to increase the generator output powers as seen in point 1 in figure 4.2.5.

4.2.5. Parameter Variation - Sensitivity Analysis

To illustrate the influence of different network parameters from the suburban model grid, a sensitivity analysis was conducted. The resulting relations between the parameter variations and the change in the achievable output power of the distributed generator are shown in figure 4.2.6. Selected parameters for the variation were:

- Distribution transformer - related impedance voltage u_k
- Distribution transformer - copper losses P_{Cu}
- Length of medium voltage lines - MV-Length
- Length of low voltage lines - LV-Length
- Attached consumer load at PCC

As seen in section 4.1.5, the parameters were varied in a range from $\delta = 0\%$ to $\delta = 200\%$ of their initial values, independently from each other in steps of 50%. For every variation, the possible output power for all distributed generators at their coupling point was evaluated while keeping the voltage levels within the constraints stated in section 2.7. Simulation number 2, performed in section 4.2.2, defines the initial state for the variations including following base values:

- $u_k = 6,0\%$
- $P_{Cu} = 5,0 \text{ kW}$
- MV-Length = 422 m
- LV-Length = 35 m / 35 m
- Load = 0,5 kW

The resulting figure 4.2.6 shows, how each parameter influences the achievable feed-in capacity of the suburban model grid. The increasing number of consumer loads resulted in a considerably higher overall low voltage length, thus making the voltage rise the limiting factor for distributed generation. When these lengths were reduced to lower values, the voltage drop was non-linearly lowered, which led to a severe increase of the achievable feed-in powers for the generators. An additional simulation with $\delta = 25\%$ of the low voltage lengths initial value was performed to illustrate the non-linear characteristics, caused by this effect. Furthermore, the low voltage line length was scaled on a secondary y-axis due to the increased value range. The comparison between the effects caused by the low voltage and medium voltage line lengths shows the dominance of the low voltage level. The highest voltage rise was as expected, observed

at the remotest point of common coupling within the remotest supplied low voltage grid at the longest medium voltage stub PCC.S.F1.20.

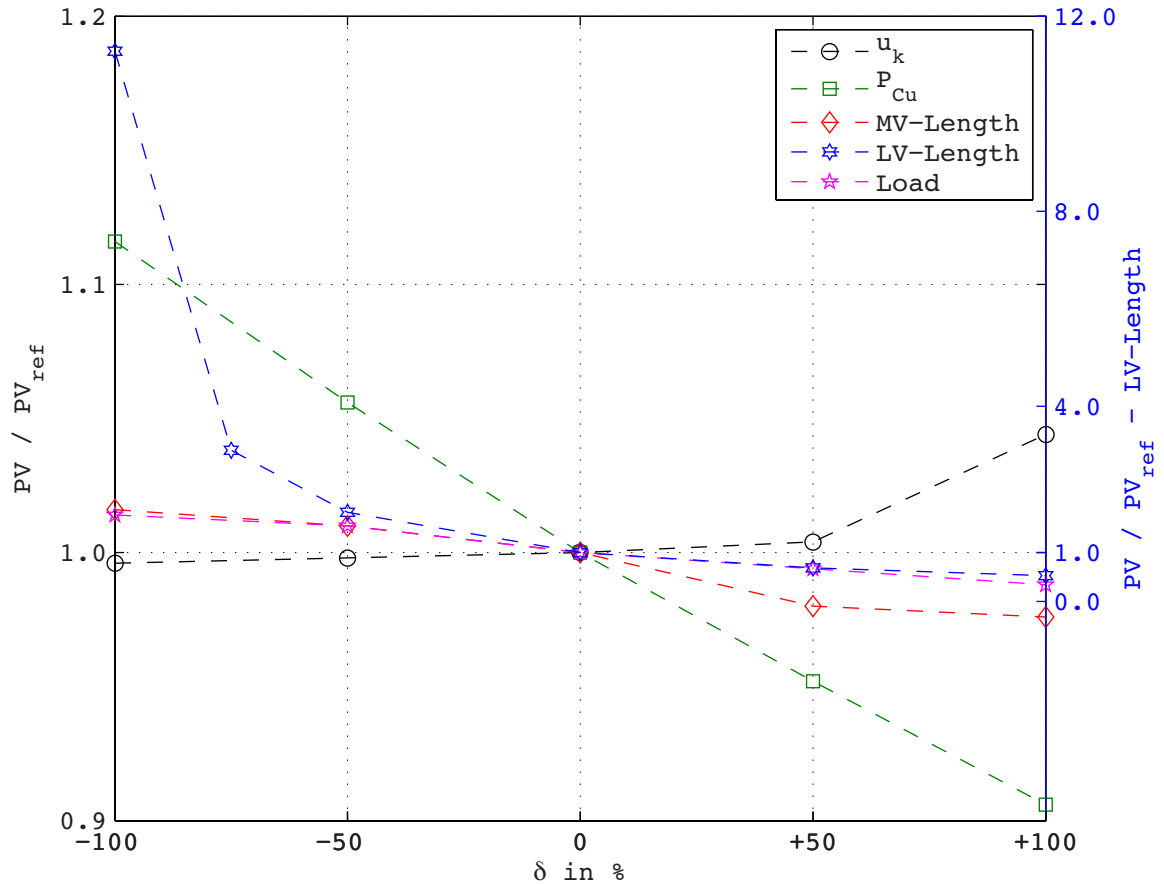


Figure 4.2.6.: Sensitivity analysis of the suburban model grid (variation of: u_k , P_{Cu} , MV-Length, LV-Length, consumer load).

4.2.6. Equipment Variation

In addition to the steady parameter variation in section 4.2.5, an equipment variation was performed for the low voltage lines of the suburban model grid. The overhead lines in section 2 were replaced with cable lines for all variations. Aluminium was used as conductor material and the cross section was varied from 50 mm² in single routing, up to 3 parallel lines with a cross section of 150 mm², regarding real cable values from the company Wien Energie Stromnetz GmbH. For both sections the same cable lines with the same cross sections were used. The constraints for the supply voltage level from section 2.7 were not violated throughout all simulations.

Figure 4.2.7 shows the linear relation between the achievable generator output power and the cross section. As mentioned before, the output power was changed in discrete steps of 0,5 kW, which led to a small divergence from a nearly linear relation. The non-linear characteristics, seen at the cable variation in the urban model grid, however did not occur in the suburban model grid, due to the relatively low

load currents. Smaller cross sections than 50 mm^2 would lead to increasing line resistances and finally to a non-linear behavior of the voltage rise.

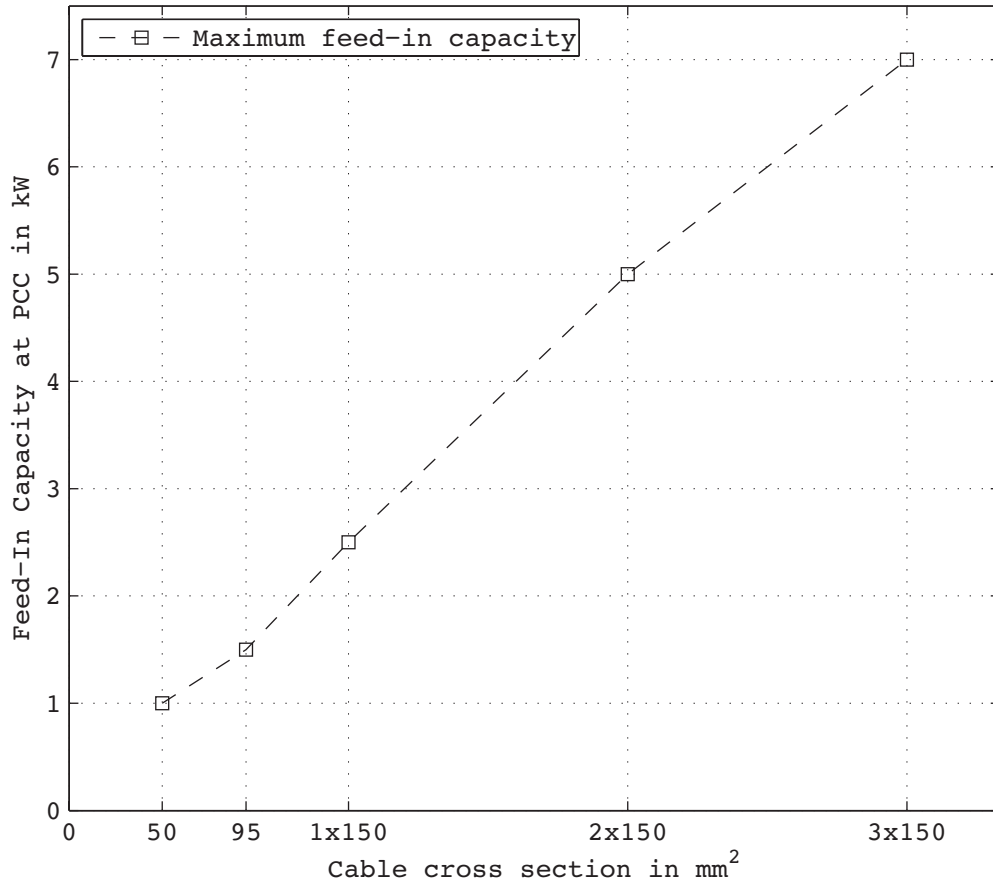


Figure 4.2.7.: Cable cross section variation for the suburban model grid.

Cross Section in mm ²	50	95	150	2×150	3×150
Max PV in kW	1,0	1,5	2,5	5,0	7,0

4.3. Rural Model Grid

The rural model grid was meant to describe the difficulties for distributed generation in so called extreme value grids. Based on real network segments with very high line lengths and low cross sections, a model grid was developed in section 3.2.3. The low voltage network structure of the rural model grid can be seen in figure 4.3.1.

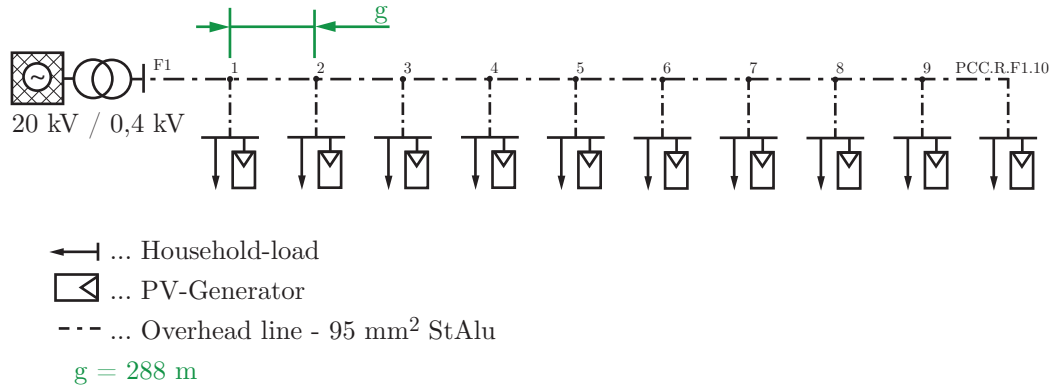


Figure 4.3.1.: Low voltage structure of the rural model grid.

In contrary to the urban and suburban grids, the medium voltage section not only included cable lines but also overhead lines. The corresponding low voltage grids were modeled as overhead line networks only. Line lengths within the low voltage section increased significantly, whereas the load density decreased. Thus, the resulting higher line impedances lead to substantial voltage drops. The power flow caused by the consumer loads in normal operation led to a high voltage difference at the remote coupling points, compared to the expected operational voltage. Therefore even a low output power of possibly available distributed generators caused a high voltage rise at their respective connection point. The threshold for the voltage rise, mentioned in chapter 2.7 represented a massive restriction for the possible output power of the installed generators.

The sizes of the chosen distribution transformers were a result of the averaging of real network segments representative for a rural supply area. For the chosen load density, the resulting rated power of 400 kVA was relatively high. Only simulations with high feed-in powers including the mentioned measures to decrease the voltage rise led to considerable loadings. However, the basic loading threshold of 60% for the transformers was never reached during the simulations. For the developed low voltage grid, the utilization of distribution transformers with smaller power ratings would be possible.

In order to reach higher feed-in capacities and to examine the effects of different line lengths in detail, the low voltage grid was simulated with the full length (288 m) developed before and also with 50% (144 m) of this length. A further shortening of the line length to 20% (57,6 m) of the standard values was performed to accomplish line lengths similar to the previous model grids, making the evaluation and comparison between the results possible. Therefore simulations were performed for the standard grid configuration (LV-Length - 100% = 288 m) developed from the real network segments, and for the two line length variations of this grid (LV-Length - 50% = 144 m, LV-Length - 20% = 57,6 m).

Figure 4.3.2 shows the structure of the performed simulations regarding the rural model grid. The standard power flow simulations were performed for all three LV-Length configurations (100% = 288 m, 50% = 144 m and 20% = 57,6 m), in order to determine their achievable feed-in capacities. Further simulations including reactive power provision by the distributed generators, the exchange from overhead lines with cable lines in the low voltage section, regulating distribution transformer and a centralized reactive power management were conducted, examining their abilities to increase the feed-in capacity of the three grid configurations.

A sensitivity analysis for the standard grid configuration with a 400 kVA distribution transformer should illustrate the general grid behavior, towards changes in the characteristic grid parameters.

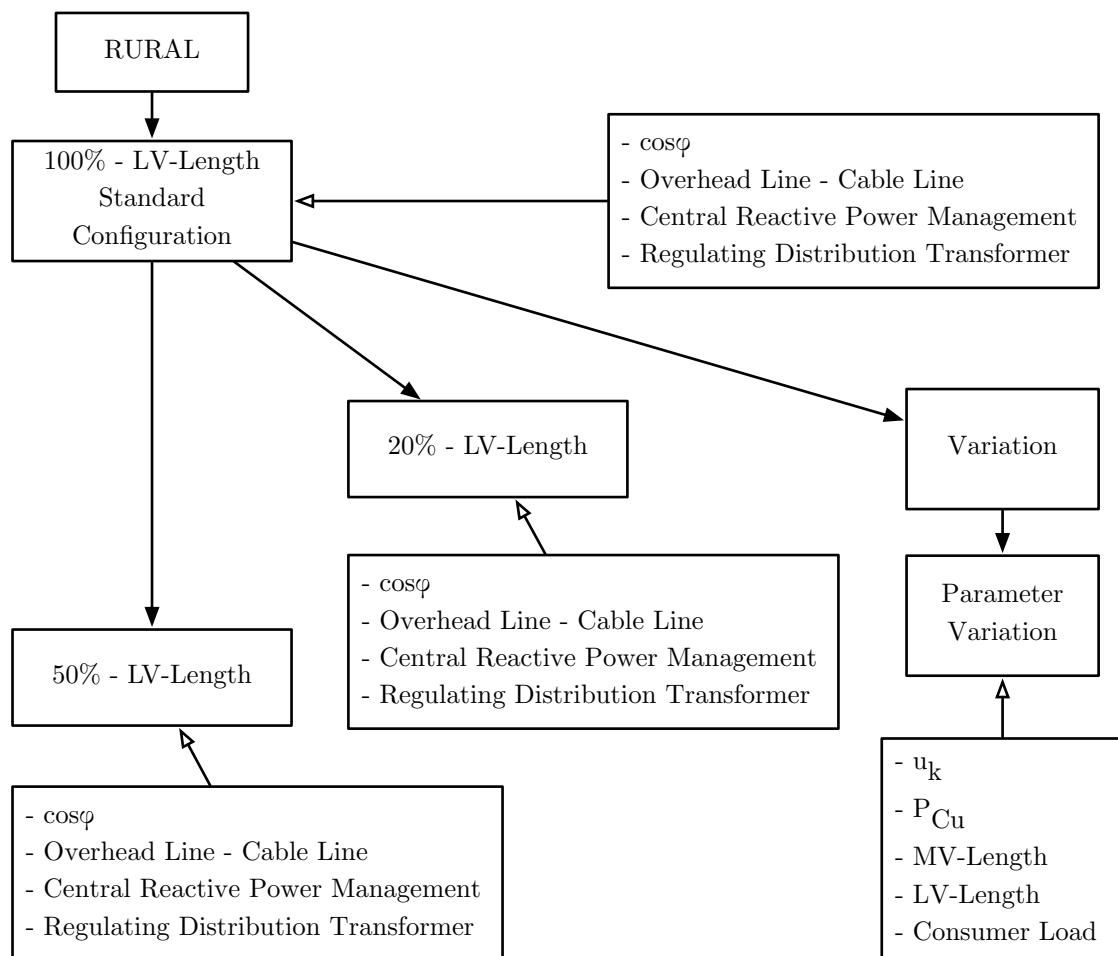


Figure 4.3.2.: Performed simulations for the rural model grid.

The increasing power flow due to the distributed generators exceeded the prior set upper loading limits of the medium and low voltage lines, if high feed-in powers were reached. Although the generator output powers were small in comparison to the urban and suburban areas, the medium voltage feeder supplied a much higher number of low voltage distribution networks. Together with the uniform allocation of the generator infeeds, high currents at the medium voltage lines near the transformer's feeder were achieved, resulting in a high equipment loading. The overhead lines, used in section two of the medium voltage grid and also for the complete low voltage grid, featured smaller cross sections. Therefore their allowed

loading values were already lower in comparison to the previously analyzed grids.

For further investigations, the fluctuating feed-in power which is a main disadvantage of renewable energy sources, could be taken into account. The developed model grid covers a large physical area, thus making local effects upon the generation determining the power flow.

4.3.1. Simulation Parameters

The following assumptions, were valid for all simulations of the rural model grid. The same 40 MVA transformer, which was already present in the urban and suburban model grid, was again used to step down the 110 kV from the overlaid high voltage transmission grid, represented by the feeding slack node. The voltage regulation of the transformer kept the voltage at the secondary busbar at the set operation voltage of 20,4 kV. Due to the discrete step size of the regulator, a permanent voltage difference was observed.

Table 4.3.1.: Simulation parameters for the rural model grid.

Transformer regulation (110 kV / 20 kV)	active
Operating voltage (20 kV)	20,4 kV
Maximum equipment loading	60%
Consumer load at PCC	0,5 kW
Node with highest voltage rise	PCC.R.F1.10

One objective for the rural grid was a lower load density in comparison to prior simulations. Therefore the number of houses supplied by one distribution transformer was reduced from 20 to 10. Represented by 10 detached houses, the loads were uniformly allocated at one single low voltage stub. In accordance with previous simulations, the consumer load was set to 0,5 kW for each detached house. With the existing structure, the total load for each low voltage grid resulted in 5 kW with the chosen operating conditions.

In the considered supply area, an increasing number of agricultural buildings are present. For these special buildings, higher consumer loads could be applied. However for the performed simulations, an increasing consumer load did not affect the possible feed-in capacity. Agricultural loads were therefore neglected for the following considerations.

However, for the estimation of possible photovoltaic system sizes within the rural area, these buildings play an important role. Due to the larger available roof sizes and the possible installation of free-standing photovoltaic systems, the real photovoltaic system capacity is not limited in terms of the needed space. The distributed generators, used for the simulations, were discretized in 0,5 kW steps. As expected, the maximum voltage rise was observed at the remotest point of common coupling within the remotest low voltage distribution grid PCC.R.F1.10. For all evaluations of the voltage levels, this point was used to verify the assessment criteria.

The observed voltage rise in the medium voltage structure, never reached values near the given threshold of $\Delta u = +2\%$ [7], although the line lengths in the medium voltage section substantially increased in comparison to the previous model grids. The evaluation of the voltage rise at the medium voltage level could therefore be disregarded.

4.3.2. Simulation Sequence

Table 4.3.2 includes the order of the performed simulations, the set feed-in power of the distributed generators and the corresponding simulation title. The results for the simulations are listed in the tables 4.3.3 and 4.3.4. All simulations were performed for the standard grid configuration and in the same way for the reduced low voltage line lengths of 50% (144 m) and 20% (57,6 m) compared to their initial reference value.

Reactive Power Provision by the Distributed Generators

The simulations 1 to 3 state the analysis for the standard configuration with the full line lengths. Simulation 1 represents the reference value for eventual voltage rises. With the existing load distribution and photovoltaic penetration, the maximum for the feed-in capacity with uniformly allocated generators was reached at 1 kW. However the threshold for the voltage rise was already exceeded with 0,4% due to the voltage drops caused by the line resistances. With the use of reactive power provision by the inverters and a power factor, set to 0,95 lagging, the voltage rise could be decreased to meet the $\Delta u = +3\%$ border. The according voltage level and equipment loadings can be seen in simulation 3. Figure 4.3.3 depicts the voltage profiles along the low voltage stub for these simulations.

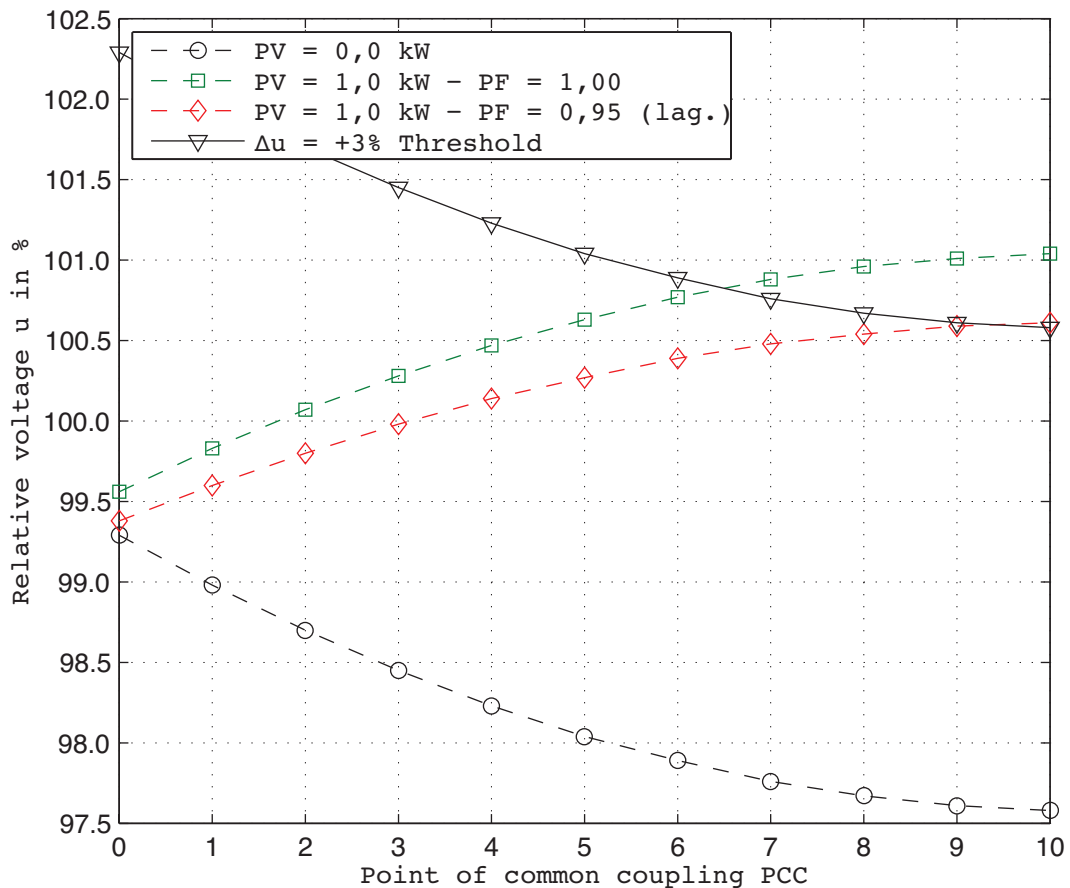


Figure 4.3.3.: Voltage profile of the suburban model grid (100% LV-Length, reactive power provision).

The same procedure was repeated for the reduced line lengths in the simulations 4 to 5 for 50%, and 7 to 8 for 20% respectively.

Table 4.3.2.: List of simulations for the rural model grid.

Standard Configuration			
Simulation #	PV in kW	Relative lengths in %	Simulation title
1	0,0	100	Idle state, load only (Reference)
2	1,0	100	Max PV
3	1,0	100	Max PV (Reactive power provision)
4	0,0	50	Idle state, load only (Reference)
5	1,5	50	Max PV
6	2,0	50	Max PV (Reactive power provision)
7	0,0	20	Idle state, load only (Reference)
8	3,0	20	Max PV
9	4,5	20	Max PV (Reactive power provision)
Overhead Lines Exchanged With Cable Lines			
Simulation #	PV in kW	Relative lengths in %	Simulation title
10	0,0	100	Idle state, load only (Reference)
11	1,0	100	Max PV
12	0,0	50	Idle state, load only (Reference)
13	2,0	50	Max PV
14	0,0	20	Idle state, load only (Reference)
15	4,5	20	Max PV
Regulating Distribution Transformer			
Simulation #	PV in kW	Relative lengths in %	Simulation title
16	0,0	100	Idle state, load only (Reference)
17	1,5	100	Max PV
18	0,0	50	Idle state, load only (Reference)
19	4,5	50	Max PV
20	0,0	20	Idle state, load only (Reference)
21	7,5	20	Max PV
Central Compensation Unit			
Simulation #	PV in kW	Relative lengths in %	Simulation title
22	1,0	100	Max PV - 50 kvar
23	1,5	100	Max PV - 100 kvar
24	2,0	100	Max PV - 150 kvar
25	3,0	50	Max PV - 50 kvar
26	4,0	50	Max PV - 100 kvar
27	4,5	50	Max PV - 150 kvar
28	6,0	20	Max PV - 50 kvar
29	8,0	20	Max PV - 100 kvar
30	10,0	20	Max PV - 150 kvar

With a low voltage line length reduced to a half of the initial value, the feed-in capacity was increased by 0,5 kW, without violating the given thresholds for the resulting voltage rise.

Reactive power provision could increase the possible feed-in powers furthermore. With the present grid configuration, however the voltage level was violated by 0,1% if the feed-in capacity was raised to 2 kW for each coupling point.

When the line lengths were reduced to 20% of the standard configurations length, the possible distributed generator feed-in power was increased to 3 kW. With reactive power provision by the inverters it was possible to increase the value to 4,5 kW for each generator. The constraints for the voltage rise were not violated.

Replacement of Overhead Lines With Cable Lines

Another possible way to reduce the line resistance and increase possible generator sizes was selective grid reinforcement in terms of line replacements. For the present model grid the existing low voltage overhead lines with a cross section of 95 mm² were replaced with cable lines featuring a cross section of 150 mm². Figure 4.3.4 depicts the change in the model grid configuration. Case A represents the standard grid configuration, whereas in Case B the overhead lines where replaced with cable lines.

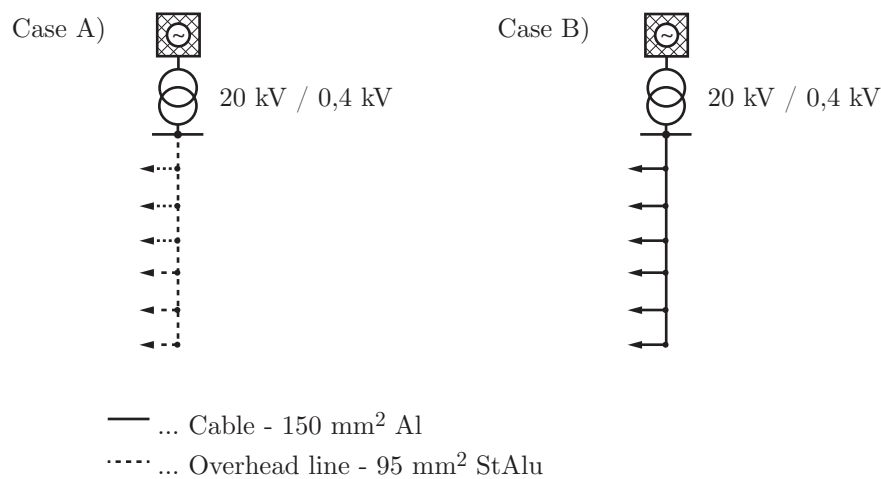


Figure 4.3.4.: Model grid configuration for the comparison between overhead lines and cable lines.

The simulations 10 to 15 show the influence of this method upon the possible generator capacities. For the standard configuration with a low voltage line length of 100% (288 m), the feed-in capacity could not be increased. The resulting line resistance remained too high to achieve reasonable voltage drops along the line elements. However the voltage rise at the remotest point of common coupling, which at the same time equals the highest rise within the whole grid, could be kept in the allowed range with a feed-in power of 1 kW. Together with the reduction of the low voltage line length, the increased cross section of the cable lines raised the possible feed-in capacity to 2 kW in the 50% (144 m) line length simulations and to 4,5 kW in the 20% (57,6 m) line length simulations. For the present grid structure, this meant the same effect upon the feed-in capacity, which was already observed in the simulations with reactive power provision by the inverters.

Regulating Distribution Transformers

The effects of regulating distribution transformers were examined in the simulations 16 to 21. The transformers regulation kept the voltage at its secondary busbar at a predefined value. Following the previous model grids, the voltage level at the remotest coupling point was chosen as a measurement value. Therefore the transformer regulated its output voltage to meet the set voltage at the remotest coupling point. For the standard configuration with 100% (288 m) line length a feed-in power of 1,5 kW was achieved. With the line length of the low voltage section reduced to 50% (144 m) and the same transformer, the generator feed-in power was increased to 4,5 kW for every single point of common coupling. For a line length of 20% (57,6 m) the achievable feed-in power was increased to 7,5 kW.

Central Reactive Power Management

A central reactive power management by central compensation units represents the last examined method to decrease the voltage rise, caused by distributed generation. Compensation unit sizes of 50 kvar, 100 kvar and 150kvar were used for the simulations 22 to 30, including the different line lengths for the low voltage grid. With the compensation units, the voltage at the corresponding coupling point was reduced, resulting in lower voltage levels along the low voltage stub. For the performed simulations, the compensation unit was connected to the low voltage busbar of the distribution transformer.

The possible feed-in capacity was increased from 1 kW to 2 kW in the standard configuration with 100% (288 m) line length. However, due to the increased transport of reactive power in the overlaid medium voltage grid, the given loading thresholds of 60% was reached at the first medium voltage lines at the medium voltage feeder. With a reduced low voltage line length in combination with central reactive power management, the feed-in capacity was increased to 4,5 kW in the grid with 50% (144 m) relative line length and 10 kW in the grid with a relative line length of 20% (57,6 m). In both cases, the line loading threshold of 60% was violated at the first medium voltage cable lines near the feeder, which carried the highest load currents. In simulation number 30 also the line loadings of the low voltage lines near the transformer busbar exceeded the threshold.

In comparison to the previously examined model grids for the urban and suburban area, one medium voltage feeder, supplied a much larger number of low voltage grids. Therefore the sum of all connected distributed generators led to proportionally higher equipment loadings. Grid reinforcement in these areas would be conceivable. Also the fluctuating feed-in power of the wide spread generators could be considered. The concurrency of the allocated generators would decrease the overall loading of the equipment.

4.3.3. Simulation Results

Table 4.3.3.: Simulation results for the suburban model grid (voltage levels at PCC.R.F1.10 and distribution transformer loading for 400 kVA transformers, in the three low voltage line lengths variations 100% = 288 m, 50% = 144 m and 20% = 56,7, including reactive power provision by the inverters, the exchange of overhead lines with cable lines, regulating transformers and a centralized reactive power management).

400 kVA - Distribution Transformer - 100% / 50% / 20% LV-Length							
#	Load in kW	PV in kW	u max in %	Δu in %	Distribution Transformer		
					I in A (sec.)	Loading in %	
1	0,5	0,0	97,6	-	8,0	1,3	
2	0,5	1,0	101,0	+3,4*	7,0	1,3	
3	0,5	1,0 (cos φ =0,95)	100,6	+3,0	10,0	1,7	
4	0,5	0,0	98,4	-	8,0	1,3	
5	0,5	1,5	101,2	+2,8	14,0	2,5	
6	0,5	2,0 (cos φ =0,95)	101,5	+3,1*	24,0	4,2	
7	0,5	0,0	99,0	-	8,0	1,3	
8	0,5	3,0	101,6	+2,6	36,0	6,2	
9	0,5	4,5 (cos φ =0,95)	101,9	+2,9	62,0	10,6	
Overhead Lines Exchanged With Cable Lines - 100% / 50% / 20% LV-Length							
10	0,5	0,0	98,2	-	8,0	1,3	
11	0,5	1,0	100,5	+2,3	7,0	1,3	
12	0,5	0,0	98,7	-	8,0	1,3	
13	0,5	2,0	101,3	+2,6	22,0	3,7	
14	0,5	0,0	99,1	-	8,0	1,3	
15	0,5	4,5	102,0	+2,9	57,0	9,9	
Regulating Distribution Transformer - 100% / 50% / 20% LV-Length							
16	0,5	0,0	98,9	-	8,0	1,3	
17	0,5	1,5	100,3	+1,4	15,0	2,5	
18	0,5	0,0	101,0	-	7,0	1,3	
19	0,5	4,5	104,1	+3,1*	57,0	9,8	
20	0,5	0,0	100,2	-	7,0	1,3	
21	0,5	7,5	103,0	+2,8	99,0	17,2	
Central Compensation Unit - 100% / 50% / 20% LV-Length							
22	0,5	1,0	99,7	+2,1	76,0	13,1	
23	0,5	1,5	99,9	+2,3	152,0	26,3	
24	0,5	2,0	100,1	+2,5	230,0	39,8	
25	0,5	3,0	101,2	+2,8	84,0	14,6	
26	0,5	4,0	101,5	+3,1*	161,0	27,9	
27	0,5	4,5	100,8	+2,4	239,0	41,4	
28	0,5	6,0	101,5	+2,5	110,0	19,0	
29	0,5	8,0	101,7	+2,7	186,0	32,2	
30	0,5	10,0	101,8	+2,8	267,0	46,2	

* Voltage threshold of +3% exceeded

Table 4.3.4.: Simulation results for the suburban model grid (line loading of the first medium voltage line at the 40 MVA medium voltage feeder and the first low voltage line at the feeder F1, for 400 kVA transformers, in the three low voltage line lengths variations 100% = 288 m, 50% = 144 m and 20% = 56,7, including reactive power provision by the inverters, the exchange of overhead lines with cable lines, regulating transformers and a centralized reactive power management).

400 kVA - Distribution Transformer - 100% / 50% / 20% LV-Length						
#	Load in kW	PV in kW	1. MV-Line		1. LV-Line	
			I in A	Loading in %	I in A	Loading in %
1	0,5	0,0	15,0	3,7	8,0	4,1
2	0,5	1,0	15,0	3,7	7,0	4,0
3	0,5	1,0 ($\cos\varphi=0,95$)	11,0	2,6	10,0	5,2
4	0,5	0,0	15,0	3,7	8,0	4,1
5	0,5	1,5	21,0	5,1	14,0	7,8
6	0,5	2,0 ($\cos\varphi=0,95$)	25,0	6,1	24,0	13,1
7	0,5	0,0	15,0	3,7	8,0	4,1
8	0,5	3,0	43,0	10,7	36,0	19,3
9	0,5	4,5 ($\cos\varphi=0,95$)	67,0	16,7	62	33,2
Overhead Lines Exchanged With Cable Lines - 100% / 50% / 20% LV-Length						
10	0,5	0,0	15,0	3,7	8,0	2,5
11	0,5	1,0	15,0	3,7	7,0	2,5
12	0,5	0,0	15,0	3,7	8,0	2,5
13	0,5	2,0	28,0	6,9	22,0	7,2
14	0,5	0,0	15,0	3,7	8,0	2,5
15	0,5	4,5	67,0	16,6	57,0	19,0
Regulating Distribution Transformer - 100% / 50% / 20% LV-Length						
16	0,5	0,0	15,0	3,7	8,0	4,0
17	0,5	1,5	21,0	5,1	15,0	7,9
18	0,5	0,0	15,0	3,7	7,0	4,0
19	0,5	4,5	65,0	16,1	57,0	30,5
20	0,5	0,0	15,0	3,7	7,0	4,0
21	0,5	7,5	113,0	28,1	99,0	53,7
Central Compensation Unit - 100% / 50% / 20% LV-Length						
22	0,5	1,0	74,0	18,4	8,0	4,1
23	0,5	1,5	162,0	40,1	15,0	7,9
24	0,5	2,0	251,0	62,4*	22,0	11,9
25	0,5	3,0	86,0	21,3	36,0	19,5
26	0,5	4,0	173,0	43,0	51,0	27,4
27	0,5	4,5	262,0	65,1*	58,0	31,6
28	0,5	6,0	118,0	29,3	79,0	42,7
29	0,5	8,0	204,0	50,7	108,0	58,4
30	0,5	10,0	297,0	73,7*	137,0	74,1*

* Loading threshold of 60% exceeded

4.3.4. Achievable Feed-In Capacity

The different measures to increase the possible distributed generator outputs, discussed in the previous simulations, were also used to examine the capabilities of the rural model grid with the three configurations of 100% (288 m), 50% (144 m) and 20% (57,6 m) low voltage line lengths.

The limiting factor was the voltage rise threshold of $\Delta u = +3\%$. However, especially for high line lengths, represented by the standard 100% length configuration, this threshold was violated several times. These threshold violations were accepted in certain simulations in order to achieve realistic generator output powers. The resulting feed-in capacities for the different measures, regarding the three grid configurations, are shown in figure 4.3.5.

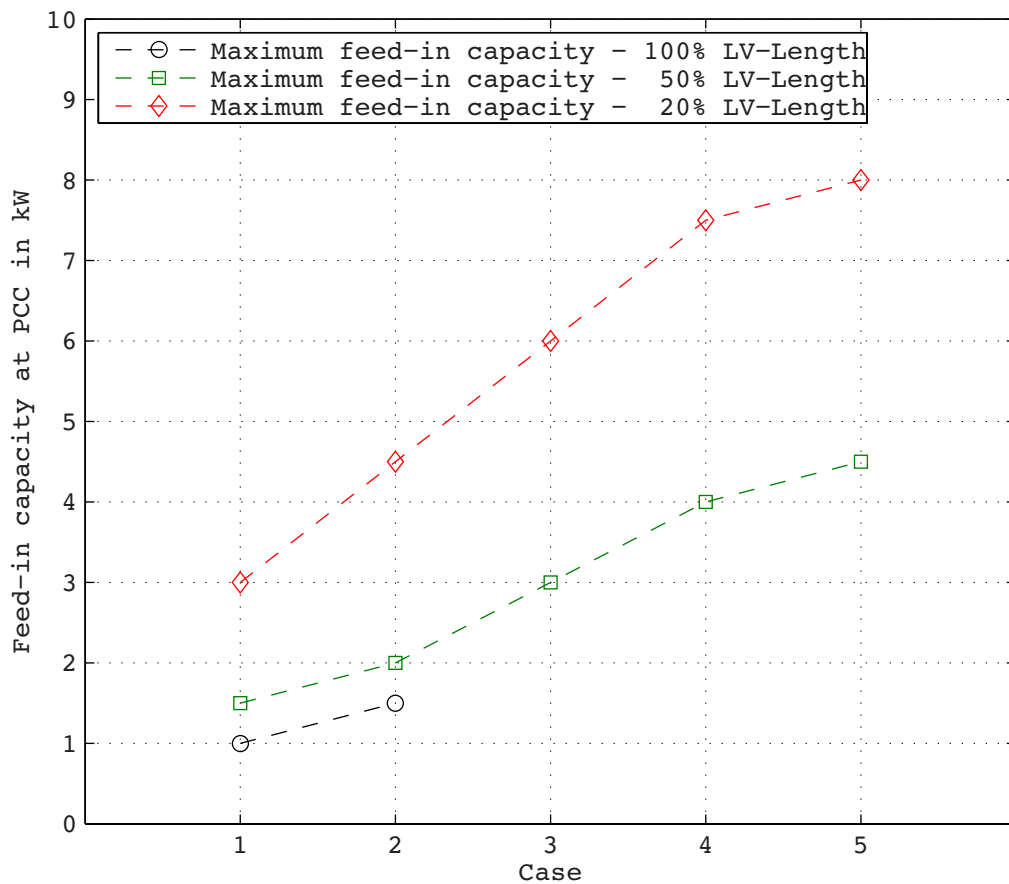


Figure 4.3.5.: Feed-In capacity of the rural model grid.

100% LV-Length (288 m)

Table 4.3.5 lists the output power of the attached distributed generators at every single point of common coupling and the corresponding measures, used to maintain the required phase voltage at every coupling point. The standard grid configuration, including a low voltage line length of 100% (288 m) of its initial value, did not offer any considerable possibilities of improvement. Only the use of a 100 kvar compensation unit at the secondary transformer busbar or the exchange of the whole transformer with an on-load tap-

changer could increase the possible generator output powers. Point 2 shows an improvement of 50% for the feed-in power at every point of common coupling.

50% LV-Length (144 m)

A reduction of the low voltage line lengths by 50% (144 m) of their initial values shows a significant increase in possible generator output powers, especially for the implementation of different measures to decrease the voltage rise, while still meeting the required constraints.

20% LV-Length (57,6 m)

The reduction of the low voltage line lengths by 20% (57,6 m) of their initial values led to a similar low voltage structure, compared to the structures already examined in the previous model grids. This resulted in the respective feed-in powers, stated for the 20% (57,6 m) length configuration in table 4.3.5.

Table 4.3.5.: Upper limits for the feed-in power regarding the voltage rise.

100% LV-Length			
Case	Simulation #	Max PV at PCC in kW	Measure to increase PV
1)	2, 3, 11, 22	1,0	$\cos\varphi = 1,00$, $\cos\varphi = 0,95$ (lagging), Cable lines, 50 kvar compensation
2)	23, 17	1,5	100 kvar compensation, regulating transformer
50% LV-Length			
Case	Simulation #	Max PV at PCC in kW	Measure to increase PV
1)	5	1,5	$\cos\varphi = 1,00$
2)	6, 13	2,0	$\cos\varphi = 0,95$ (lagging), cable lines
3)	25	3,0	50 kvar compensation
4)	26	4,0	100 kvar compensation
5)	19	4,5	150 kvar compensation, regulating transformer
20% LV-Length			
Case	Simulation #	Max PV at PCC in kW	Measure to increase PV
1)	8	3,0	$\cos\varphi = 1,00$
2)	9, 15	4,5	$\cos\varphi = 0,95$ (lagging), cable lines
3)	28	6,0	50 kvar compensation
4)	21	7,5	Regulating transformer
5)	29	8,0	100 kvar compensation

The resulting relation between the achievable feed-in power for the distributed generators and the low voltage lengths, illustrates the non linear influence of lower line lengths. The same effects can be observed at the sensitivity analysis for the low voltage length in figure 4.3.6.

4.3.5. Parameter Variation - Sensitivity Analysis

The influence of different network parameters from the rural model grid was examined with the help of a sensitivity analysis for the standard grid configuration with a low voltage line length of 100% of its initial value. The resulting relations between the parameter variations and the change in the achievable output power of the distributed generators are shown in figure 4.3.6.

Selected parameters for the variation were:

- Distribution transformer - related impedance voltage u_k
- Distribution transformer - copper losses P_{Cu}
- Length of medium voltage lines - MV-Length
- Length of low voltage lines - LV-Length
- Attached consumer load at PCC

Like in the previous sections, the listed parameters were varied in a range from $\delta = -100\%$ to $\delta = +100\%$ of their initial values, independently from each other in steps of 50%. For every variation, the possible output power for all distributed generators at their coupling point was evaluated while keeping the voltage levels within the constraints stated in section 2.7. Due to the voltage violations in section 4.3.2, an additional simulation defines the initial state for the variations including following base values:

- $u_k = 6,0\%$
- $P_{Cu} = 5,0 \text{ kW}$
- MV-Length = 840 m (cable lines) / 280 m (overhead lines)
- LV-Length = 288 m
- Load = 0,5 kW

The resulting diagram in figure 4.3.6 shows, how each parameter influences the achievable feed-in capacity of the rural model grid. Due to the higher line lengths, increased voltage drops were observed, thus making the resulting voltage rise the limiting factor for distributed generator output powers. The variation of the low voltage line length shows the nonlinear relation at lower values, which was already present in the urban and suburban model grid. An additional simulation was performed, reducing the low voltage line length to $\delta = 25\%$ of its initial value in order to emphasize this effect. The achievable feed-in power for the variation of the low voltage line length was scaled on a secondary y-axis due to the high value range.

The comparison between the influences caused by the low voltage and medium voltage line lengths shows the dominance of the low voltage level lengths. The highest voltage rise was as expected, observed at the remotest point of common coupling within the remotest supplied low voltage grid at the longest medium voltage stub PCC.R.F1.10.

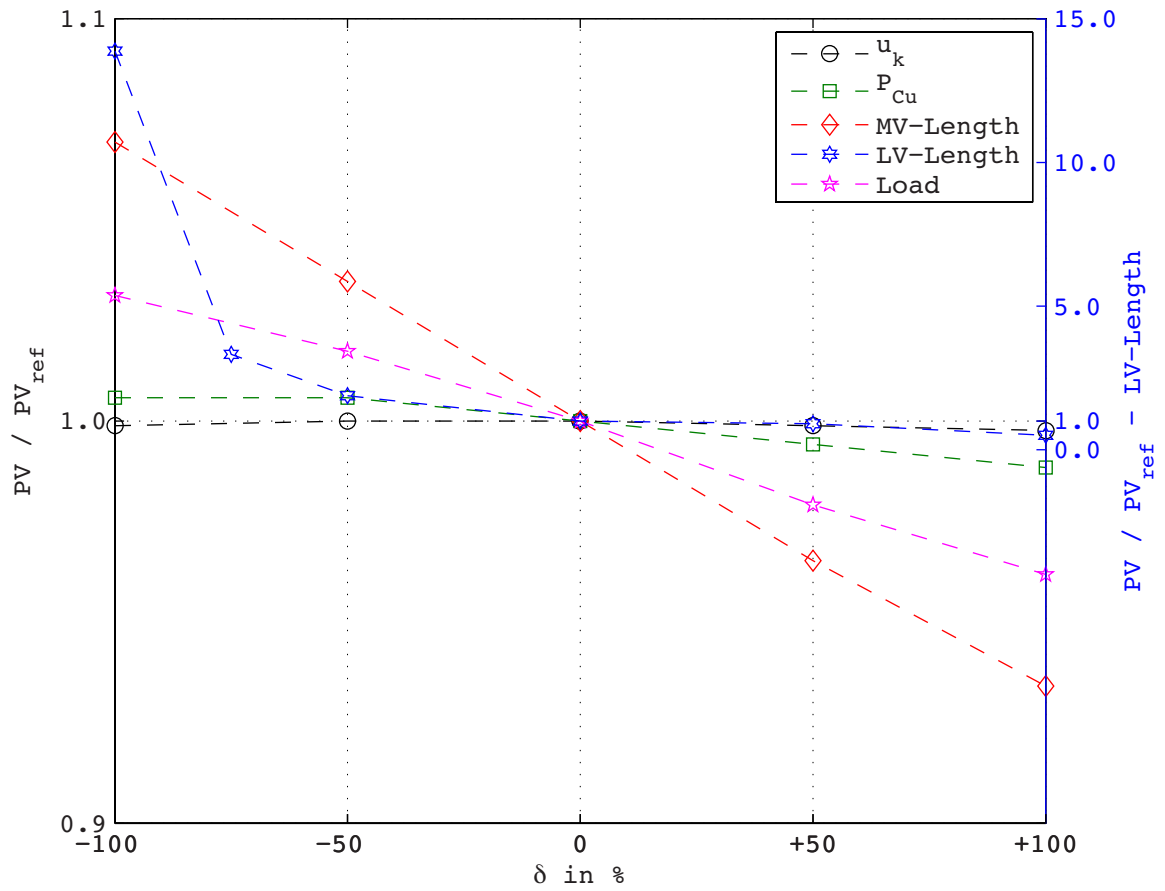


Figure 4.3.6.: Sensitivity analysis of the rural model grid (variation of: u_k , P_{Cu} , MV-Length, LV-Length, consumer load).

5. Conclusion

To examine the effects of distributed micro-generation in medium and low voltage supply networks, this thesis centers on the following questions:

- Is it possible to create distinctive and generally valid generic model grids, which reflect the main characteristics of common supply areas?
- Which network parameters have the most significant effects onto the developed model grids?
- What is the possible feed-in capacity for distributed micro-generation within the developed model grids?
- Which measures can be taken into consideration to increase the possible feed-in capacity for an existing grid and how practical and effective are they?

In order to answer these research questions, three model grids were developed and analyzed. Several power flow simulations were conducted with different distributed generation feed-in powers and the mentioned methods to increase the possible generator output. The evaluation of these simulations led to the following conclusions:

The averaging of real network structures, present in the supply area of the Wien Energie Stromnetz GmbH, resulted in usable and generally applicable model grids for the respective network structure and the desired load densities. However, in most cases specific changes in the structure and network parameters had to be carried out to emphasize special effects of distributed generation onto the particular model grid. The structures and parameters of the developed model grids are heavily depending on the real grid sections, they are based on.

The possible feed-in capacity for the model grids was in most cases restricted by the upper limit of the allowed voltage rise at the remote points of common coupling due to the distributed micro-generation. Therefore the line impedance, with its mostly resistive character, was the main influencing parameter. However, line reinforcement can only be applied in certain network areas to effectively reduce the voltage drop along the line, thus increasing the possible generator feed-in capacity.

In areas with very low line lengths and high load densities, as seen in the urban model grid, the equipment loading restrictions can have a further decreasing effect onto the feed-in capacity.

For the standard configuration of the chosen network structures and the stated load densities, the feed-in capacities, seen in table 5.0.1 could be achieved at every single point of common coupling in the respective low voltage grid.

Table 5.0.1.: Comparison of the achievable feed-in capacities for the different model grids

Model Grid	Capacity (Standard)	Capacity (Increased)	Measure
Urban	26,0 kW	28,0 kW	1000 kVA Distr. Transformer
Suburban	2,5 kW	5,5 kW	Regulating Distr. Transformer
Rural	<1,0 kW	1,5 kW	Regulating Distr. Transformer

The values in table 5.0.1 can be seen as reference points for supply areas with similar structures and load densities. The reduction of the low voltage line lengths in the low voltage grid of the rural model grid improved the achievable feed-in capacity furthermore, resulting in a possible generator output power, comparable with the suburban model grid.

For this document, a grid reinforcement with cable lines, the participation of the photovoltaic inverters in the reactive power management, a centralized reactive power management system and regulating on-load tap-changers as a replacement for the existing distribution transformers were considered as valid measures to increase the possible distributed feed-in capacity.

In areas with a high length of the low voltage lines, a grid reinforcement can improve the possible generator output power by lowering the resulting voltage rise caused by a smaller line voltage drop. The improvement due to the line reinforcement depends on the existing line configuration and grid structure.

The participation of the distributed generators in the reactive power management by providing reactive output power with various power factors is a simple and effective way to influence the voltage rise at the corresponding coupling point. The loss of active power output, which comes with the reactive power provision, is outweighed by the additional achievable active power output due to the decrease in the voltage at the coupling point. This method represents a way to increase the possible distributed generator sizes without any costs for the distribution system operator.

A centralized reactive power management for a low voltage grid in terms of an inductive reactive power consumer represents another way to influence the voltage levels within the network. If the appropriate grid code does not include guidelines for a reactive power management by the inverters themselves, a centralized power factor correction system can help to achieve the same effects.

The most effective way to increase the possible feed-in capacity of distributed generators in the suburban and rural grid is the use of regulating distribution transformers. However, regulating distribution transformers are still in development and not state of the art. Furthermore the increased costs for the regulation outweigh the benefits gained by the higher achievable feed-in capacity.

In general the efficiency of the different methods depends on the existing grid in which they are applied. The simulation showed that in most cases, the use of regulating distribution transformers leads to the highest possible feed-in capacity for the respective grid. The effects of the other methods however, vary with the different network parameters of the examined grids. No general statements can be made about their suitability.

Bibliography

- [1] KJAER S. B., PEDERSEN J. K., and BLAABJERG F. A Review of Single-Phase Grid-Connected Inverters for Photovoltaic Modules. *IEEE TRANSACTIONS ON INDUSTRY APPLICATIONS*, 41(5), SEPTEMBER/OCTOBER 2005.
- [2] SOLARPLAZA International BV. Top 10 World's Most Efficient Solar PV Modules (Mono-Crystalline). <http://www.solarplaza.com/top10-crystalline-module-efficiency/>, June 2011.
- [3] SOLARPLAZA International BV. Top 10 World's Most Efficient Solar PV Modules (Poly-Crystalline). <http://www.solarplaza.com/top10-polycrystalline-module-efficiency/>, December 2011.
- [4] SOLARPLAZA International BV. Top 10 World's Most Efficient String Inverters (<5 kW). <http://www.solarplaza.com/top10-inverters-5kw-efficiency/>, January 2012.
- [5] EN 50160 - Voltage Characteristics of Electricity Supplied by Public Electricity Networks, 2010.
- [6] KERBER G. *Aufnahmefähigkeit von Niederspannungsverteilnetzen für die Einspeisung aus Photovoltaikkleinanlagen*. PhD thesis, Technische Universität München - Fachgebiet Elektrische Energieversorgungsnetze, 2010.
- [7] Energie-Control GmbH. Technische und organisatorische Regeln für Betreiber und Benutzer von Netzen. Teil D: Besondere technische Regeln. Hauptabschnitt D2: Richtlinie zur Beurteilung von Netzzrückwirkungen, 2006.
- [8] SCHMIESING J. Selbstregelnde Ortsnetztrafos – Erfahrungen und Ideen. In *2. Siemens Transformatoren – Symposium*, March 2011.
- [9] HEUCK K., DETTMANN K.-D., and SCHULZ D. *Elektrische Energieversorgung*. Friedr. Vieweg & Sohn Verlag - GWV Fachverlage GmbH, 7 edition, 2007.
- [10] ALBACH M. *Grundlagen der Elektrotechnik 1 - Erfahrungssätze, Bauelemente, Gleichstromschaltungen*. Pearson Education, 2004.
- [11] SAKULIN M., FICKERT L., HIPPEL W., STRANNER B., RENNER H., and SCHMAUTZER E. Der Einfluss dezentraler Erzeugung auf die Verteilnetze. Technical Report VEÖ-EFG Projektnummer 10.36, Technische Universität Graz - Institut für Elektrische Anlagen, 2004.
- [12] CRASTAN V. *Elektrische Energieversorgung 2*. Springer-Verlag Berlin Heidelberg, 2 edition, 2009.
- [13] VDE-AR-N 4105 - Generators connected to the low-voltage distribution network – Technical requirements for the connection to and parallel operation with low-voltage distribution networks, 2011.

A. Voltage Profiles - Urban Model Grid

A.1. 630 kVA Distribution Transformers

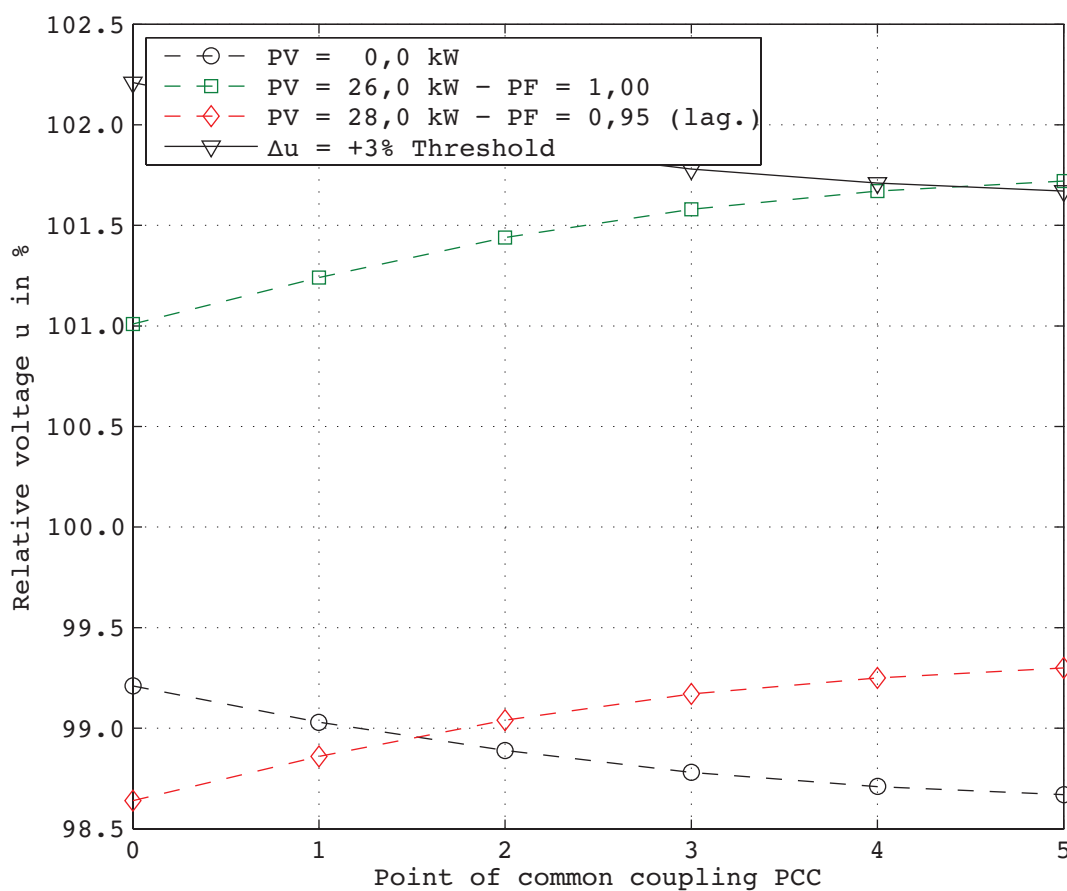


Figure A.1.1.: Voltage profile of one low voltage stub - urban model grid (630 kVA distribution transformers, reactive power provision by the generators).

#	$\cos\varphi$	Load in kW	PV in kW	u_{PCC5} in %	Δu_{PCC5} in %
1	-	$20 \times 0,5$	0,0	98,7	-
7	1,00	$20 \times 0,5$	26,0	101,7	+3,0
9	0,95 (lag.)	$20 \times 0,5$	28,0	99,3	+0,6

A.2. 800 kVA Distribution Transformers

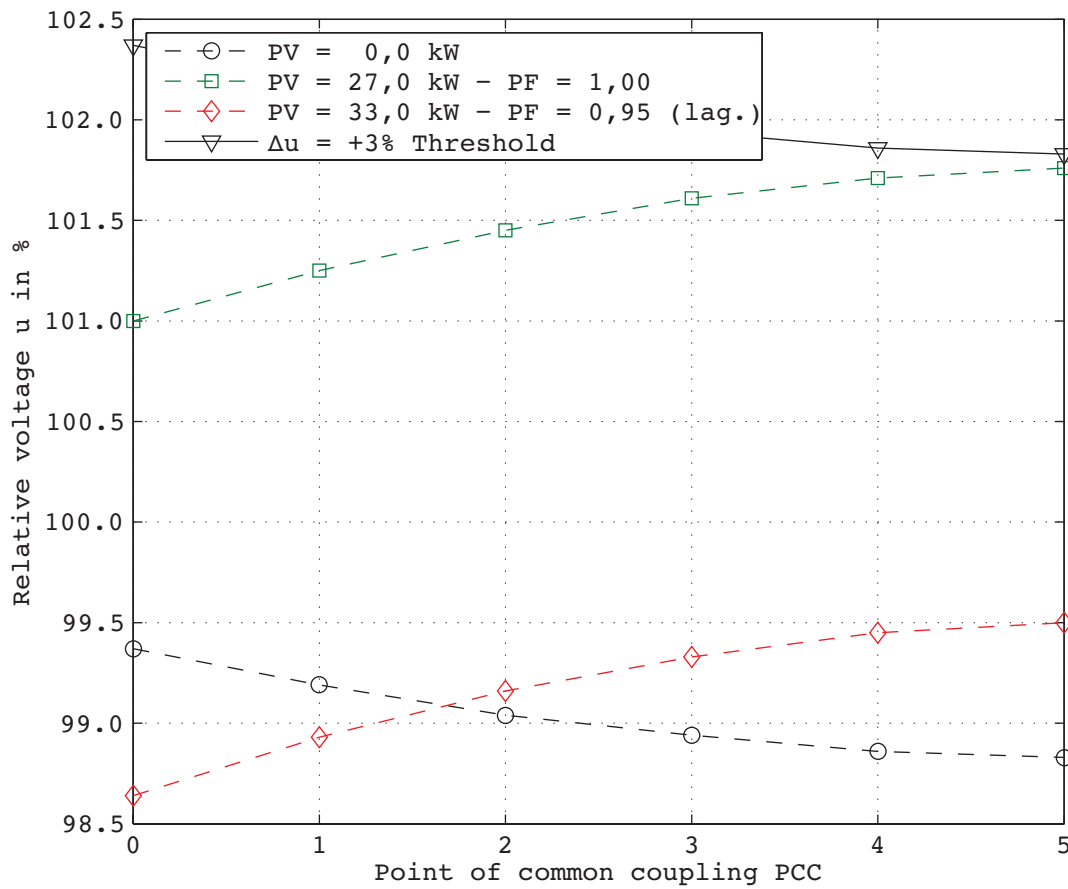


Figure A.2.1.: Voltage profile of one low voltage stub - urban model grid (800 kVA distribution transformers, reactive power provision by the generators).

#	$\cos\varphi$	Load in kW	PV in kW	u_{PCC5} in %	Δu_{PCC5} in %
10	-	$20 \times 0,5$	0,0	98,8	-
12	1,00	$20 \times 0,5$	27,0	101,8	+3,0
16	0,95 (lag.)	$20 \times 0,5$	33,0	99,5	+0,7

A.3. 1000 kVA Distribution Transformers

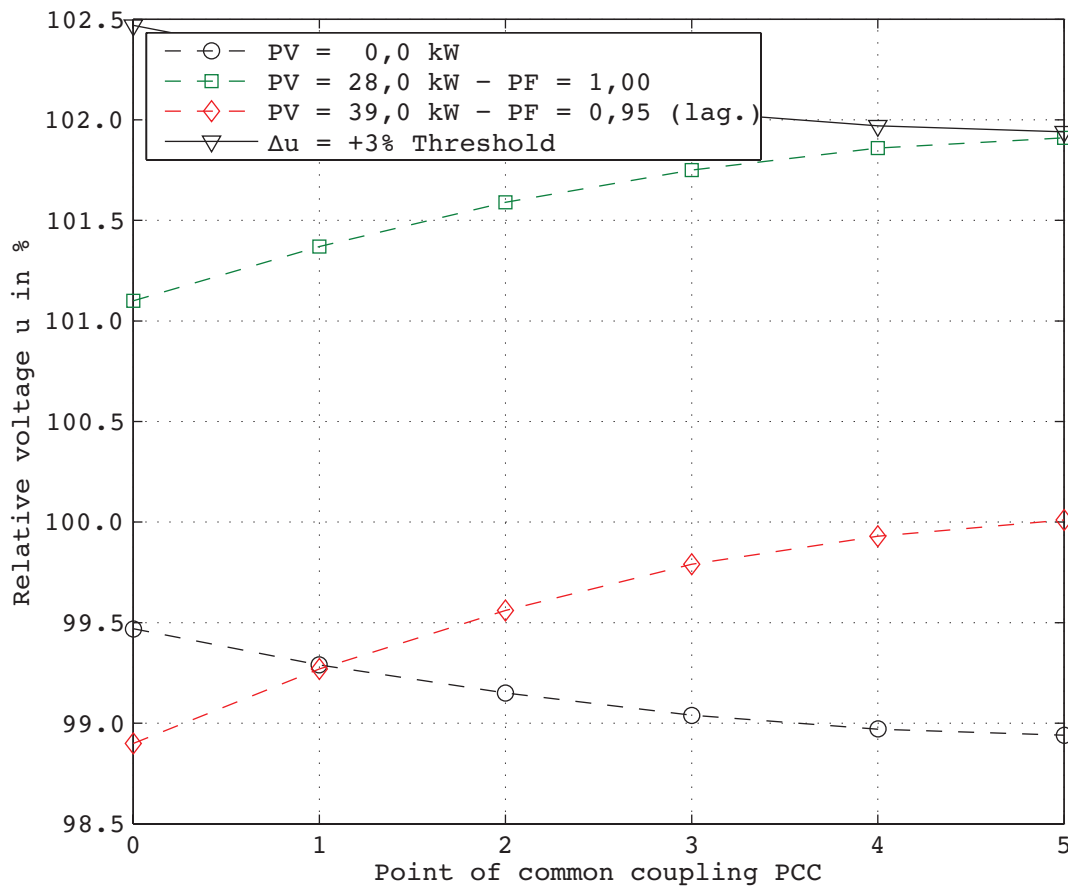


Figure A.3.1.: Voltage profile of one low voltage stub - urban model grid (1000 kVA distribution transformers, reactive power provision by the generators).

#	$\cos\varphi$	Load in kW	PV in kW	u_{PCC5} in %	Δu_{PCC5} in %
17	-	$20 \times 0,5$	0,0	98,9	-
19	1,00	$20 \times 0,5$	28,0	101,9	+3,0
23	0,95 (lag.)	$20 \times 0,5$	39,0	100,0	+1,1

B. Voltage Profiles - Suburban Model Grid

B.1. Reactive Power Provision through PV-Systems

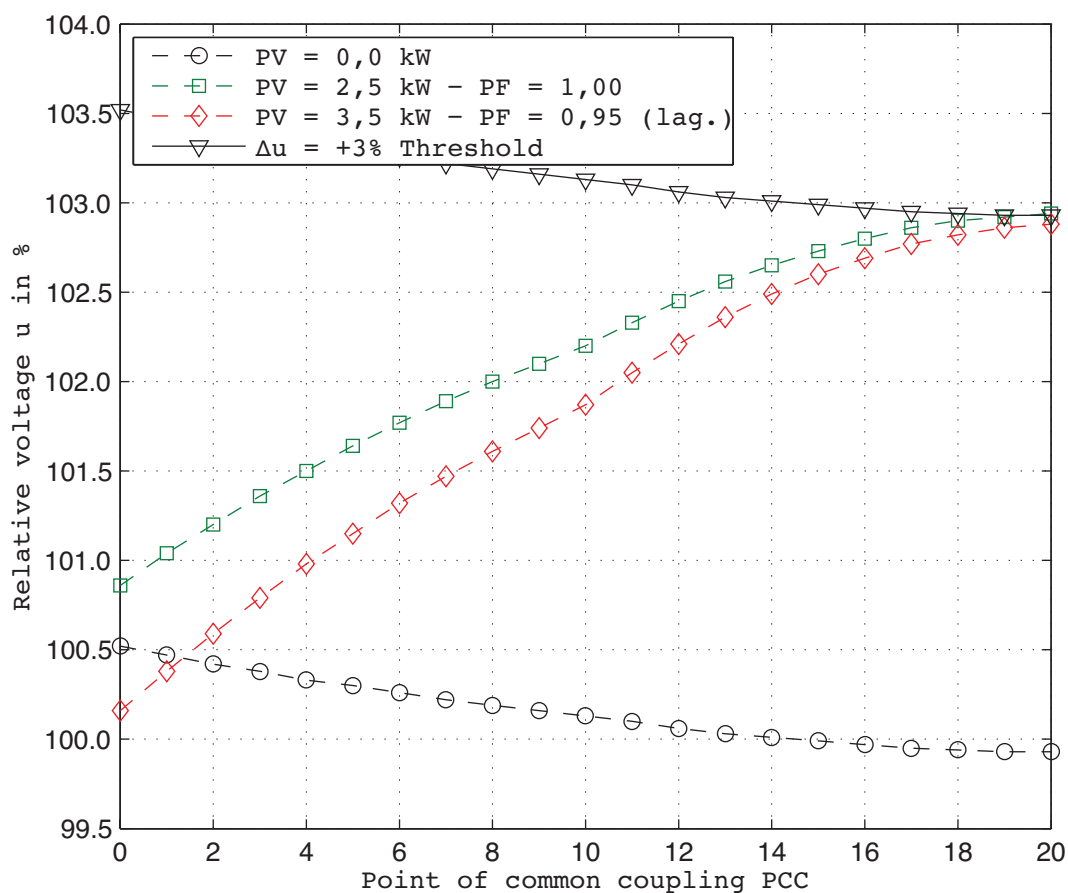


Figure B.1.1.: Voltage profile of one low voltage stub - suburban model grid (400 kVA distribution transformers, reactive power provision by the generators).

#	$\cos\varphi$	Load in kW	PV in kW	u_{PCC20} in %	Δu_{PCC20} in %
1	-	0,5	0,0	99,9	-
2	1,00	0,5	2,5	102,9	+3,0
3	0,95 (lag.)	0,5	3,5	102,9	+3,0

B.2. Overhead Line / Cable Comparison

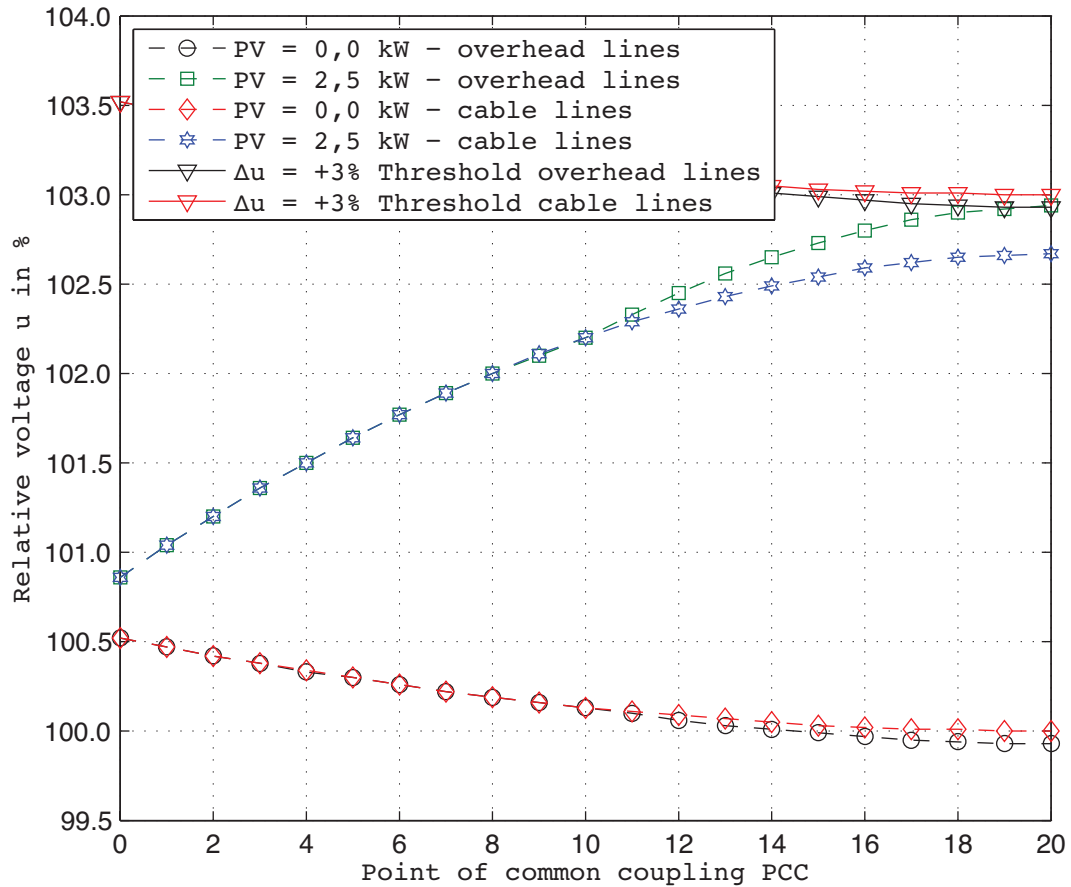


Figure B.2.1.: Voltage profile of one low voltage stub - suburban model grid (400 kVA distribution transformers, overhead lines exchanged with cable lines).

#		Load in kW	PV in kW	u_{PCC20} in %	Δu_{PCC20} in %
1	Overhead line - 95 mm ² StAlu	0,5	0,0	99,9	-
2		0,5	2,5	102,9	+3,0
4	Cable - 150 mm ² Al	0,5	0,0	100,0	-
5		0,5	2,5	102,7	+2,7

B.3. Regulating Distribution Transformer

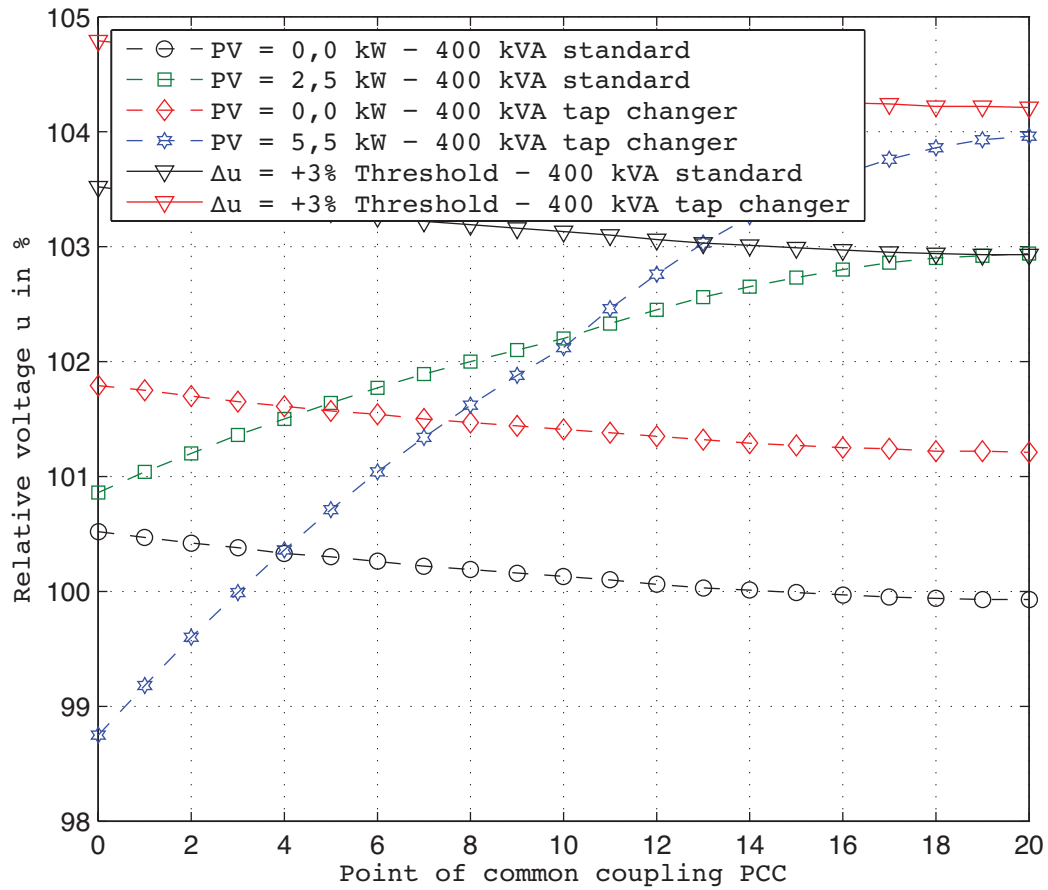


Figure B.3.1.: Voltage profile of one low voltage stub - suburban model grid (400 kVA regulating distribution transformers).

#		Load in kW	PV in kW	u_{PCC20} in %	Δu_{PCC20} in %
1	400 kVA standard	0,5	0,0	99,9	-
2		0,5	2,5	102,9	+3,0
6	400 kVA tap changer	0,5	0,0	101,2	-
7		0,5	5,5	104,0	+2,8

B.4. Central Reactive Power Management at 0,4 kV Busbar

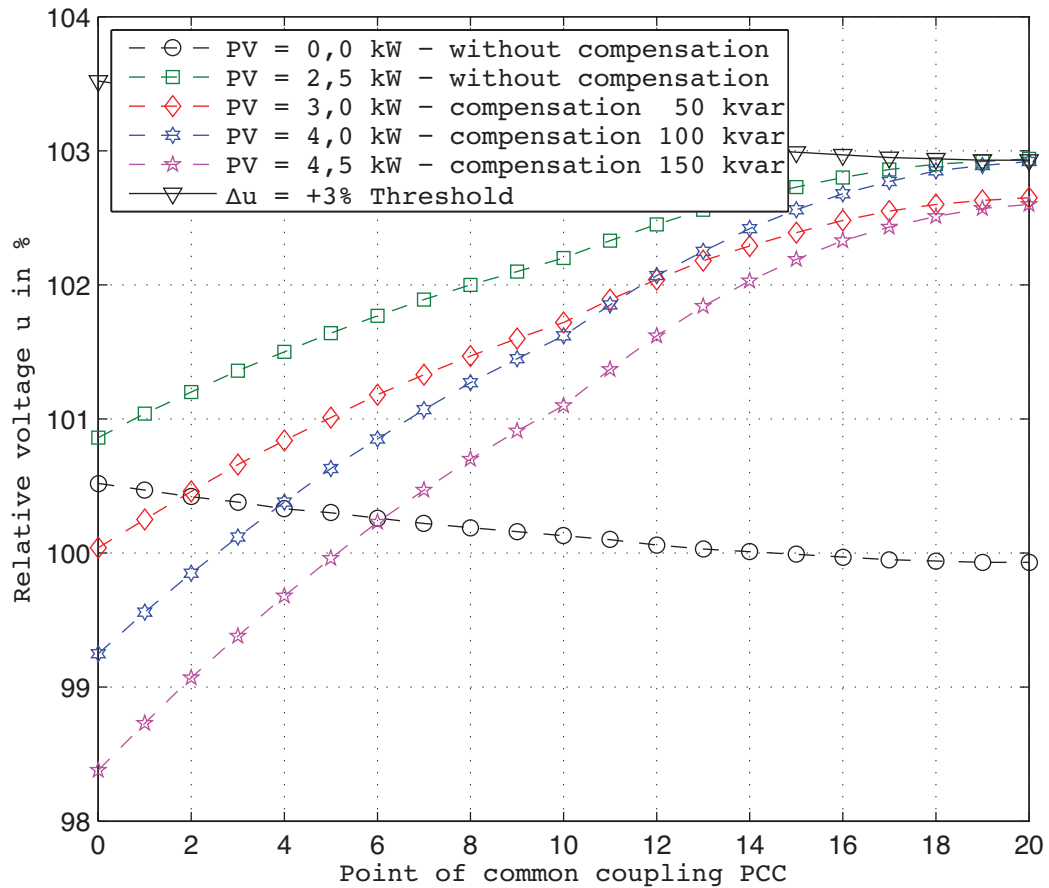


Figure B.4.1.: Voltage profile of one low voltage stub - suburban model grid (400 kVA distribution transformers, central compensation unit).

#	Compensation in kvar	Load in kW	PV in kW	u_{PCC20} in %	Δu_{PCC20} in %
1	-	0,5	0,0	99,9	-
2	-	0,5	2,5	102,9	+3,0
8	50	0,5	3,0	102,7	+2,8
9	100	0,5	4,0	102,9	+3,0
10	150	0,5	4,5	102,6	+2,7

C. Voltage Profiles - Rural Model Grid

C.1. Reactive Power Provision through PV-Systems

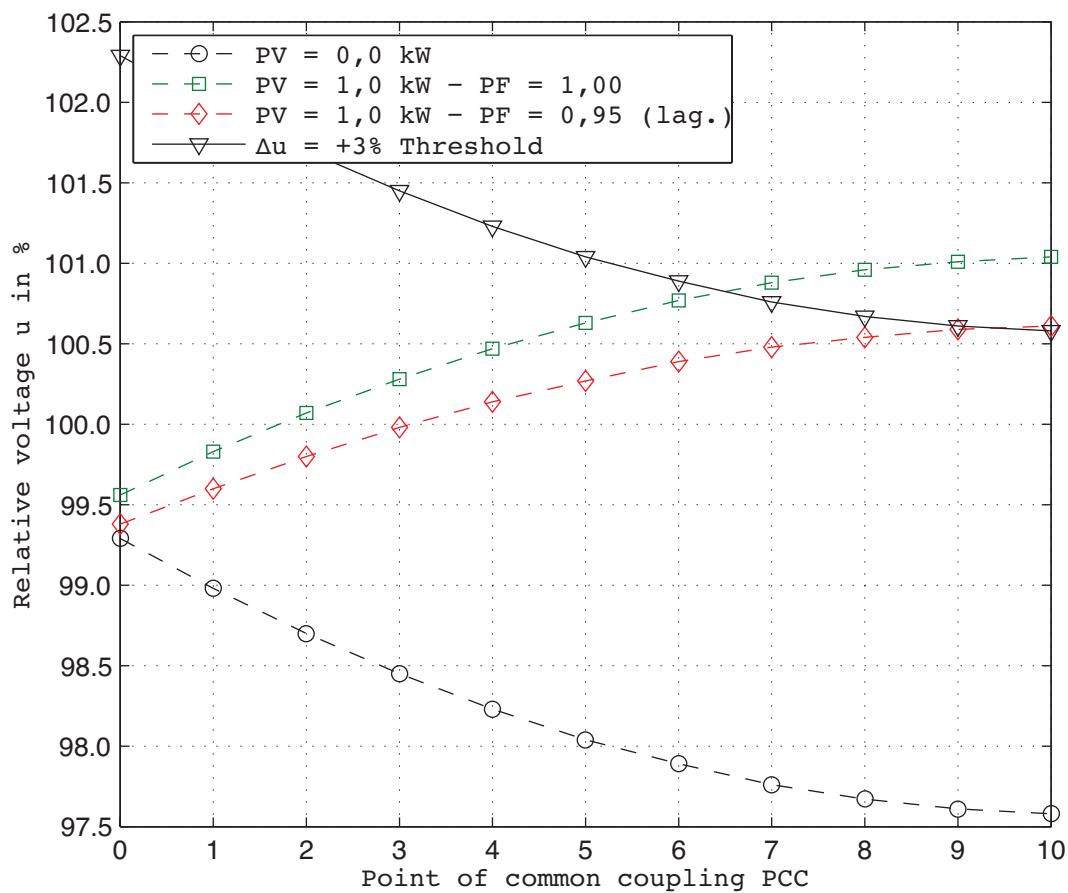


Figure C.1.1.: Voltage profile of one low voltage stub - rural model grid (100% LV-Length, 400 kVA distribution transformers, reactive power provision by the generators).

#	$\cos\varphi$	Load in kW	PV in kW	u_{PCC10} in %	Δu_{PCC10} in %
1	-	0,5	0,0	97,6	-
2	1,00	0,5	1,0	101,0	+3,4
3	0,95 (lag.)	0,5	1,0	100,6	+3,0

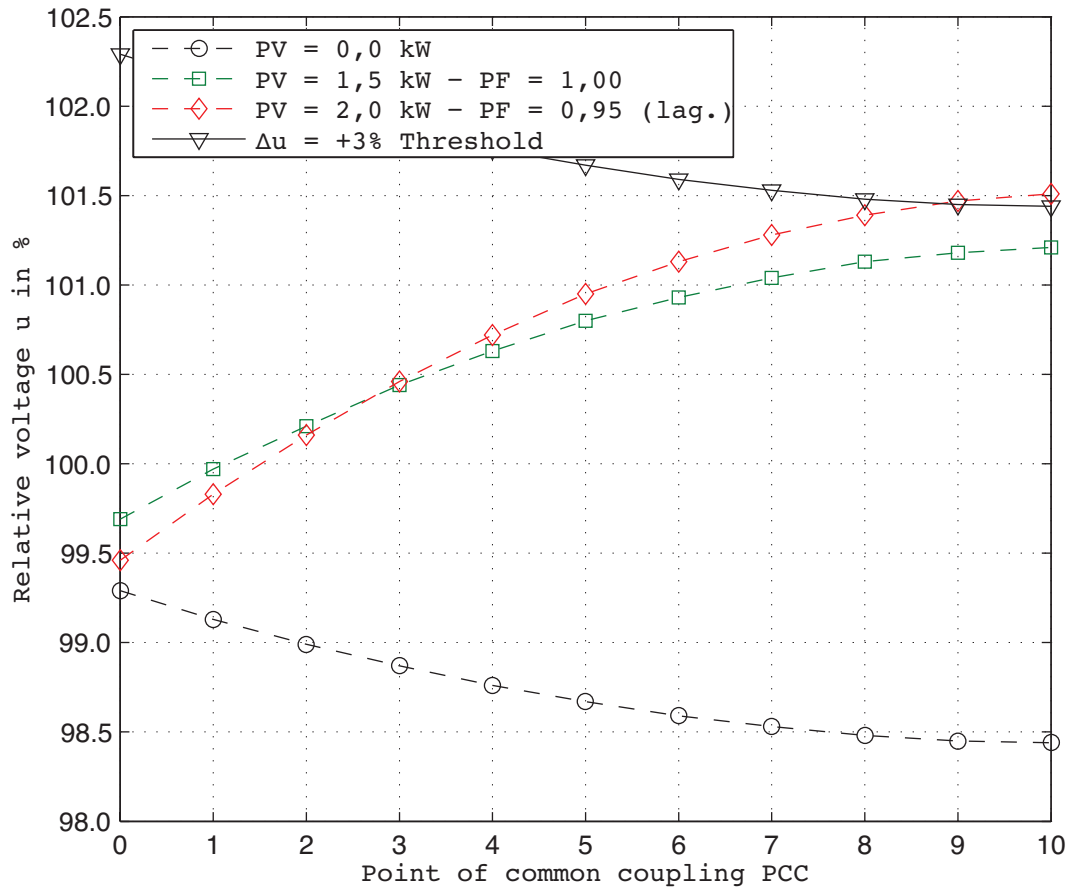


Figure C.1.2.: Voltage profile of one low voltage stub - rural model grid (50% LV-Length, 400 kVA distribution transformers, reactive power provision by the generators).

#	$\cos\varphi$	Load in kW	PV in kW	u_{PCC10} in %	Δu_{PCC10} in %
4	-	0,5	0,0	98,4	-
5	1,00	0,5	1,5	101,2	+2,8
6	0,95 (lag.)	0,5	2,0	101,5	+3,1

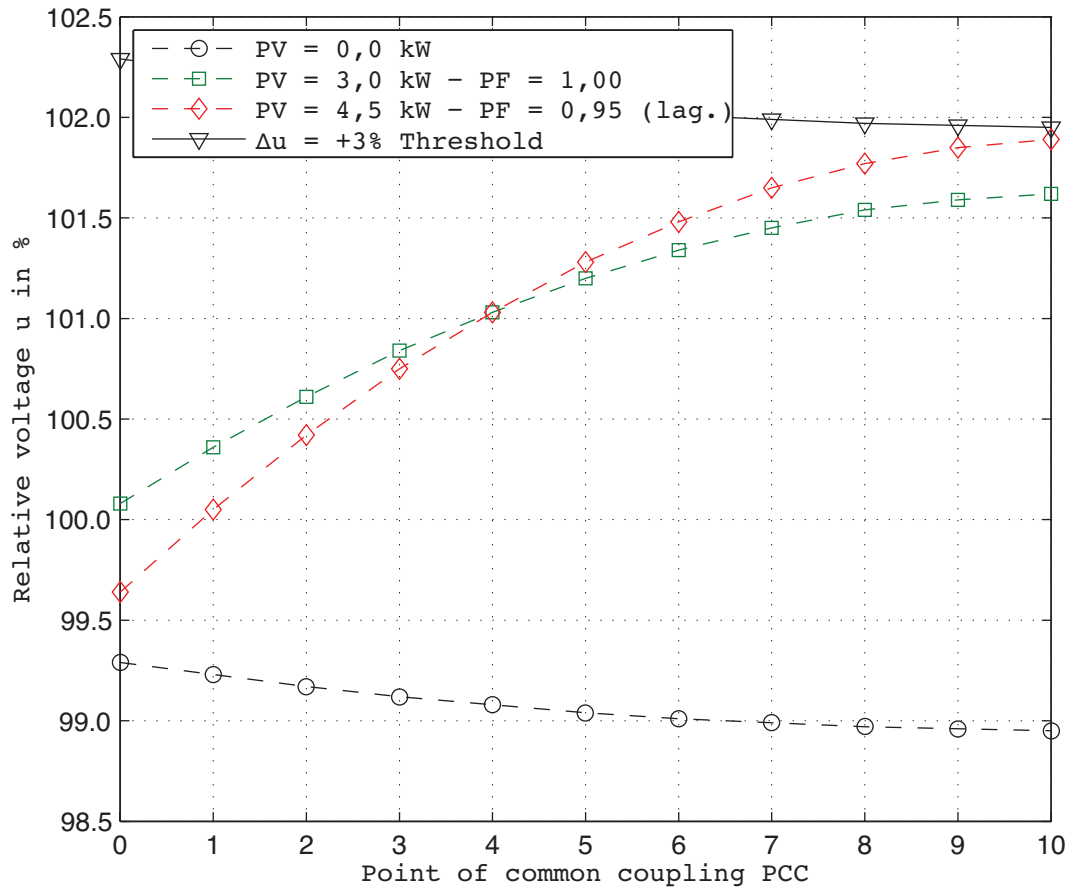


Figure C.1.3.: Voltage profile of one low voltage stub - rural model grid (20% LV-Length, 400 kVA distribution transformers, reactive power provision by the generators).

#	$\cos\varphi$	Load in kW	PV in kW	u_{PCC10} in %	Δu_{PCC10} in %
7	-	0,5	0,0	99,0	-
8	1,00	0,5	3,0	101,6	+2,6
9	0,95 (lag.)	0,5	4,5	101,9	+2,9

C.2. Overhead Line / Cable Comparison

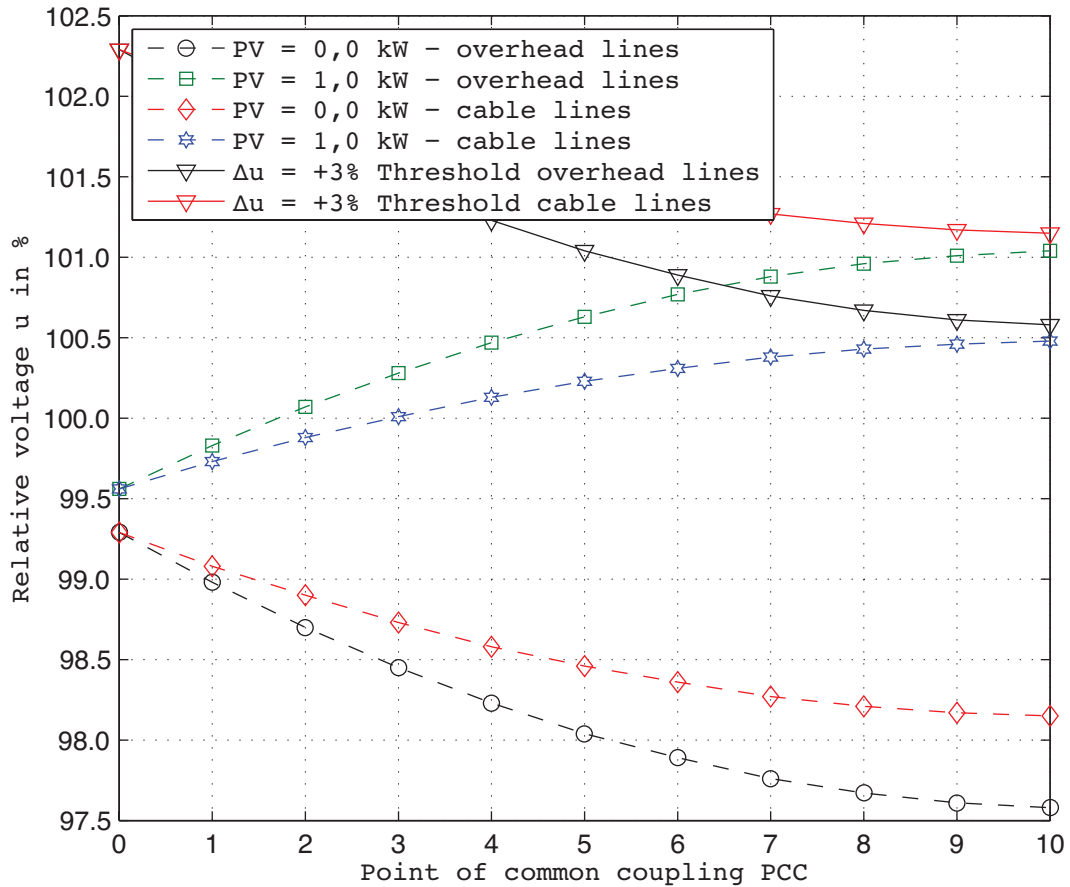


Figure C.2.1.: Voltage profile of one low voltage stub - rural model grid (100% LV-Length, 400 kVA distribution transformers, overhead lines exchanged with cable lines).

#		Load in kW	PV in kW	u_{PCC10} in %	Δu_{PCC10} in %
1	Overhead lines - 95 mm ² StAlu	0,5	0,0	97,6	-
2		0,5	1,0	101,0	+3,4
10	Cable lines - 150 mm ² Al	0,5	0,0	98,2	-
11		0,5	1,0	100,5	+2,3

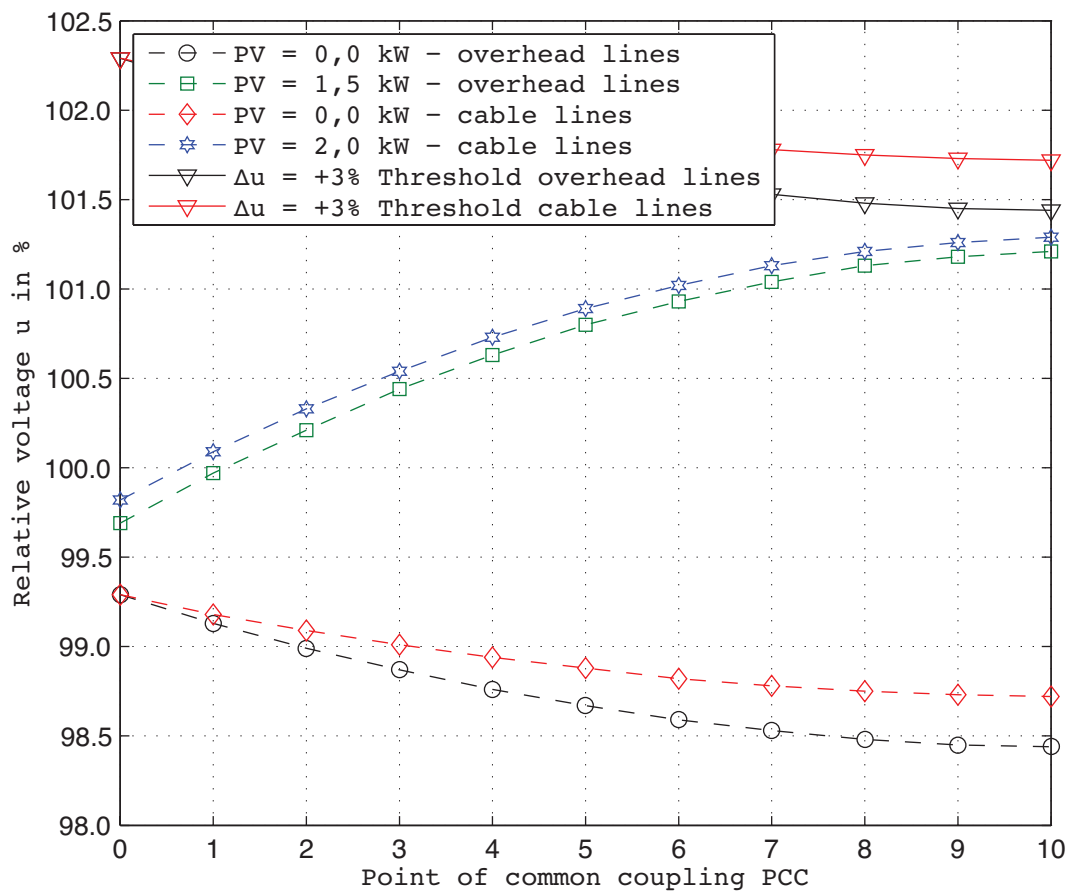


Figure C.2.2.: Voltage profile of one low voltage stub - rural model grid (50% LV-Length, 400 kVA distribution transformers, overhead lines exchanged with cable lines).

#		Load in kW	PV in kW	u_{PCC10} in %	Δu_{PCC10} in %
4	Overhead lines - 95 mm ² StAlu	0,5	0,0	98,4	-
5		0,5	1,5	101,2	+2,8
12	Cable lines - 150 mm ² Al	0,5	0,0	98,7	-
13		0,5	2,0	101,3	+2,6

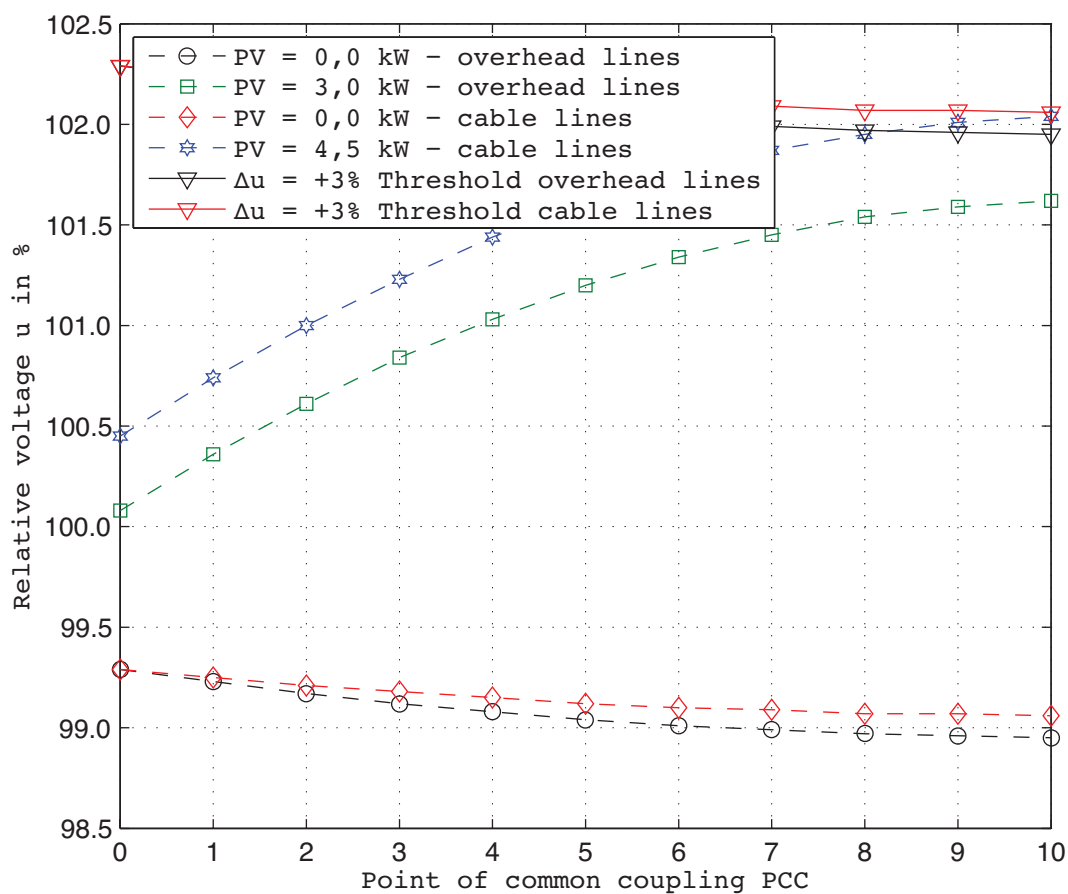


Figure C.2.3.: Voltage profile of one low voltage stub - rural model grid (20% LV-Length, 400 kVA distribution transformers, overhead lines exchanged with cable lines).

#		Load in kW	PV in kW	u_{PCC10} in %	Δu_{PCC10} in %
7	Overhead lines - 95 mm ² StAlu	0,5	0,0	99,0	-
8		0,5	3,0	101,6	+2,6
14	Cable lines - 150 mm ² Al	0,5	0,0	99,1	-
15		0,5	4,5	102,0	+2,9

C.3. Regulating Distribution Transformer

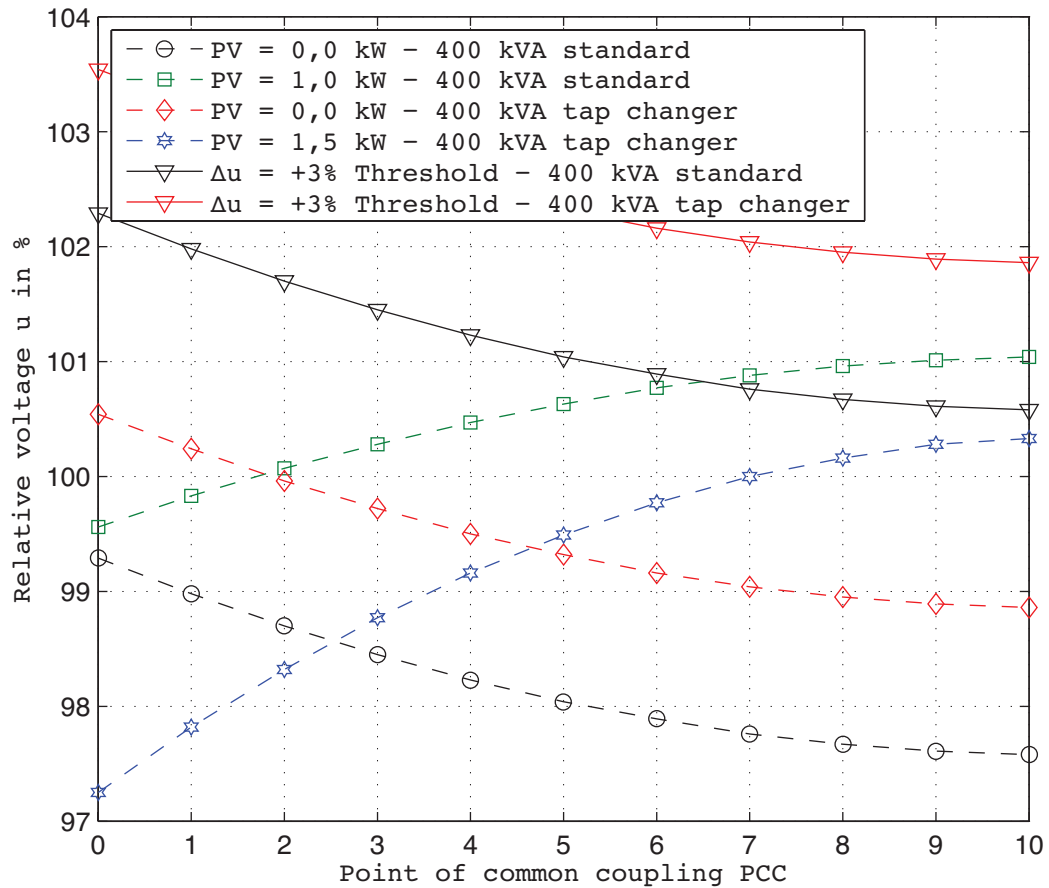


Figure C.3.1.: Voltage profile of one low voltage stub - rural model grid (100% LV-Length, 400 kVA regulating distribution transformers).

#	Load in kW	PV in kW	u_{PCC10} in %	Δu_{PCC10} in %
1	400 kVA standard	0,5	97,6	-
2		0,5	101,0	+3,4
16	400 kVA tap changer	0,5	98,9	-
17		0,5	100,3	+1,4

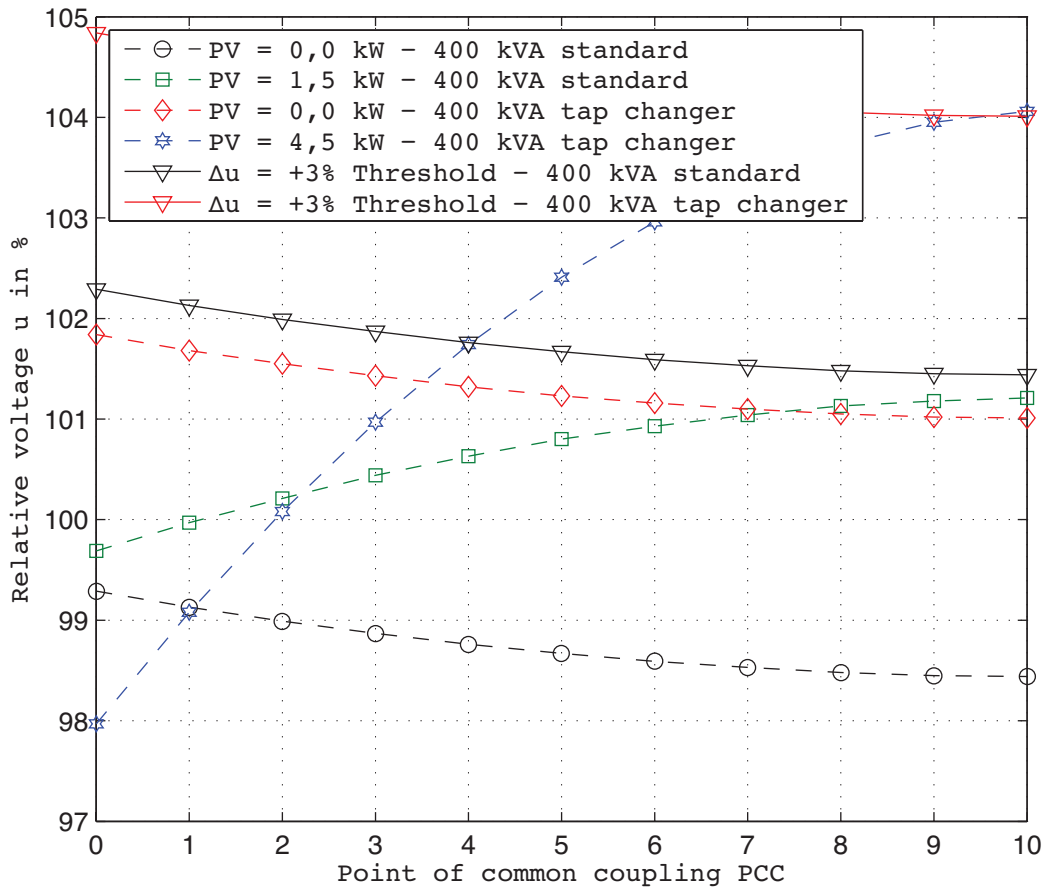


Figure C.3.2.: Voltage profile of one low voltage stub - rural model grid (50% LV-Length, 400 kVA regulating distribution transformers).

#		Load in kW	PV in kW	u_{PCC10} in %	Δu_{PCC10} in %
4	400 kVA standard	0,5	0,0	98,4	-
5		0,5	1,5	101,2	+2,8
18	400 kVA tap changer	0,5	0,0	101,0	-
19		0,5	4,5	104,1	+3,1

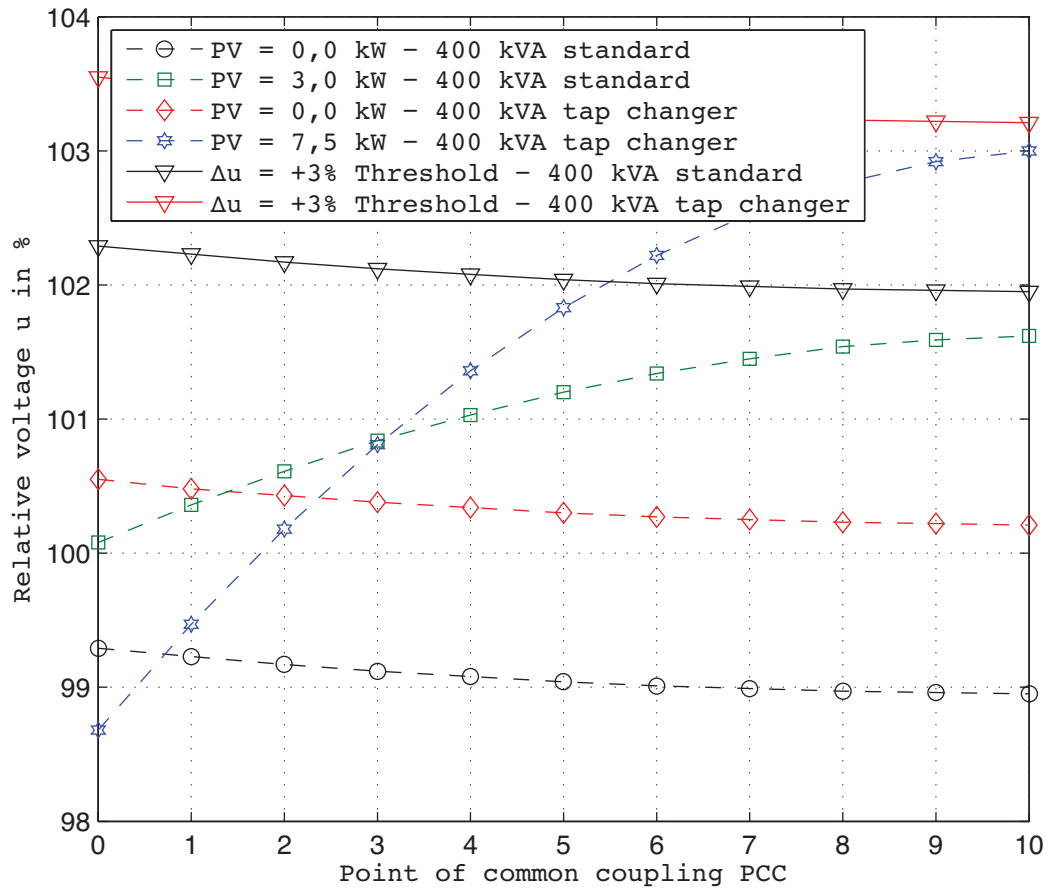


Figure C.3.3.: Voltage profile of one low voltage stub - rural model grid (20% LV-Length, 400 kVA regulating distribution transformers).

#		Load in kW	PV in kW	u_{PCC10} in %	Δu_{PCC10} in %
7	400 kVA standard	0,5	0,0	99,0	-
8		0,5	3,0	101,6	+2,6
20	400 kVA tap changer	0,5	0,0	100,2	-
21		0,5	7,5	103,0	+2,8

C.4. Central Reactive Power Management at 0,4 kV Busbar

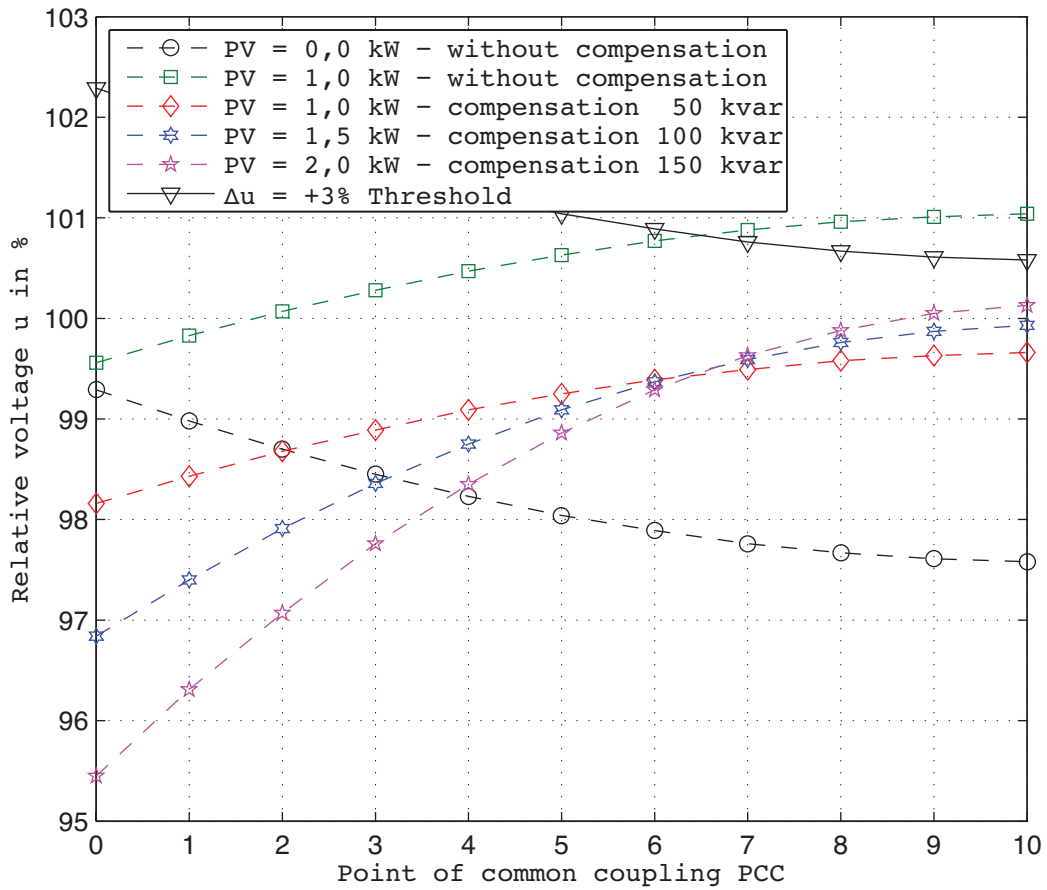


Figure C.4.1.: Voltage profile of one low voltage stub - rural model grid (100% LV-Length, 400 kVA distribution transformers, central compensation unit).

#	Compensation in kvar	Load in kW	PV in kW	u_{PCC10} in %	Δu_{PCC10} in %
1	-	0,5	0,0	97,6	-
2	-	0,5	1,0	101,0	+3,4
22	50	0,5	1,0	99,7	+2,1
23	100	0,5	1,5	99,9	+2,3
24	150	0,5	2,0	100,1	+2,5

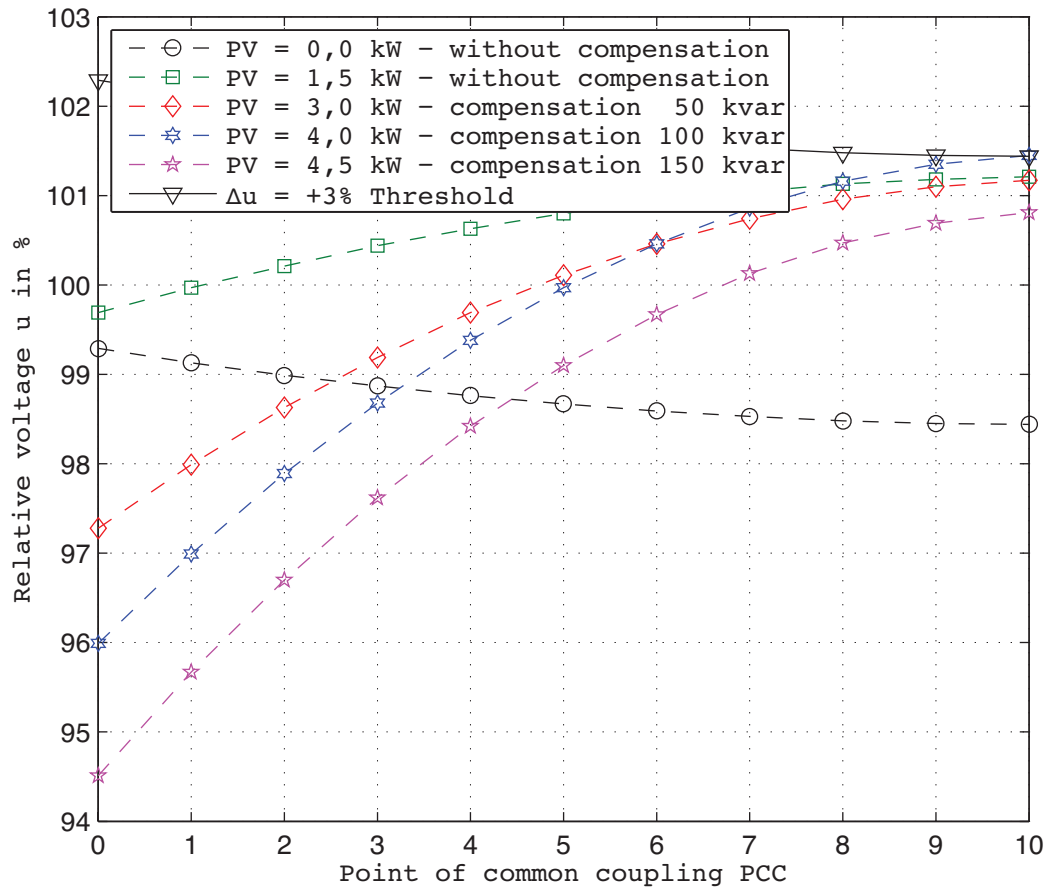


Figure C.4.2.: Voltage profile of one low voltage stub - rural model grid (50% LV-Length, 400 kVA distribution transformers, central compensation unit).

#	Compensation in kvar	Load in kW	PV in kW	u_{PCC10} in %	Δu_{PCC10} in %
4	-	0,5	0,0	98,4	-
5	-	0,5	1,5	101,2	+2,8
25	50	0,5	3,0	101,2	+2,8
25	100	0,5	4,0	101,5	+3,1
27	150	0,5	4,5	100,8	+2,4

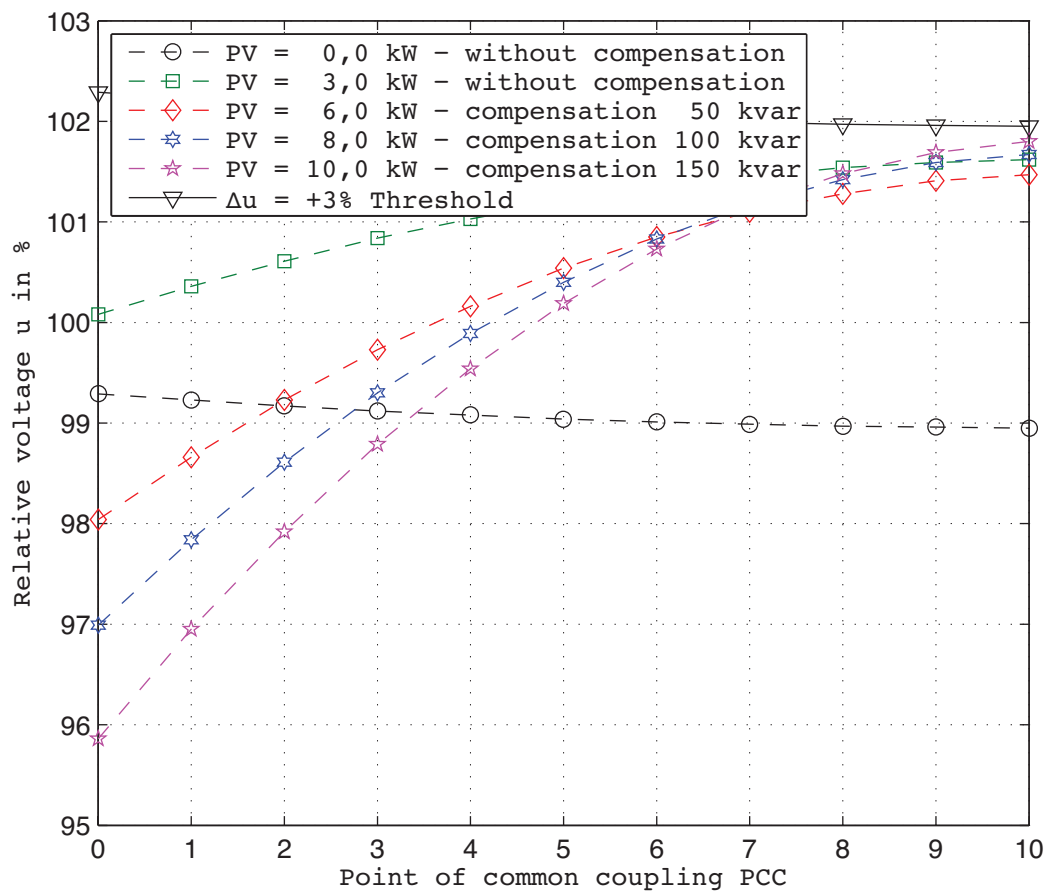


Figure C.4.3.: Voltage profile of one low voltage stub - rural model grid (20% LV-Length, 400 kVA distribution transformers, central compensation unit).

Compensation in kvar	Load in kW	PV in kW	u_{PCC10} in %	Δu_{PCC10} in %
7	-	0,5	99,0	-
8	-	0,5	101,6	+2,6
28	50	0,5	101,5	+2,5
29	100	0,5	101,7	+2,7
30	150	0,5	101,8	+2,8